8-2015

FUNCTIONAL ANALYSIS OF SYNTHETIC GENE CIRCUITS CONTROLLING A PROTEIN PUMP IN YEAST

Junchen Diao

FUNCTIONAL ANALYSIS OF SYNTHETIC GENE CIRCUITS CONTROLLING A PROTEIN PUMP IN YEAST

By

Junchen Diao B.S.

APPROVED:

_____
Gábor Balázsi, Ph.D. Supervisory Professor

_____
Gregory S. May, Ph.D. On-site Advisor

_____
Michael C. Lorenz, Ph.D.

_____
Guang Peng, M.D. Ph.D.

_____
Matthew R. Bennett, Ph.D.

_____
Timothy Cooper, Ph.D.

APPROVED:

_____

Dean, The University of Texas

Graduate School of Biomedical Sciences at Houston

FUNCTIONAL ANALYSIS OF SYNTHETIC GENE CIRCUITS CONTROLLING A PROTEIN PUMP IN YEASTS

A

DISSERTATION

Presented to the Faculty of

The University of Texas

Health Science Center at Houston

and

The University of Texas

MD Anderson Cancer Center

Graduate School of Biomedical Sciences

in Partial Fulfillment

of the Requirements

for the Degree of

DOCTOR OF PHILOSOPHY

by

Junchen Diao B.S.

Houston, Texas

August, 2015

Dedication

I dedicate my dissertation to my grandpa. Together with my grandma, he raised me up with in my early years. He taught me the qualities to be a good person, and was always extremely supportive for my education, and gave me encourage and confidence to push forward in difficult situations. He set himself as an example to true devotion to work, family and the society. He will be missed.

Acknowledgement

During my entire Ph.D. study, I got help from many people. Now I want to give my deepest thanks to all of them.

First of all, I want to thank my Ph.D. mentor, Dr. Gabor Balazsi for his belief in me and continuous guidance and support. He accepted me as a graduate student from a pure biology background to do highly interdisciplinary research. During my study here, he has been teaching me with great patience, and was always there to help whenever I was in trouble. Doing scientific research can be exhaustive and extremely difficult sometimes, but Dr. Balazsi encouraged me during the whole journey, and trained me to deal with tough situations with confidence and belief. He is a true teacher; even at the time that research funding was very tight, he still placed great emphasis on training students. He gave me the freedom to explore, and taught me to be an independent thinker. He is also a true scientist, his dedication to scientific research and striving for excellence serves great example to me for my further career. This dissertation could not be finished without his support and dedication.

Besides Dr. Balazsi, I want to thank all the members in Balazsi lab. I grew with them in the past over 4 years, and received tremendous help. They addressed technical troubles I had with experiments, data analysis and mathematical models. Here I want to give my special thanks to Dr. Dmitry Nevozhay, who laid the foundation for my research projects, and helped me with experimental design and technical problems. I also want to thank Dr. Daniel Charlebois, who performed stochastic simulations for my projects, which facilitated my research progress.

I also want to express my gratitude to my supervisory committee, their criticism and suggestions pushed my research to a higher level. Besides, they also trained my

scientific thinking, expanded my scientific knowledge and writing skills. Among them, I want to thank Dr. Gregory May as my on-site advisor, he has been very supportive after Gabor left, and gave me courage and confidence to finish my research and dissertation.

Next, I want to thank my family and friends. Without their support and company in the past 5 years, it is impossible for me to finish this dissertation. Their love and care completed me as a full person and helped me to grow along the way.

Finally, I want to thank the University of Texas Graduate School of Biomedical Sciences for offering me a position to pursue my Ph.D. and all the assistance in my study here. I also want to thank all the employees in the Department of Systems Biology at MD Anderson Cancer Center; I cannot complete my research without the support from this department.

FUNCTIONAL ANALYSIS OF SYNTHETIC GENE CIRCUITS CONTROLLING A PROTEIN PUMP IN YEAST

Junchen Diao B.S.

Supervisory Professor: Gábor Balázsi, Ph.D.

Abstract

Synthetic biology aims to build biological devices to understand living systems and explore new applications. Synthetic gene circuits such as genetic switches, oscillators and logic gates are at the core of many synthetic biology applications. These gene circuits often include a sensor/regulator protein capable to detect small molecules and then transduce them into a regulatory signal to generate measurable output. Similar signal transduction networks are also abundant in nature. However, in many natural and engineered scenarios, the output also affects the regulator/sensor protein. How such interactions between the regulator/sensor and the output affect synthetic gene circuit function has not been investigated. In order to address this question, I took advantage of *Saccharomyces cerevisiae* synthetic gene circuits built previously in our laboratory: Negative Regulation (NR), Negative Feedback (NF) and Positive Feedback (PF). Previous research had characterized the behavior of these gene circuits at various inducer (anhydrotetracycline, ATc) concentrations when they controlled the bifunctional Zeocin Resistance gene (ZeoR) fused to the reporter yEGFP. In these gene circuits, yGFP::ZeoR was a passive target, which did not interact with its upstream transcriptional regulator. In order to study the effect of an

active target on gene network dynamics, I replaced yEGFP::ZeoR with *PDR5::GFP* to create three new gene circuits, NRpump, NFpump and PFpump. The *PDR5* gene produces a multidrug resistance pump that belongs to the ATP-binding cassette protein family. Once Pdr5 is expressed, it pumps out various small molecule chemicals including the inducer, altering the activity of its upstream transcriptional regulators, and thereby creating a feedback loop. Therefore, these reconfigured gene circuits enabled the investigation of the question: how the protein pump alters the characteristics of the original NR, NF and PF gene circuits.

In this dissertation, I show that the dose response behavior of the NRpump, NFpump and PFpump gene circuits differs from their non-pump counterparts. Studying gene circuits controlling non-functional *PDR5* mutants indicated that the efflux pumping activity of Pdr5 caused loss of linearity in NFpump compared to NF dose-response. However, the dose-response behavior of NRpump and NFpump with the *PDR5* mutant still differed from the behavior of the original NR and NF gene circuits. With the help of stochastic models developed by my collaborator, I hypothesized and then proved experimentally that lower expression level of the regulator, TetR, in all NRpump and NFpump strains (both with functional and non-functional Pdr5) compared to NR and NF, should be responsible for the remaining dose response differences. Similar to the other pump-controlling gene circuits, the PFpump gene circuit had a more sensitive dose-response compared to the original PF. Although both gene circuits produced bimodal distributions, the finesses and cellular transition rates between the two subpopulations were different.

Finally, I tested the evolution of non-induced NRpump, NFpump and PFpump strains in a fluconazole-containing environment. While PFpump cells maintained fluconazole sensitivity, NRpump and NFpump cells started to develop fluconazole resistance after 48 hours. Expression of Pdr5 was the cause of resistance. The

elevated Pdr5 expression level remained the same after fluconazole removal, suggesting mutational breakdown of these gene circuits. However, bimodal expression patterns evolved in some NRpump and NFpump cell cultures after 256 hours in fluconazole environment suggesting that other mutations might have occurred besides those causing gene circuits' breakdown.

Table of Contents

List of Figure

List of Tables

Chapter 1 Introduction

1.1 Introduction and background

1.1.1 Synthetic biology

Synthetic biology is an interdisciplinary subject which combines biology, physics, engineering and computer science. It emerged as an independent field marked by the development of the genetic toggle switch [1] and genetic oscillator [2] in the year 2000. The field has been developing so rapidly that no clear definition is widely accepted for now. The one used by the Synthetic Biology Community (www.syntheticbiology.org) is 'the design of new biological parts, devices and systems, and the re-design of existing, natural biological systems for useful purposes'. By this definition, synthetic biology creates and modifies existing biological systems. In order to do that, synthetic biologists employ a variety of tools in existing subjects, for example, concepts and technologies developed in molecular biology, systems biology, bioengineering, evolutionary biology and biophysics.

Although synthetic biology is still a very young subject, the idea of building biological parts and systems dates back to the mid-70s in the 20th century: the discovery and utilization of restriction enzymes and the subsequent emergence of DNA recombination technology. Restriction enzymes were discovered by Werner Arber, Daniel Nathans, and Hamilton O. Smith, whose work won the Nobel Prize in Physiology and Medicine in 1978 [3-9]. This significant discovery immediately led scientists to be able to map DNA and manipulate nucleotide sequence. The advances in DNA recombination technology in the following years then led to a series of breakthrough achievements in science and medicine, for example, the modern molecular cloning technology and the production of protein drugs. Inspired by these technology

advancements while being aware of their limitations in complexity, scientists hoped to build novel biological systems or even artificial organisms to further advance understanding of biology and expanding its application. Synthetic biology emerged to study the engineering of biological systems. With the aim to engineer biology, synthetic biologists use four major approaches. The most common one is building standardized biological parts, including DNA, RNA and protein sequence. A variety of existing biological elements have been used, for example, promoter, terminator, activator and repressor sequence on the transcriptional regulation level, and UTR, splicing sequence and ribosome binding site (RBS) on the translational level [10-19]. Several existing inventories for standardized DNA elements are also available online, such as BioBricks, which has been used widely internationally. Besides standardizing existing biological parts, another widely used approach for synthetic biologists is DNA synthesis. Nowadays with the rapid advancement of DNA synthesis technology, we are able to synthetize DNA sequence up to 5 kb in length, which has significantly improved the plasmid construction efficiency and accuracy. It also allows scientists to design DNA sequence with certain mutations, or special sequences that do not exist naturally. The third approach that advanced synthetic biology is DNA sequencing technology. Because synthetic biology requires high accuracy, advanced DNA sequencing technology works faster, cheaper and with higher accuracy rate that will definitely benefit synthetic biology. The last but not least used approach is mathematical modeling. Because synthetic biologists use standardized elements to engineer biology, computational simulation that is able to predict possible outcomes can provide useful insight on how the engineered system will behave, and save time and cost for experimental construction.

Although synthetic biology appeared as an independent subject only 15 years ago, numerous achievements have been made. Biomaterial production is among the biggest one. Thanks to synthetic biology technology, greener energy sources such as biofuel for jets and vehicles is being produced by microorganisms. Cosmetics and food ingredients, vaccine and

pharmaceuticals are also being produced by synthetic biology means in biotech and pharmaceutical industries. Besides facilitating drugs production, synthetic biology also accelerated the discovery of drug targets and facilitated drug delivery. Synthetic systems built with controllable biological elements can assist the discovery of disease mechanisms and identification of drug target [20]; synthetic gene circuits built to work as oscillators can deliver a drug periodically as desired [2, 21]. In addition, biosensor design is another active research area in synthetic biology, which generated influential applications. A series of biosensors were developed for both basic scientific research and industrial applications. For example, synthetic de-greening biosensors in plants were used to detect explosive molecules in the air [22]; metal detection biosensors were able to detect certain chemicals underground and were used in a mining startup. More fancy research and applications have been created with synthetic biology tools. For example, in May 2010, Craig Venter's group announced that they had been able to assemble a complete genome composed of millions of deoxyribonucleic acid base pairs. When it was used to replace the original genome in a cell, the cell was able to replicate [23], which was the first artificial life built in the laboratory. Scientists also use DNA sequence for information storage. George Church's group encoded one of his books on synthetic biology into DNA [24].

Behind most of these advanced technologies developed by synthetic biologists are synthetic gene circuits. 'Gene circuit' is a term borrowed from electronic engineering, and it reflects the idea that synthetic biologists are treating gene elements as electronic elements, aiming to completely control the outcome signal. Under the influence of this concept, toggle switches [1], oscillators [2] and digital logic gates [25] were built as first-generation systems. These systems successfully integrated regulatory DNA elements into microbial genomes and were able to program the behavior of those microorganisms. By doing so, they also discovered the switches, oscillators and logic gates in natural biological systems [26]. The exciting news of programmable cells and natural regulators attracted a number of scientists to work in this field.

Initially, they engineered natural promoter sequences to be inducible in order to utilize natural transcription factors such as Gal4, TetR and LacI. While the intracellular level of TetR and LacI can be regulated by tetracycline family molecules and IPTG respectively [27, 28], synthetic gene circuits based on these systems are subsequently under control of these inducers to a range of expression. Later on, more complicated gene circuits involving negative feedback loops and positive feedback loops were built, and their behaviors were studied [29]. With the growth of synthetic biology research, the regulation of gene circuits evolved from the transcriptional level to include translational and post-translational level regulation. The clustered regularly interspaced short palindromic repeat (CRISPR)/Cas9 system was initially discovered as part of a bacterial immune system, but now it is used for gene editing and RNA driven gene modification [30].

Despite numerous advances in the study of gene circuits and gene networks, obstacles and challenges exist. Living cells are more complicated than electronics; simply applying the concepts from electronic engineering is insufficient to engineer biological systems. With mutation and evolution playing a critical role in biology, variability of genetic elements created big problems. Besides, although our knowledge and information in biology and medicine increased exponentially, the unknown expanded to in a greater degree. Therefore, it is very difficult to standardize and modularize elements in biology as experts did in the field of electronic engineering. Great effort is still needed in order to overcome these challenges in the future.

1.1.2 Gene expression noise

Gene expression is a stochastic process. The variation generated during the gene expression process is called gene expression noise. Genomically identical cells growing in the

same environment have different expression levels for a gene of particular interest. For example, considering a population of cells with identical genomes cultured in the same medium, any particular gene of interest can express different amounts of RNA from cell to cell and over time in a single cell. The reason for this difference is random factors, for example, unpredictable thermodynamic movement of transcription factors and promoters in the cell, random partition of molecules during cell division, response to unpredictable environmental stimuli, etc. This phenomena was first observed in experiment by Novick and Weiner that the production of β-galactosidase was different in each bacterial cell [31]. A few decades later, another group confirmed their discovery and further showed that the difference in terms of β-galactosidase in individual cells was enlarged by increased induction level [32]. However, the effort to study stochasticity of gene expression was not done until 2000 when Elowitz et al designed a synthetic gene circuit that produced oscillations, which were triggered by stochastic gene expression [2]. Two years later, the same group designed two gene circuits that have identical promoters, but different reporters. Then these two gene circuits were inserted in the symmetrical position on the genome of *E.coli*. Two observations were obtained; first, the expression of two reporters showed the same level across the entire experiment; second, two reporters showed different expression level [25]. These results led to the discovery of two types of gene expression noise, extrinsic noise and intrinsic noise. Intrinsic noise refers to gene specific variation that comes from the stochasticity of biochemical reactions in the cell such as transcription and translation, and it is specific for the particular gene of interest. Intrinsic noise leads to cell-to-cell variation in terms of expression level of a particular gene in a cell population. There are many factors that contribute to intrinsic noise such as promoter sequence and structure and location on the chromosome [33]. Extrinsic noise is caused by global factors that indirectly linked to the gene of interest in biochemical reaction processes such as transcription, translation and biomolecule degradation. For example, the amount of RNA pol II, ribosome and proteasome available in the cells contribute to the extrinsic noise in the expression of target genes. Other

factors such as variable molecule partitioning during cell division and asynchronous timings of their cell cycle also result in extrinsic noise. Extrinsic noise can be categorized into two types based on the origin: pathway specific and global. Pathway specific noise can be caused by the availability of specific transcription factors, while global noise usually comes from chromatin remodeling or ribosome abundance [33]. Elowitz et al also discovered that promoter strength was related to both intrinsic and extrinsic noise [25]. Their conclusion was later confirmed by the discovery that transcription and translation occurred in bursts in bacteria [34-37].

After these discoveries in bacteria, research on gene expression noise in eukaryotes attracted more attention. Although transcriptional busts have been confirmed as one of the sources for gene expression noise in yeast cells, research in budding yeast has discovered that gene expression noise in eukaryotes is different from bacteria [38-41]. The most important difference is chromatin remodeling. In eukaryotic cells, DNA is packed with nucleosome to form a compact structure, the chromosome. When transcription begins, chromatin structure switches into open and acetylated state from a condensed structure, where transcription is blocked. Studies also identified that essential genes tend to cluster together while non-essential gene cluster together on the genome, and established the correlation between the location of gene clusters and gene expression noise. They found that essential gene expression is much less noisy than non-essential genes and this was because of their location on the chromosome [42]. The location where essential genes cluster showed open chromatin structure, while location where non-essential genes cluster had more condensed structure on the genome [43]. Locations of transcription factors were also found to be influential over gene expression noise [44]. Additional studies indicated that the gene expression noise in yeast cells is mostly from extrinsic origins, which was confirmed by the fact that different genes showed the same noisy expression pattern [38, 45-47]. Cell size and chromatin remodeling were considered the major contributors [46-48].

However, the theoretical studies of extrinsic noise are still lacking because of lack of robust mathematical models [49].

With technical advancement and increasing knowledge of gene expression noise in budding yeast, more interest has been attracted to study that in mammalian cells. In the beginning, gene expression noise was expected to be much lower in mammalian cells, because of their low protein numbers the lower number of molecules, the higher randomness it becomes [50]. However, more and more research has found the opposite. Measurement of mRNA expression in single cell observed burst of transcription [51-54], which showed similar pattern as it was observed in bacterial cells, but lasting longer and less frequent. Similarly, protein expression was also observed to happen in bursts in mammalian cells, which resulted in cell-cell variation [43].

The discovery that essential genes tend to cluster together on chromatin open locations suggested that noisy expression of essential genes may have lethal consequences. However, the relatively more noisy expression of nonessential genes triggered the idea that noise can be beneficial to certain cells or in certain circumstances. One major outcome of noisy gene expression is to create diversity of phenotypes. One example is the expression of odorant receptors in sensory neurons in mice. Over a thousand odorant receptors have been found in different sensory neurons, their expression was random and mutually exclusive [55, 56]. Our traditional view of stem cell diffraction and development is deterministic. However, stochastic gene expression has been shown to play a major role. Researchers found that genomically identical individual cells with expression of certain stem cell markers correlate with their further fate of differentiation [57]. Not only was an advantage of gene expression noise was found in mammalian cells, it was also discovered in unicellular organisms. Genes encoding metabolic pathways are stochastically switched between on and off states. For example, gene products that utilize lactose as energy source in *E. coli* [58, 59] and the *GAL3* gene in yeast [60]. Some

attempts have been made to explain the causes of these phenomena. Some researchers claimed that stochastic switching between two states maximize the growth rate of cells population when environment change frequently [35, 61]. Bacterial cells use expression noise of drug resistance gene as a protective strategy against adverse environment [62]. When adverse environment comes, cells with high expression of drug resistance genes are more likely to survive. Another example involves the competence in *B. subtilis*. Two survival states exist in *B. subtilis*, competence and vegetative states. In competence state, comK expression was activated and its expression amplified by a positive feedback loop, while vegetative state showed only basal level of comK expression. The two states resulted in bimodal expression of comK in a cell population, and they transit between each other [63]. In summary, gene expression noise is random, and can be both good and bad depending on the situations. To really answer these questions, we ought to ask, can noise be regulated? The answer is yes, synthetic biologists are already using different regulatory network to regulate gene expression noise.

1.1.3 Synthetic gene circuits for noise control

Based on the studies to understand and characterize gene expression noise in both natural and synthetic systems, researchers also attempted to control noise by building synthetic gene circuits. The first attempt was to control a downstream reporter by upstream regulatory elements to study its gene expression noise [36, 64, 65]. They found that the variation in the upstream regulatory parts can affect expression noise in the downstream genes, and the effect was heritable. Later on, more research has been done to investigate more complex synthetic gene circuits. I am going to talk about the basic gene circuits in the following context.

Auto regulation

Auto regulation is the simplest regulatory cascade in the transcriptional level. Basically, it needs a transcription factor that binds to its own promoter and regulates its own expression. Auto regulation can happen in either self-inhibition or self-activation forms. Research has found that the auto regulation on gene circuit was able to reduce noise by decreasing the size of transcriptional bursts, which caused the reduction of time to reach steady states [66-70]. Besides, auto regulation is also involved in oscillation induction and reduces the metabolic cost by reducing mRNA usage [2, 71, 72]. On the contrary, positive auto regulation has been found to increase gene expression noise and take longer time to reach steady states [67].

Negative feedback (NF) gene circuit

Negative feedback gene circuit involves more complex regulatory components. On the transcriptional level, usually there is a repressor that represses the transcription of both the transcription factor and downstream target gene. It has been found that negative feedback loop was able to reduce gene expression noise (for both transcription factor and the downstream target gene) and speed up the response time [66, 73, 74]. Because only one steady state has been demonstrated to exist, any fluctuations deviating from the mean would be pushed back [35, 74-77]. It was also able to generate linear response to inducer up to saturation [29]. By modifying the number of repressor binding sites on the target promoter region, the authors were able to change the linearity of the dose response curve, which indicated the correlation between promoter sequence and the noise expression in synthetic gene circuits [29].

Positive feedback (PF) gene circuit

Positive feedback regulatory network is usually composed of a transcription factor that regulates a downstream target gene. An activator is able to activate the transcription of both itself and its downstream target gene. Positive gene circuits have been found to amplify noise. Therefore, a low activator expression is able to activate further expression of it and the target gene, which usually led to the two stable steady states, one with maximum level of expression, and one with basal level. It has also been found that cells in these two states were able to switch between states [1, 77-80]. Further studies discovered that the switching rates between the two states were different, and the existence of stable bimodal expression states were a result of different cellular growth rate memory in the two states [81]. Cellular memory refers to the time an individual cell staying in one stable steady state [60].

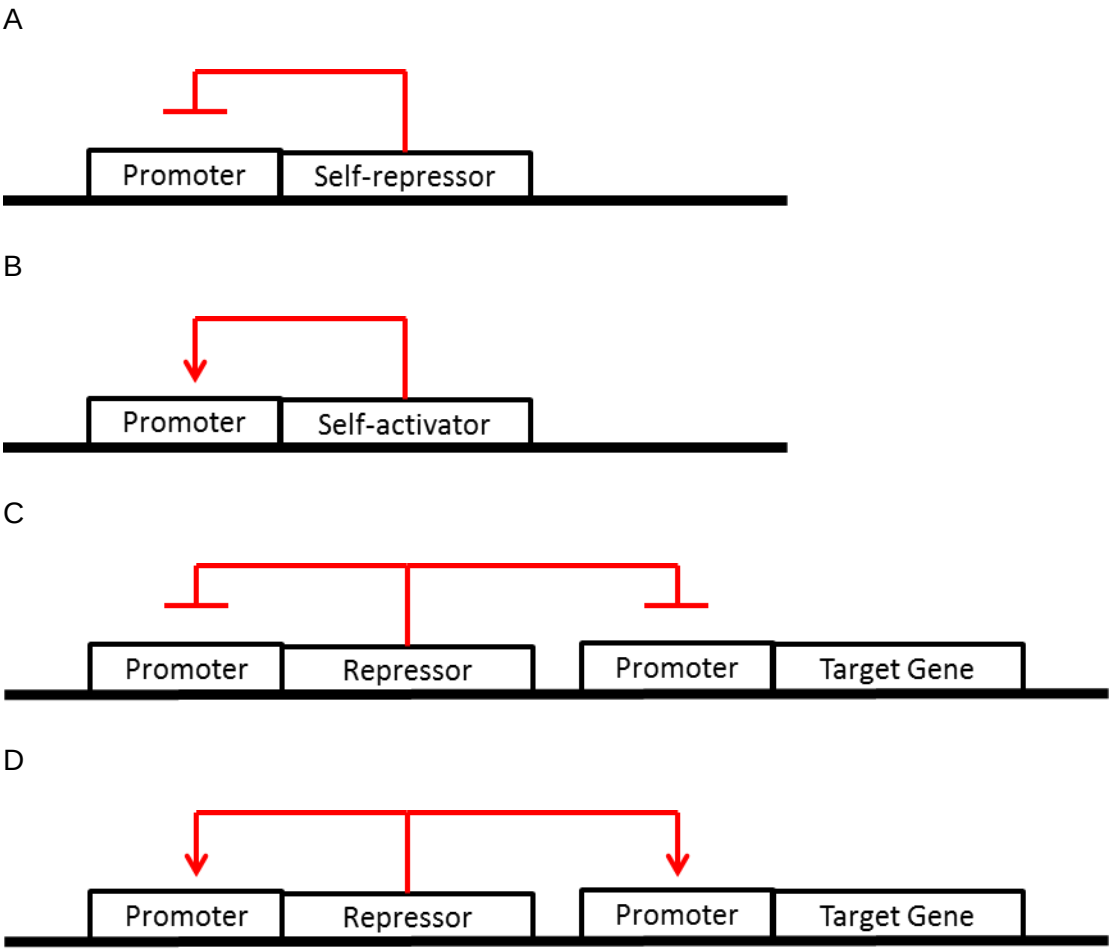

Figure 1.1 Scheme of auto regulation and feedback regulation.

A. Auto regulation (Inhibitor). B. Auto regulation (Activator). C. Negative feedback regulation. D. Positive feedback regulation

1.1.4 Tetracycline controlled transcription

Tetracycline controlled transcription is a system that was developed from the tetracycline resistance operon in *E.coli* [28]. The natural operon functions to protect bacterial cells from antibiotics such as tetracycline. It is composed of a Tet repressor, TetR, which inhibits the transcription of the tetracycline resistance protein, TetA. The TetR binding sites on the promoter are called TetO sites. It's been reported that the binding of tetracycline or its derivatives (doxycycline, etc) are able to reduce the affinity between TetR and TetO by 9 orders of magnitude, which leads to the release of TetR from the promoter and therefore activation of target gene transcription. Researchers started to use this natural system to study the gene of interest by placing it under the control of a natural tetracycline resistance promoter. This is called the T-REx system. Later on, Tet-on and Tet-off were distinguished; since then, more research has been done to modify and improve the system [82-86]. Placing the TetO sequence on other natural promoters in other bacteria, yeast and mammalian cells revealed that the modified Tet systems were able to induce transcription of target gene of interest again as well. Further modifications also led to the construction of Tet-On system. This system is composed of an activator instead of the repressor in the T-REx system, and the TetO sequence in the promoter region. The activator activates the transcription of the target gene in two ways, induced by tetracycline or not. Other modification has also been done to increase the activator's sensitivity and specificity to doxycycline, which works better than tetracycline in terms of its lower light sensitivity [83]. The activator in Tet-on system, tTA, was originally created by fusing TetR with the acidic domain of HSV VP16, which is a transcriptional transactivation domain in eukaryotic cells. As a result, binding of tetracycline family molecules leads to the release of rTA from the promoter and inhibits transcription of target genes. Another activator that has been used widely is rtTA, which was modified on the basis of tTA by introducing a few mutations on TetR, which transferred the function of transactivator to bind DNA in the presence of inducer. rtTA requires binding of tetracycline to activate the transcription of target genes. Recently, a more advanced

Tet-on system was created, Tet-Oh 3G, which showed reduced basal expression and higher sensitivity to inducers. This new system was constructed by using human optimized codons [84].

1.1.5 ATP-Binding Cassette (ABC) family

The ATP-binding cassette (ABC) superfamily was first discovered in bacteria [87]. Early biochemists studying molecules across cell membranes discovered that the transporter in charge of the process was also responsible for regulatory and other functions. Researchers later discovered that some of the transportation processes were coupled with ATP hydrolysis, which led to the identification of a group of closely related proteins in several bacterial species [88-90]. These proteins are both functionally and structurally related, as they are all involved in cell division, and substrate transport across the membrane and ATP hydrolysis. Later on, ABC family proteins were discovered in eukaryotes, including yeasts and humans, and their importance rose significantly after the discovery of their role in multidrug resistance in a variety of diseases. Increased expression of ABC family proteins was associated with resistance to chemotherapy in cancer and fungal infections, which usually led to the failure of medical treatment. Since then ABC family proteins received considerable attention. The structure of ABC transporters is highly conserved, including a phosphate binding domain and the consensus sequence 'LSGGQ'. It has been reported that 1% to 3% of the genome in microbes encodes ABC transporters [91]. 48 ABC transporters have been identified in human so far [92, 93].

In *Saccharomyces cerevisiae*, 31 ABC transporters have been discovered, and they have been divided into 5 subfamilies based on their phylogenetic features [94]. Among them, the Pleiotropic drug resistance (PDR) proteins are mainly responsible for multidrug resistance by exporting toxic molecules across cell membrane. There are 9 full sized proteins in the PDR

subfamily, *PDR5*, *PDR10*, *PDR11*, *PDR12*, *PDR15*, *PDR18*, *SNQ2*, *AUS1* and *YOL075c* [95]. Pdr5 plays the most important role in transporting molecules across cell membrane.

1.1.6 *PDR5*

PDR5 gene was discovered in 1990 when Leppert G et al. cloned a DNA fragment that was able to confer resistance to cycloheximide and sulfometuron methyl treatment by overexpression in yeast cells [96], while mutants with disruptive mutation on *PDR5* showed hypersensitivity to these drugs. Then *PDR5* was identified to be regulated by the transcription factor, PDR1 in *S. cerevisiae*. Four years later, the complete sequence of *PDR5* was published and then this 160-kDa protein was officially considered as a member of ABC family. Further studies by Leonard et al and Kolaczowski et al indicated that the non-functional *PDR5* mutant led to reduced R6G (a fluorescent dye) and drug efflux, and demonstrated that *PDR5* deficient cells were more sensitive to anti-cancer drugs [97, 98].

The Pdr5 protein is composed of two transmembrane domains (TMDs) and two cytoplasmic domains (NBDs). TMDs include 12 alpha helices on transmembrane segments (TMSs) and several of them associate with each other compromising the substrate binding sites [99, 100]. Site-directed mutagenesis studies revealed that individual TMSs sequences predominantly determined substrate specificity. Function and position of several TMSs have been identified. TMS 2 locates at the binding pocket of Pdr5, and TMDs10 is on the opposite position. TMS1 and TMS7 are responsible for membrane localization of the entire TMDs [101]. Although effort and progress regarding the structure and function of TMDs have been made, no exact structure of TMDs have been discovered so far, Rutledge et al proposed computational simulation of Pdr5 structure based on its amino acid sequence [102, 103], which might give insight for further study on TMDs structure. NBDs are located at the cytoplasmic side of Pdr5 protein

and are mainly responsible for ATP hydrolysis, which provide energy for the conformational change on TMDs. Unlike TMDs, which have rare sequence homology across different ABC transporters, NBDs are relatively well conserved. Certain sequences are highly conserved on NBDs and play very important functions. These sequences include the Walker A motif, Walker B motif and ABC signature. Research discovered that the association between Walker A motif and the β- and γ-phosphates of ribonucleotide is essential for ATP hydrolysis [101].

ABC family proteins have an enormous variety of substrates. Generally, the two trans membrane domains (TMDs) are responsible for substrate recognition and binding while the two nuclear binding domains (NMDs) provide the energy source and facilitate the conformational change [100]. The TMDs can switch between two structures, the inward facing substrate binding structure, and outward facing substrate release structure [89]. It has been discovered that TMDs with these two conformations have different affinities towards the substrates, which might explain one way efflux pumping function of Pdr5. Based on previous research and discoveries, a simple model of substrate efflux pumping has been proposed. The process starts with TMDs in the inward facing conformation, while their substrate binding sites are active. Once TMDs recognize their substrates and bind to them, NBDs bind to ATP and start to hydrolyze it into ADP, which provides the energy for the conformational change on TMDs. Then TMDs change from inward facing position to outward facing position, substrates are transferred from the cytoplasm to the outer site of cell membrane. Because TMDs' affinity for the substrates is significantly reduced in outward facing conformation, substrates are released to the outside environment. Recent research found that this decreased affinity for substrates in outward position might be due to the position change of active binding sites on TMDs. After the substrates release, TMDs switch back to inward facing conformation, and ADP is converted into ATP and released from NBDs. This model explained the efflux pumping function of Pdr5 well, but some detailed mechanism are still unclear and the order of steps in the model is in debate.

Robert et al discovered that the two NBDs on Pdr5 do not function equivalently. Site directed mutation assays indicated that the ATP hydrolysis at NBD2 active sites is important to initiate TMD conformational change, while the ATP hydrolysis site at NBD1 is negligible. Higgins & Linton proposed that the ATP hydrolysis only occurred after substrates release from TMDs in the outward facing conformation. However, 3 years later a contradictory conclusion was made by Oldham et al that the cross talk between TMDs and NBDs are essential mechanism to prevent ATP hydrolysis and NBDs dimerization without binding to substrates.

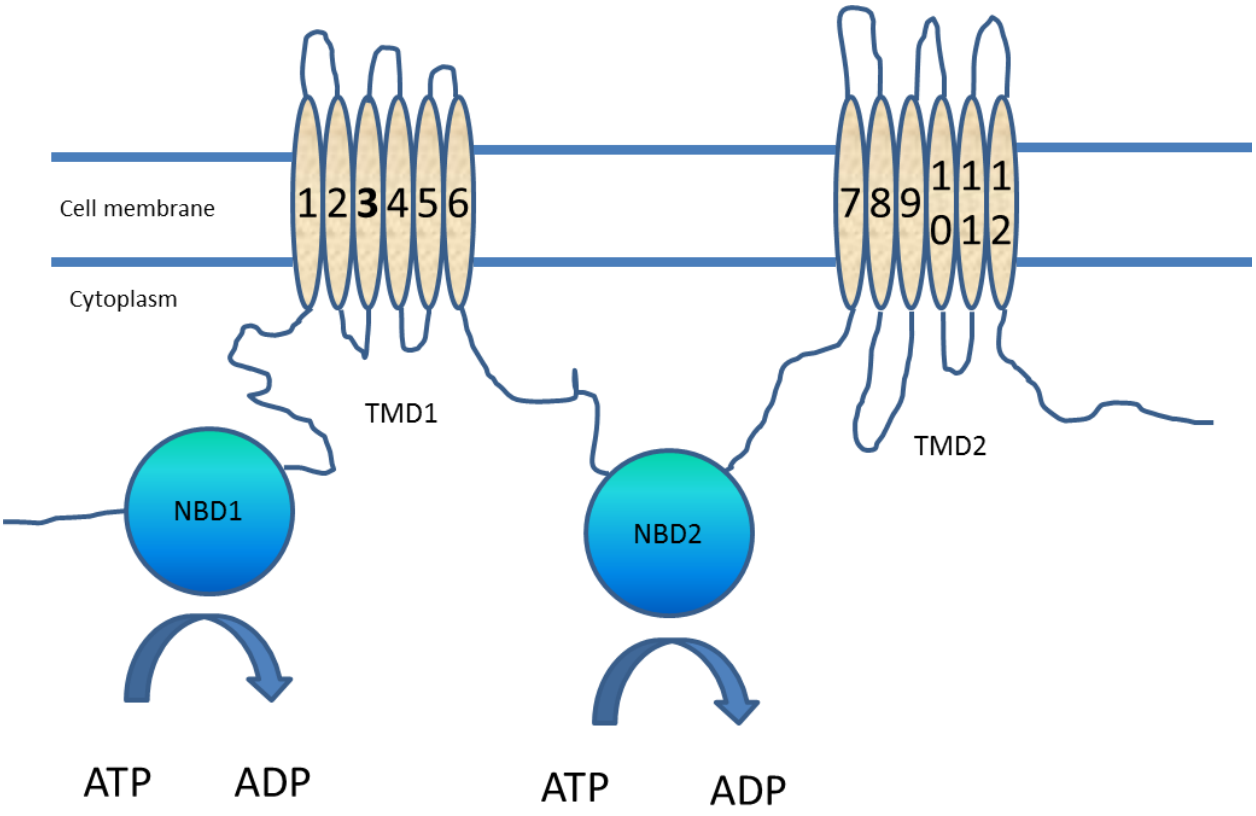

Figure 1.2 Structure of Pdr5.

Pdr5 has four domains, two transmembrane domains (TMDs) and two nuclear binding domains (NBDs). NBDs were initially associate with ATP, once TMDs bind to the substrates, ATP was hydrolyzed into ADP, which then changed the conformation of TMD, and the substrates were pumped out.

Another intriguing question that has been studied for years was the extremely diverse substrates of Pdr5. In order to study this, researchers replied on the experience from studies of other ABC family transporters. The Pdr5 homologous protein in human cells, p-glycoprotein was discovered in 1971, almost 20 years before the first identification of Pdr5. Its importance drew much attention since its involvement was found in resistance to anticancer drugs. Although rare similarities had been found on their sequence, their functions and substrate recognition were similar, Marcin Kolaczkowski et al discovered that the two proteins share 22 substrates and their efflux pumping function were both inhibited by the same inhibitors [104-106]. A series of random and site directed mutagenesis assays revealed that the transponder inhibitor and some of the mutants with impaired efflux pumping function depend on the same structural feature. Further studies using different types of substrates found that Pdr5 might have two or three substrate binding sites. However, even though multiple substrate binding sites have been identified, the mechanism of selection of various types of substrate is still unclear. In 2003, Golin et al reported that Pdr5's recognition of substrates is site-dependent; the optimum size of Pdr5 substrates is around 200 to 225 Angstron [107]. In 2007, the same group published another discovery that hydrogen bonds formed between TMD and the substrates also contribute to the substrate selection [108-110]. However, debate in this field is still ongoing. In 2009, R. Ernst proposed the kinetic substrate selection model, namely that the substrate selection of Pdr5 was determined by the kinetics of transporter-substrates and transporter-nucleotide [111]. In the model, the authors argued that more substrates being transported out of the cytoplasm did not necessarily equal higher substrate affinity. For example, given the same affinities of fast and slow substrate kinetics, the one with fast kinetics is transported more efficiently, which resulted in more substrates transported out by Pdr5.

1.1.7 Biofuels and their production

Industrialization improved the quality of human lives significantly, but on the other hand, it aggravated the environment we all depend on. According to United States Environmental Protection Agency, the emission of greenhouse gases has been increasing dramatically since 1950, when the consumption of fossil fuels was 1/7 of the amount used in 2008, and it along accounted for 57% of the total greenhouse gas emission globally. The use of fossil fuels has changed our climate irreversibly and caused global warming, it also resulted in the production of acid rain, smog and harmful particles in the atmosphere. This adverse effect endangered hundreds of living organisms and is threatening our own lives as well. Therefore, the demand for clean energy sources now has become stronger than ever. The mainstream alternative energy sources are wind, solar, nuclear and bioenergy. Bioenergy refers to the energy sources generated from living organisms or organic products. The huge benefit of bioenergy and the leading potential of bio-economy therefore attracted attention from the scientific community. Research in the field of biofuel production has been intense and numerous improvements had been made. The first generation biofuels were mostly bioethanol, biodiesel and biogas made from sugar, starch, vegetable oils or animal fat. They are able to blend with current petroleum based fuels, fit the internal combustion engines and distribute through existing infrastructure. Therefore, it has been widely used in transportation today [112]. However, the first generation biofuels also caused concerns. They were produced from food sources, and naturally competed with food consumption [113]. With a strong will to produce economically advantageous biofuel in the scientific community, second generation biofuels appeared. This novel biofuel type produced from plant biomass, which mainly refers to the lignocellulosic feedstock. Those lingocellulosic materials are abundant and cheap. Most importantly, it is not food source, and on the contrary, it is mostly waste and need to be degraded. However, the cost of production of second generation biofuel turned to be much higher than fossil fuel. The major obstacle now is the biofuel productivity and yield. A number of microorganism hosts have been studied to

produce biofuel, such as *Escherichia coli*, *Saccharomyces cerevisiae*, *Zymomonas mobilis*, and *Clostridium acetobutylicum*. These microbes' metabolic pathways were modified to maximize the production of biofuel. The genome of *Escherichia coli* was engineered to do *both* plant biomass digestion and hydrocarbon production at the same time [114]. The metabolism of fatty acid production were rewired in the DNA level in *E. coli* to overproduce fatty acyl-CoA, which is a general substrate for the production of esters and alcohols [115, 116]. Hydrogen production pathways were modified in algae and cyanobacteria to enhance photosynthesis and sugar storage [117, 118]. Non-essential metabolic pathways were also eliminated [119]. In order to maximize the production of biofuels, scientists not only work on the genome level, even RNA and proteins were engineered as scaffolds for metabolic pathway optimization [120].

Although tremendous effort has been put on the research to improve biofuel production, one major challenge still remained. Too many biofuel molecules are toxic to the microbe hosts, which will decrease their growth rate and therefore, further biofuel production. Over production of biofuel molecules in those microbes cause direct damage to proteins or other large molecules that are essential for the cells to maintain growth rate, and therefore cause stress response [121-124]. Other damage that biofuel molecules may cause is cell membrane permeability. Biofuels are easily attached to the cell membrane because of the high carbon and fatty acid in both complexes, and therefore, unbalance the chemical and electronic gradients across the cell membrane. One solution is to select microbe strains that are highly tolerated with high intracellular biofuel concentration. The other one is to use efflux pumps to exclude biofuel and keep the microbes growing at an optimized rate.

1.2 Significance of the study

Synthetic biology aims to build biological devices for predefined purposes [26, 125-128]. One important goal for synthetic biologists is to construct synthetic gene circuits [129, 130] that function as switches, oscillators, logic gates, precise dimmers, or counters [1, 2, 29, 71, 131-135]. Small molecule inducers that bind to the protein components of such gene circuits are often used to control their function externally. The hope is that by placing specific genes under the control of such inducible synthetic gene circuits, users can deliver precise stimuli to cell populations. For example, the use of synthetic gene circuits can improve the controlled secretion of drugs or biofuel compounds for clinical or industrial purposes [123, 136]. Secreting drugs and biofuels requires protein pumps that actively move them across the cell membrane. ATP-binding cassette (ABC) family multidrug resistance pumps are prime candidates to fulfill this function. Highly conserved across bacteria, fungi, and mammals, ABC family pumps cause microbial resistance to antibiotic treatment and chemo resistance to tumors by pumping out a wide range of compounds into the extracellular medium [137]. However, protein pumps controlled by synthetic gene networks that respond to inducers can secrete the intracellular inducer and thereby lower its concentration (in addition to the molecule species they are intended to secrete). This introduces a feedback [138] that may alter the function of synthetic gene networks, and may be important to understand if protein pumps are to be used as parts of synthetic gene circuits. Yet, the effect of protein pumps on synthetic gene circuit function has not been thoroughly investigated.

The major goal of this dissertation was to study the interaction between a protein pump and three gene circuits that regulate it. To answer this question, I modified three previously characterized, TetR-based synthetic gene circuits inducible by tetracycline analogs, called the negative regulation (NR), negative feedback (NF), and positive feedback (PF) gene circuits. My lab members have characterized previous versions of these gene circuits that control a passive

target gene (yEGFP::zeoR), which does not affect its upstream transcriptional regulators [29, 81]. Here, I replaced this passive target gene with the yeast pleiotropic drug resistance pump-fluorescent reporter fusion gene *PDR5::GFP*. Once *PDR5::GFP* is expressed, it pumps out the inducer, altering the activity of its upstream transcriptional regulators, and creating a negative feedback loop. I showed by experiment how this feedback loop altered the dose-response of the original three gene circuits. Moreover, I also identified mechanisms underlying an additional, unexpected change from introducing the gene that encoded the protein pump that applied to NR and NF gene circuits. Additional changes for PF gene circuit caused by *PDR5* was discovered as well in terms of growth rate and cellular memory.

Another question this dissertation addressed was the evolution of gene circuits. One goal of synthetic gene circuits was to study regulatory networks that commonly exist in natural systems. Study of the evolutionary course of synthetic gene circuits was able to provide clues on the evolution and natural selection of natural regulatory networks, such as the positive loops in the transcriptional regulation of natural *PDR5* gene. Here I evolved these three gene circuits controlling *PDR5::GFP* fused gene in constant fluconazole environment. The results were unexpected, and potential evolutionary mechanisms were identified. The results uncovered the interaction between *PDR5* and its upstream regulatory elements during evolution course in fluconazole containing environment.

Chapter 2 Materials and methods

2.1 Experiments

2.1.1 Construction of synthetic gene circuits

Each synthetic gene circuit we used consisted of two parts originating from separate plasmids: a bifunctional reporter and the regulator (Figure 1). We obtained the *PDR5::GFP* fusion by PCR amplification from whole-genome extraction of the GFP-tagged yeast library [139] and cloned it into the pRS4D1 integrative yeast plasmid, which was used to build the NRpump, and NFpump gene circuits [39, 40], chromosomally integrated into the GAL1-GAL10 locus as previously described [29, 140]. In each NRpump558/312 NFpump558/312 version, a single nucleotide mutation was introduced on *PDR5* gene before following the same procedure for yeast genome integration. In the S558Y mutant, the C was changed to A at position 1673 in the *PDR5* gene. In the G312A mutant, the G was changed to C at position 935 in the *PDR5* gene. For the construction of two color gene circuits, TetR gene in the regulator plasmid was replaced with TetR::mCherry fusion gene. Other construction procedures were the same.

Primers used for the construction and verification of gene circuits:

PDR5::GFP fusion primers:

PDR5-BamHI-f: 5’-gcgcggatcctattaaaATGCCCGAGGCCAAGCTTAAC-3’

neGFP-XhoI-r: 5’-gcgcctcgagCTATTTGTATAGTTCATCCATGC-3’

Primers for sequencing PDR5::GFP fusion:

PG-Seq1 –f: 5’-ACAGAACCGTATCAAGGGTGTC-3’

PG-Seq2 –f: 5’-TTCTTCTCTGTTAGAAATCTTTTCG-3’

PG-Seq3 –f: 5’-TATTTCACTGGAGAAACCTTTGTTACG-3’

PG-Seq4 –f: 5’-GAAAGGTTCGATAACTGCAGCTG-3’

PG-Seq5 –f: 5’-TCTACGTTTATGTTGGTTCTATGG-3’

PG-Seq6 –f: 5’-GGAAACATTCTTGGACACAAATTGG-3’

PG-Seq7 –r: 5’-CATCTCTCACTGTAGAAAGAATTG-3’

PG-Seq8 –r: 5’-TCAGCTGCAGTTATCGAACCTTTC-3’

PG-Seq9 –r: 5’-CTTCGTAACAAAGGTTTCTCCAGTG-3’

PG-SeqA –r: 5’-AAAAGATTTCTAACAGAGAAGAAAATGC-3’

PG-SeqB –r: 5’-CTATCGACACCCTTGATACGGTTCTG-3’

PG-SeqC –f: 5’-ACTCATGGTTTTGATCTTGGTGCAGATAC-3’

PG-SeqD –f: 5’-TGTACTAACTGAAAAGAATGCAAATGACC-3’

PG-SeqE –f: 5’-ATGGTGCTCATAAATGCCCTGCTGACG-3’

Orientation of the insert after inserting into pRS403 (his marker) plasmid:

Insert-f: 5’-AATTGGAGCGACCTCATGCTATACCTG-3’

Backbone-r: 5’-CGCGTTGGCCGATTCATTAATGC-3’

2.1.2 Strains and Media

The haploid *S. cerevisiae* strain YPH500 (α, *ura3-52*, *lys2-801*, *ade2-101*, *trp1*Δ*63*, *his3*Δ*200*, and *leu2*Δ*1*) (Stratagene) was used as a parental strain. The reporter plasmid was integrated into the native Gal1-Gal10 locus first. Then the regulator plasmid was integrated into the AmpR gene in the reporter plasmid by homologous recombination. The transformation procedure was described before [141]. Strains with single integration were selected by PCR and flow cytometry. All cell cultures were grown in synthetic drop-out (SD) medium with appropriate selection markers and 2% galactose.

Primers used for strains verification:

Before2TRP-r: 5’-CACATATATTACGATGCTGTTCTATTAAATGCTTCC-3’

TetREnd-f: 5’-ATGCGGATTAGAAAAACAACTTAAATGTGAAAGTGG-3’

HIS-f: 5’-ATGACAGAGCAGAAAGCCCTAGTAAAGC-3’

HIS-r: 5’-CTACATAAGAACACCTTTGGTGGAGGG-3’

TRPSeq-f: 5’-GGTGAAAACCTCTGACACATGCAGCTCC-3’

HIS-Begin-r: 5’-ACGCTTTACTAGGGCTTTCTGCTCTGTC-3’

TetR-BamHI-f: 5’-GCGCGGATCCTATTAAAATGTCTAGATTAGATAAAAG-3’

TetR-XhoI-r: 5’-GCGCCTCGAGTTAAGACCCACTTTCACATTTAAG-3’

2.1.3 Endogenous Pdr5 knockout

KanMX4 cassette was used for Pdr5 knockout. This cassette confers resistance to geneticin (G418), and was used as selection marker for successful knockout. First of all, a dose killing curve was done to optimize geneticin concentration for selection. A series of geneticin solution were made with different concentration and used to treat target strains, a positive control was used as reference. 200mg/ml geneticin was selected for my target strains. KanMX4 cassette was amplified to include upstream 45 nucleotides and downstream 45 nucleotides of native *PDR5* gene. Then the *PDR5* specific KanMX4 cassette was transformed into target strains to replace endogenous *PDR5* gene through homologous recombination. Transformation was done with the method describe by R Daniel Gietz’s methods [142]. 0.3 µg KanMX4 cassette was use for transformation. Deletion of endogenous *PDR5* gene was confirmed by PCR.

Primers used for *PDR5* knockout:

PDR5-deletion-UP45:

5’-TTAAGTTTTCGTATCCGCTCGTCGAAAGACTTTAGACAAAAATG-3’

PDR5-deletion-DN45:

5’-CATCTTGGTAAGTTTCTTTTCTTAACCAAATTCAAAATTCTATTA-3’

PDR5-deletion A: 5’-TTGAACGTAATCTGAGCAATACAAA-3’

PDR5-deletion B: 5’-TACCTAAAACGACTAGCAATTCA-3’

PDR5-deletion C: 5’-GCCTCTTTGTTGTTTACAATGTC-3’

PDR5-deletion D: 5’-TCACACTAAATGCTGATGCCTAT-3’

Kan B: 5’-CTGCAGCGAGGAGCCGTAAT-3’

Kan C: 5’-TGATTTTGATGACGAGCGTAAT-3’

2.1.4 Site directed mutagenesis

Reporter plasmid (pDN-G1PGlbh) containing *PDR5::GFP* fusion gene was modified with site directed mutagenesis in order to create non-functional Pdr5 protein. In the first mutant, No. 4734 nucleotide, cytosine, on the plasmid pDN-G1PGlbh was converted to thymine. In the second mutant, the nucleotide No.3997, guanine, on the plasmid pDN-G1PGlbh was converted to adenine. This procedure was done with QuikChange II XL Site-Directed Mutagenesis Kit. Desired mutation was introduced on one pair of primers, which were used to amplify the entire plasmid pDN-G1PGlbh. Then the PCR product was digested with Dpn1 restriction enzyme, which recognized parental plasmid (PCR template) and digested it. Then the digested PDR product was transferred to XL10-Gold ultracompetent cells which connected the two ends of the PCR product and repaired the nick, new plasmid with desired site mutation was created.

Primers used for site directed mutagenesis:

PDR5-S558Y-f:

5’-CTATTTCCGTGGTTATGCTATGTTTTTTGCAATTCTATTCAATGC-3’

PDR5-S558Y-r: 5’-CATAGCATAACCACGGAAATAGAATGTAGAAGTATCACC-3’

PDR5-G312A-f:

5’-GTTTCCGGTGCTGAAAGGAAGCGTGTCTCCATTGCTGAAGTCTCC-3’

PDR5-G312A-r:

5’-CGCTTCCTTTCAGCACCGGAAACACCTCTGACGATGTCGTTACC-3’

2.1.5 Identification of optimal resuspension period for cell culture

In order to maintain stable cellular growth condition for the experiments, cells need to be kept growing in exponential phase. In order to optimize culturing time and cell density to maintain them growing in exponential phase, growth curve was measured. This measurement was to determine the starting cell density and the time for each strain to reach saturation in no drug and no inducer environment. Cells were streaked on plate with corresponding selection marker and 2% glucose, and were grown in 30 °C for 2 days. Single colony was inoculated in liquid medium with corresponding selection marker and 2 % glucose, and was grown in 30 °C over night. Start new cell culture with cell density at $5*10^5$ cells/ml liquid medium with corresponding selection marker and 2% galactose. Cell density was measured by Nexcelum cell counter every 2 hours until 24^{th} hour. Growth curve was plotted. Cells kept growing in exponential phase up to 16 hours, and then reached saturation. Based on the data, cell culture was resuspened every 12 hours to maintain their growth in exponential phase.

2.1.6 Measurement of growth rate

Cellular growth rate was measured for each strain. Cells were streaked on selection plate with 2% glucose, and were cultured in 30 °C for 2 days. Single colony was inoculated in liquid medium with corresponding selection marker and 2% glucose in 30 °C overnight. The next day, fresh cell culture with cell density at $5*10^5$ cells/ml was started in liquid medium with the same selection marker, but 2% galactose. Cell density was measured every 12 hours, and then cell cultures were resuspended in fresh medium with starting cell density $5*10^5$ cells/ml. Measurement of cell density was done during the entire dose-response experiment. In PFpump strain, the growth rate of the two subpopulations was measured as well after cell sorting.

2.1.7 Characterization of synthetic gene circuits behavior

All the cells used for dose response characterization were kept growing in exponential phase. Based on the results from growth curve measurement that cells with starting density $5*10^5$ cells/ml would reach saturation after 16 hours growth, each cell culture was started with the same cell density and re-suspended every 12 hours. At each re-suspension, cell number of each culture was counted by Nexcelom cellometer and then the cell density was calculated. In each re-suspension, new cell culture was started with density $5*10^5$ cells/ml again. In the cases that cells were treated with doxycycline or fluconazole, the degradation of both drugs in 30 degree for 12 hours were both considered when re-suspending cells into new cell culture. A re-suspension formula was developed to calculate the volume of cells from old cell culture, fresh medium, doxycycline or fluconazole at different concentration. In order to avoid system error of Nexcelom cellometer cell counter, cell density in culture was diluted to the range of $5*10^6$ cells/ml to $1.5*10^7$ cells/ml.

2.1.8 Flow cytometry

Flow cytometry was done every 24 hours for normal dose-response characterization. For strains with only GFP fluorescence, FACSCan (Becton Dikinson) was used, while FACSAria II (Becton Dikinson) was used for 2 color strains dose-response and Calcein-AM red dye experiment to test Pdr5 functionality. Flow cytometry data was used to monitor the expression of target gene in the cell population, once the target gene expression became stable, flow cytometry data was used to analyze dose-response behavior.

2.1.9 Pdr5 function test by Calcein-AM red

NRpump and NFpump strains were streaked on plate with corresponding selection marker and 2% glucose, and were grown in 30 °C for 2 days. Single colony was inoculated in liquid medium with corresponding selection marker and 2 % glucose, and was grown in 30 °C overnight. Inoculate 10 µl of overnight culture to new synthetic medium with the same selection marker and 2% galactose. Cells were induced with the same set of concentrations of doxycycline for 3 days. Cells were suspended in fresh medium and inducer every 12 hours. Flow cytometry was used to check expression of Pdr5 every 24 hours. When Pdr5 expression became stable, cells were collected and washed with pre-cold PBS twice. Then cells were suspended in synthetic medium with cell density at $5*10^5$ cells/ml. Then a set of Calcein-AM red was added in the cell culture (0 µg/ml, 1 µg/ml, 2µg/ml, 3µg/ml, 4µg/ml and 5µg/ml). Cells were cultured for 3 hours and the Calcein-AM red fluorescence intensity was measured every hour. YPH500 strain was used as negative control, RFpump strain was used as positive control.

2.1.10 Measurement of cellular memory in PFpump strain

In order to measure the cellular memory of each subpopulation in PFpump strain, PFpump cells were first induced with the doxycycline concentration that gave almost identical number of cells in of the two subpopulations. Cell culture was resuspend every 12 hours, and Pdr5 expression was monitored by flow cytometry. When the expression became stable, cells were sorted into two subpopulations based on a threshold of 500 a.u. The growth rate and distribution of Pdr5 expression in the two subpopulations and a non-sorted control was measured by counting cell number and flow cytometry every 2 hours in the first 12 hours, and then every 12 hours until both of the subpopulations reached the same Pdr5 expression as the non-sorted control did.

2.2 Data analysis

2.2.1 FACScan data analysis

FACScan data was read by matlab code, the value of three parameters, FSC, SSC and FL1 (green fluorescence intensity), was extracted. A 10*10 gate based on FSC and SSC was applied to the area with highest cell density in each sample in order to exclude extrinsic noise. Then fluorescence data was read and processed in the gated area. Frist, the arithmetic mean and standard deviation were calculated and any data that was outside 3 times standard deviation was considered outliners and therefore excluded from the dataset. Fluorescence intensity of YPH500 strain cultured in complete synthetic medium was used as background, and then its value was subtracted from the fluorescence intensity of each experimental sample. The mean of each sample was then normalized to the sample in its corresponding strain that was induced at the highest doxycycline concentration. Finally the mean and CV was calculated and plotted against doxycycline concentration that was used for the induction of each strain separately.

2.2.2 FACSAria II data analysis

FACSAria II data was read by matlab code as well. Four parameters, FSC, SSC, FL1 (green fluorescence intensity) and FL3 (red fluorescence intensity), were extracted. The following processing steps were the same as FACScan data processing, except that the mean and CV was calculated for both green and red fluorescence intensity, and them plotted vs doxycycline concentrations used for each 2 color strain.

2.2.3 Deterministic simulation of GFP expression

This simulation was based on previous published differential equations [29].

$$\frac{dx}{dt} = a - bxy - dx$$

$$\frac{dy}{dt} = C - bxy - fy$$

$$\frac{dz}{dt} = aF(x) - dz$$

Where x, y and z represent TetR, intracellular doxycycline and GFP, b is the binding coefficient between TetR and doxycycline, d and f represent degradation coefficient. F(x) is inhibitory hill function.

$$\mathrm{F(x)} = \frac{\Theta^{n}}{\Theta^{n} + \mathrm{x}^{n}}$$

Where Θ is the induction threshold and n is the hill coefficient. The parameters are a = 50 nMh^{-1}, b = 3.6 nM^{-1} h^{-1}, C = 0.6 [doxycycline] h^{-1}, f = 1.2 h^{-1}, Θ = 0.44, n = 4, F = 1.5.

Here, in order to simulate different fluorescence intensity, I used two GFP degradation rate d in the equation above. d = 0.12 h^{-1} was used in NR 1, d = 1.2 h^{-1} was used in NR 2

Chapter 3 Effect of protein pump on Negative Regulation (NR) and Negative Feedback (NF) gene circuits

3.1 Introduction

Protein pumps function to exclude intracellular toxins. This property fits the scenario in the production of clinical and industrial molecules, over production of which is usually toxic to the host organisms, and therefore they need to be excluded to keep the host cells growing at the fittest condition. Efforts have been made to select protein pumps in *E. coli* for the optimal production of biofuel molecules [123]. However, the work has not been done in eukaryotes to control and optimize the exclusion of toxic molecules with a protein pump under the control of different regulatory networks. My goal here was to study the interaction between the protein pump and the networks that regulate it. Recently this question was addressed computationally for a natural gene regulatory network involving positive feedback [20]. To answer this question experimentally for additional networks in eukaryotes, I modified two previously characterized, TetR-based synthetic gene circuits inducible by tetracycline analogs, called the negative regulation (NR), and negative feedback (NF) gene circuits. I first characterized the original versions of these gene circuits that control a passive target gene, which does not affect its upstream transcriptional regulators. Here, I replaced this passive target gene with the yeast pleiotropic drug resistance pump-fluorescent reporter fusion gene *PDR5::GFP*. Once *PDR5::GFP* is expressed, it pumps out the inducer, altering the activity of its upstream transcriptional regulators, creating a feedback loop. We show by experiment and mathematical modeling how this feedback loop alters the dose response of synthetic gene circuits. Moreover, we identify mechanisms underlying an additional, unexpected difference between the dose-response curves.

3.2 NR and NRpump gene circuit design and dose response in doxycycline

3.2.1 NR and NRpump gene circuits composition (regulatory network)

The NR gene circuit is composed of two parts: the reporter and the regulator. The reporter consists of the *yEGFP* and *ZeoR* fusion gene, yEGFP::ZeoR. This fusion gene is under the control of a modified *GAL1* promoter, which bears 2 TetR binding sites, TetO, and therefore becomes inducible by tetracycline family molecules, such as doxycycline. The regulator contains the TetR gene under the control of the natural Gal1 promoter, which is constitutively active in the presence of galactose. TetR is a bacterial repressor whose binding with TetO sites blocks the transcription. However, TetR will dissociate from TetO sites in the presence of doxycycline which is able to bind to TetR competitively, leading to transcription of the downstream gene, yEGPF::ZepR (Figure 3.1 A). The NRpump gene circuit has the same regulator as the NR gene circuit, which is the TetR gene under the control of the natural *GAL1* promoter. However, the yEGFP::ZeoR fusion gene on the reporter of NR gene circuit was replaced by *PDR5::GFP* fusion gene, while the promoter remained the same modified Gal1 promoter, which is inducible by doxycycline. Since Pdr5 is able to pump out intracellular doxycycline, it introduces another negative feedback loop into the NRpump gene circuit (Figure 3.1 B).

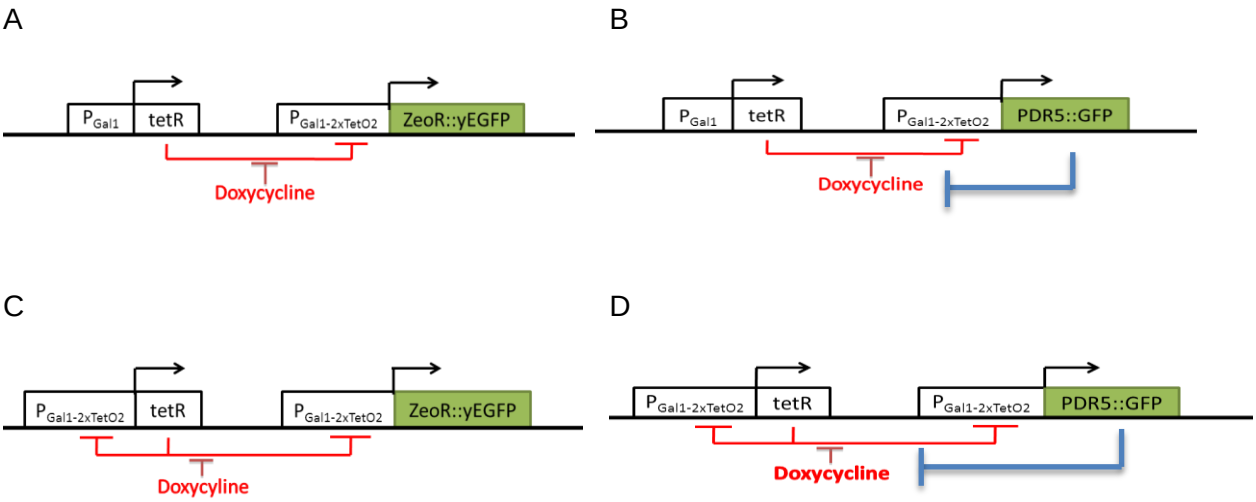

Figure 3.1 Regulation scheme for synthetic gene circuits

(A) Negative Regulation (NR) gene circuit. (B) Negative Regulation pump (NRpump) gene circuit. (C) Negative Feedback (NF) gene circuit. (D) Negative Feedback pump (NFpump) gene circuit.

3.2.2 NR dose-response

Although the dose-response of NR has been characterized before [29], it was induced by ATc, which is light sensitive and prone to degradation. Here I used doxycycline to induce the transcription of the yEGFP::ZeoR gene in the NR gene circuit to see how the yEGFP::ZeoR expression in this circuit responds to different doxycycline concentrations. This is called the dose-response. Here I used 10 concentrations of doxycycline to induce the expression of yEGFP::ZeoR gene in the NR gene circuit. Then the expression level of yEGPF::ZeoR in each individual cell was measured and quantified by flow cytometry. At zero and low doxycycline concentrations, the expression level of yEGFP::ZeoR was low in each individual cell in the whole population. With the increase of doxycycline concentration, a small portion of cells started to express a higher level of yEGFP::ZeoR, and the number of high expressing cells and their yEGFP::ZeoR expression level kept increasing with further increase of doxycycline concentration. When the doxycycline concentration reached intermediate level, some of the high expressing cells reached their maximum yEGFP::ZeoR expression level, while a portion of low expressing cells remained, and the other cells were in between. With further increase of doxycycline concentration, the majority of cells in the population shifted to higher yEGFP::ZeoR expression. Where doxycycline concentration was at high level (6 µg/ml), all cells in the population became high expressers reaching maximum expression level of yEGFP::ZeoR in each individual cell, and the expression remained the same at all the doxycycline concentrations above 6 µg/ml. In other words, the NR gene circuit's expression reached saturation (Figure 3.2).

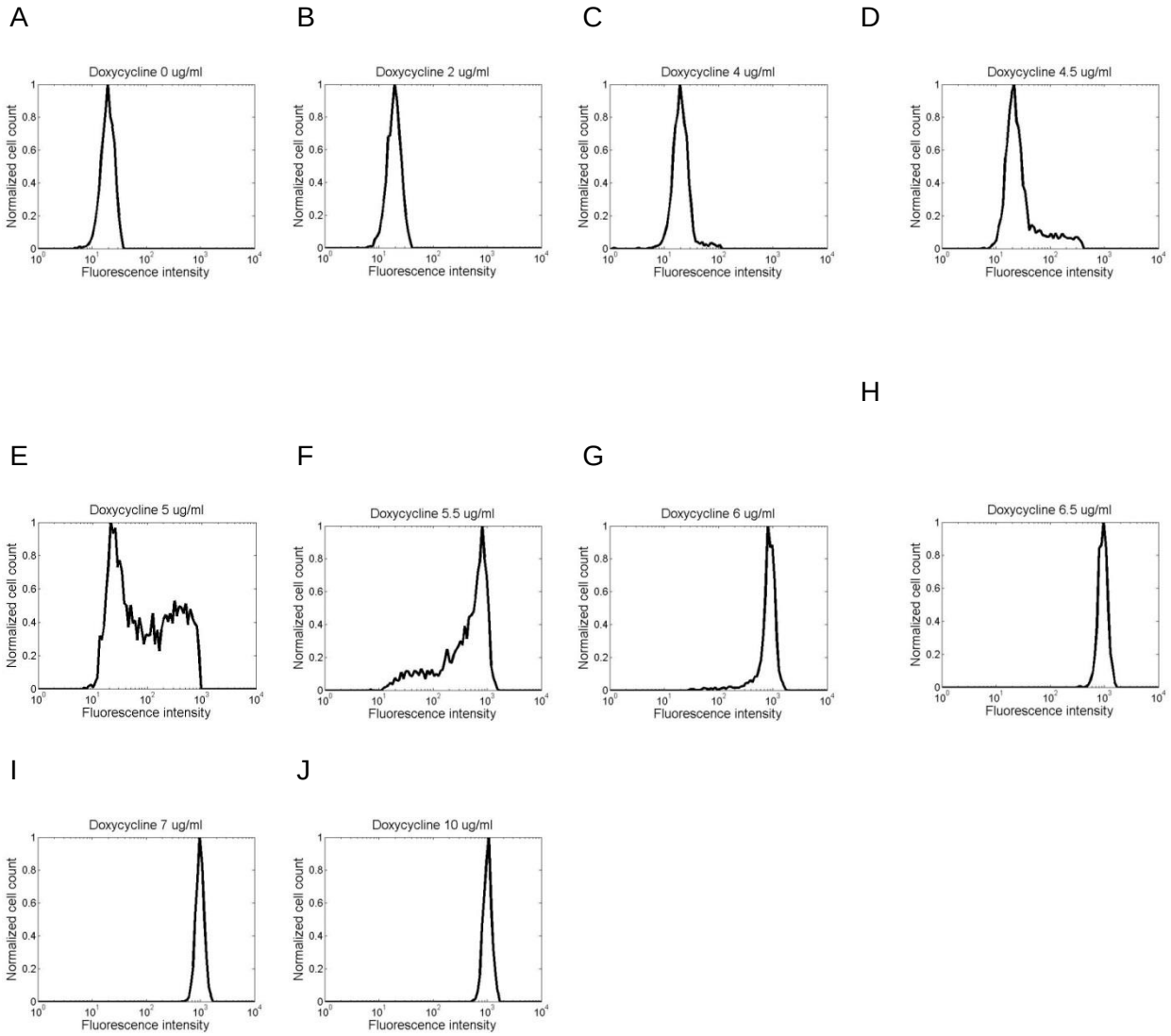

Figure 3.2 Histograms of NR dose-response.

NR gene circuit was induced at 10 doxycycline concentrations, 0, 2, 4, 4.5, 5, 5.5, 6, 6.5, 7 and 10 µg/ml; the histograms of yEGFP::ZeoR expression at each doxycycline concentration were shown. In each sample, cell culture was started with 0.5 x 10^6 cells/ml, and every 12 hours, cell density was measured by Nexolum, a small amount of cell culture based on calculated was inoculated into fresh medium to start new culture with the cell density, 0.5 x 10^6 cells/ml.

The mean of each histogram was calculated and plotted versus the corresponding doxycycline concentrations. By looking at the mean dose-response plot, we are able to understand the change of the mean expression over the entire dose response course. At zero and low doxycycline concentration, the means were very low. The only yEGFP::ZeoR expression was from gene circuit leakage. However, the population mean showed a steep increase at intermediate doxycycline concentration, and reached saturation immediately after further increase of doxycycline concentration (Figure 3.3 A). The NR gene circuit was sensitive to doxycycline at a narrow concentration range. The noise of the population was measured by the coefficient of variation (CV). CV is defined as the standard deviation divided by the mean, and is used to describe the deviation of a population from its mean. Here the CV was calculated for each histogram in Figure 3.2 as well. At zero and low doxycycline concentrations, the CV was low because all the cells expressed the same level of yEGFP::ZeoR. The CV began to increase with the increase of doxycycline concentration, and reached its peak at intermediate doxycycline concentration, which corresponded to the most diverse yEGFP::ZeoR expression level in the population shown in the histogram (Figure 3.2 E). With further increase of doxycycline concentration, the CV bounced back to a low level as indicated by uniformly high expression of yEGFP::ZeoR in the whole cell population (Figure 3.3 B).

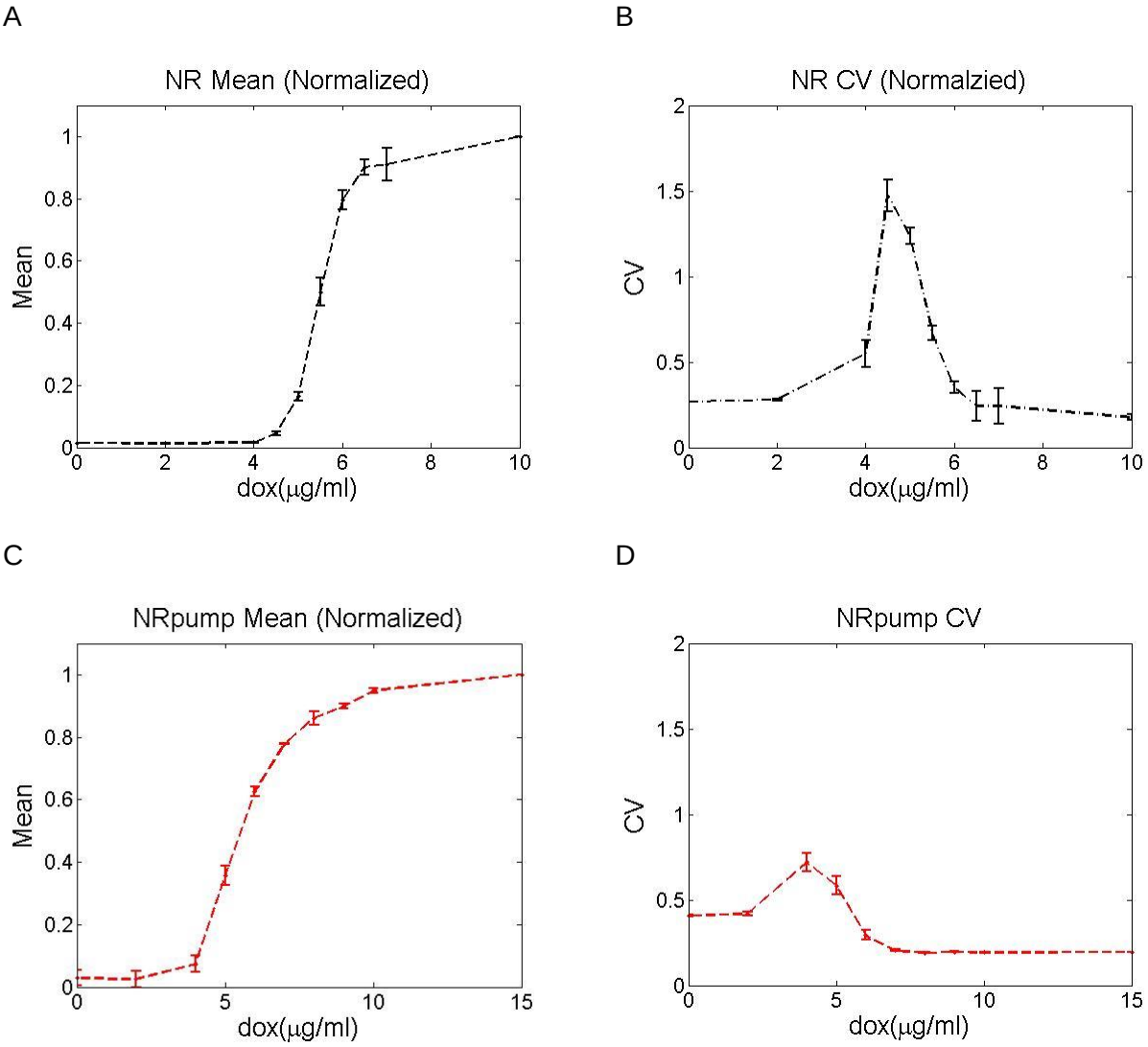

Figure 3.3 The Mean and CV of NR dose-response.

Doxycycline at 10 different concentration was used to induce yEGPF::ZeoR expression in the NR gene circuit: 0, 2, 4, 4.5, 5, 6, 6.5, 7, 10 μg/ml. Doxycycline at 10 different concentrations was used to induce *PDR5::GFP* expression in the NRpump gene circuit: 0, 2, 4, 5, 6, 7, 8, 9, 10, and 15 μg/ml. (A) NR Mean dose-response; (B) NR Coefficient of Variation (CV) dose-response. (C) NRpump Mean dose-response; (D) NRpump Coefficient of Variation (CV) dose-response. Data shown here was an average of 3 replicates. Error bar refers to the SD of the 3 replicates' mean value.

3.2.3 NRpump dose response mean and CV

After obtaining the dose response for the NR gene circuit, I wanted to know if the pump would change the behavior of the NR gene circuit, and if so, how would it change it. In order to have a fair comparison, I followed exactly the same experimental procedures as I did for the NR gene circuit to characterize the dose-response for the NRpump gene circuit. Initially, the same set of the doxycycline concentrations were used to induce the NRpump gene circuit. However, NRpump required higher doxycycline concentration to reach saturation compared to NR. Therefore, I increased doxycycline concentrations to induce NRpump, and 10 of them were selected to represent the dose response behavior. The selected doxycycline concentrations were slightly different from the concentrations used to induce NR gene circuit; because Pdr5 changed the dose-response curve and higher doxycycline concentration was required to achieve saturation. At no and low doxycycline concentrations, the expression level of *PDR5::GFP* in each individual cell was at the basal level, and the expression was uniform across the whole cell population. At intermediate doxycycline concentrations, a number of cells began to express higher *PDR5::GFP*, while most of the cells in the population remained low expression level. With increase of doxycycline concentration, a higher percentage of cells in the population expressed high level of *PDR5::GFP*. When doxycycline concentration was further increased, the majority of cells in the population became high *PDR5::GFP* expressers. At high doxycycline concentrations, all the cells in the population expressed a high level of *PDR5::GFP*, and the histograms would not change with any further increase of doxycycline concentration after 10 µg/ml.

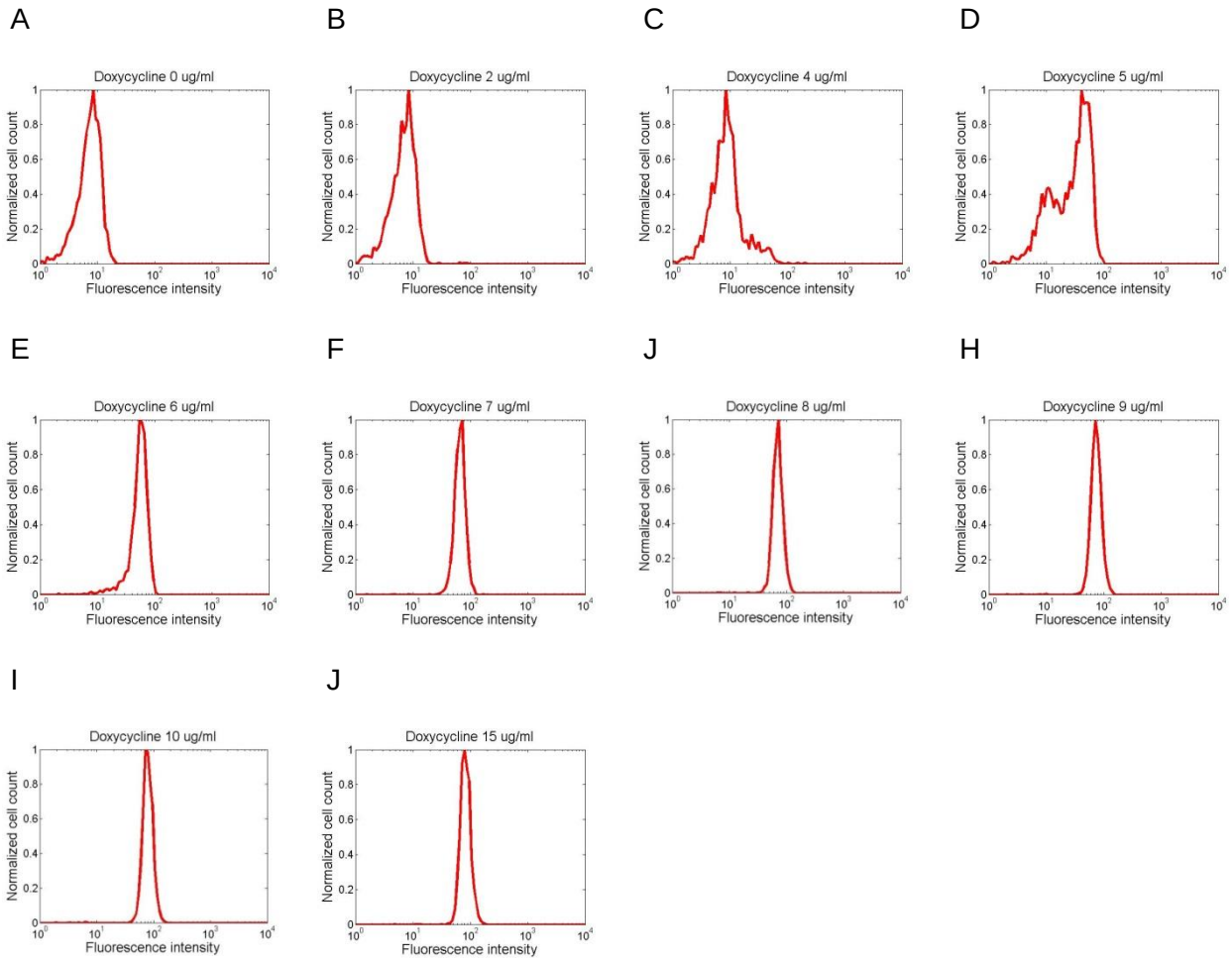

Figure 3.4 Histograms of NRpump dose-response.

Cells carrying NRpump gene circuit were induced at 10 doxycycline concentrations, 0, 2, 4, 5, 6, 7, 8, 9, 10 and 15 µg/ml; the histograms of *PDR5::GFP* expression at each doxycycline concentration were shown. In each sample, cell culture was started with 0.5 x 10^6 cells/ml, and every 12 hours, cell density was measured by Nexolum, a small amount of cell culture based on the calculation was inoculated into fresh medium to start new culture with the cell density, 0.5 x 10^6 cells/ml.

The mean for the NRpump histograms at each doxycycline concentration was calculated as for the NR gene circuit. At no and low doxycycline concentrations, the mean was low, then it started to increase at doxycycline 4 µg/ml and showed a significant increase from 5 µg/ml to 9 µg/ml, and then reached saturation at doxycycline concentration 10 µg/ml (Figure 3.3 C). The CV was calculated and plotted versus the doxycycline concentration as well. It was low at zero and low doxycycline concentrations, and showed a peak at intermediate doxycycline concentration, 4 µg/ml, which corresponded well to the diverse *PDR5::GFP* expression in the cell population at that particular doxycycline concentration, shown on the histogram (Figure 3.4). The CV decreased after further increase of doxycycline concentrations and became flat after 6 µg/ml doxycycline (Figure 3.3 D), which indicated homogenous *PDR5::GFP* expression.

3.2.4 Dose response comparison between NR and NRpump strains

Since the mean and CV for NR and NRpump gene circuits were all calculated and plotted, I could compare them side by side after normalization. At zero and low doxycycline concentrations, both NR and NRpump showed low fluorescence intensity mean (low target gene expression). However, at doxycycline concentration 4 µg/ml, NRpump started to respond while NR still remained at low expression (Figure 3.5 A). With increasing doxycycline concentration, the dose response mean of NR showed a steep increase and reached saturation right after it. However, compared to NR, the NRpump dose response mean showed a relatively slower increase, and reached saturation at higher doxycycline concentration. In other words, NRpump was more sensitive to doxycycline induction than NR at low doxycycline concentrations, but became less sensitive at high doxycycline concentrations. Besides, NRpump has a wider dose response range for doxycycline induction, between 4 µg/ml and 10 µg/ml, which was 4.5 µg/ml to 7 µg/ml for NR (Figure 3.5 A). Gene expression noise, measured by the CV, peaked at a slightly lower intermediate doxycycline concentration and reached a lower maximum for

NRpump than for NR (Figure 3.5 B). The lower CV peak for NRpump could be due to weaker GFP fluorescence intensity of the *PDR5::GFP* fused protein than of yEGFP in NR, which caused less broad distributions when the basal expression does not change. Another reason for the lower CV could be pump-mediated negative feedback (negative feedback, known to reduce noise). The broad histograms at intermediate doxycycline concentrations indicated heterogeneous reporter expression in individual cells and were consistent with the CV peaks (Figures 3.5 C and D). Therefore, the efflux pump, Pdr5, managed to change the dose response behavior of the NR gene circuit.

3.2.5 ODE models demonstrating effect of GFP fluorescence intensity

Since NR and NRpump used different GFP connected to the target protein, the two versions of GFP differed in their green fluorescence intensity. In order to compare the dose-response of NR and NRpump, I normalized fluorescence intensity at each doxycycline concentration to the fluorescence intensity at highest doxycycline concentration used in the experiment for each strain. Here I want to demonstrate that the different fluorescence intensity does not affect the dose-response curve after normalization. In order to do that, I first used previously established mathematical models to simulate two NR dose-responses, NR1 and NR2, then used different degradation rate for GFP in the two NR dose-responses, which resulted in different GFP fluorescence intensity. As a result, NR1 and NR2 have different GFP fluorescence intensity (Figure 3.6 A). However, they show exactly the same dose-response after normalization (Figure 3.6 B).

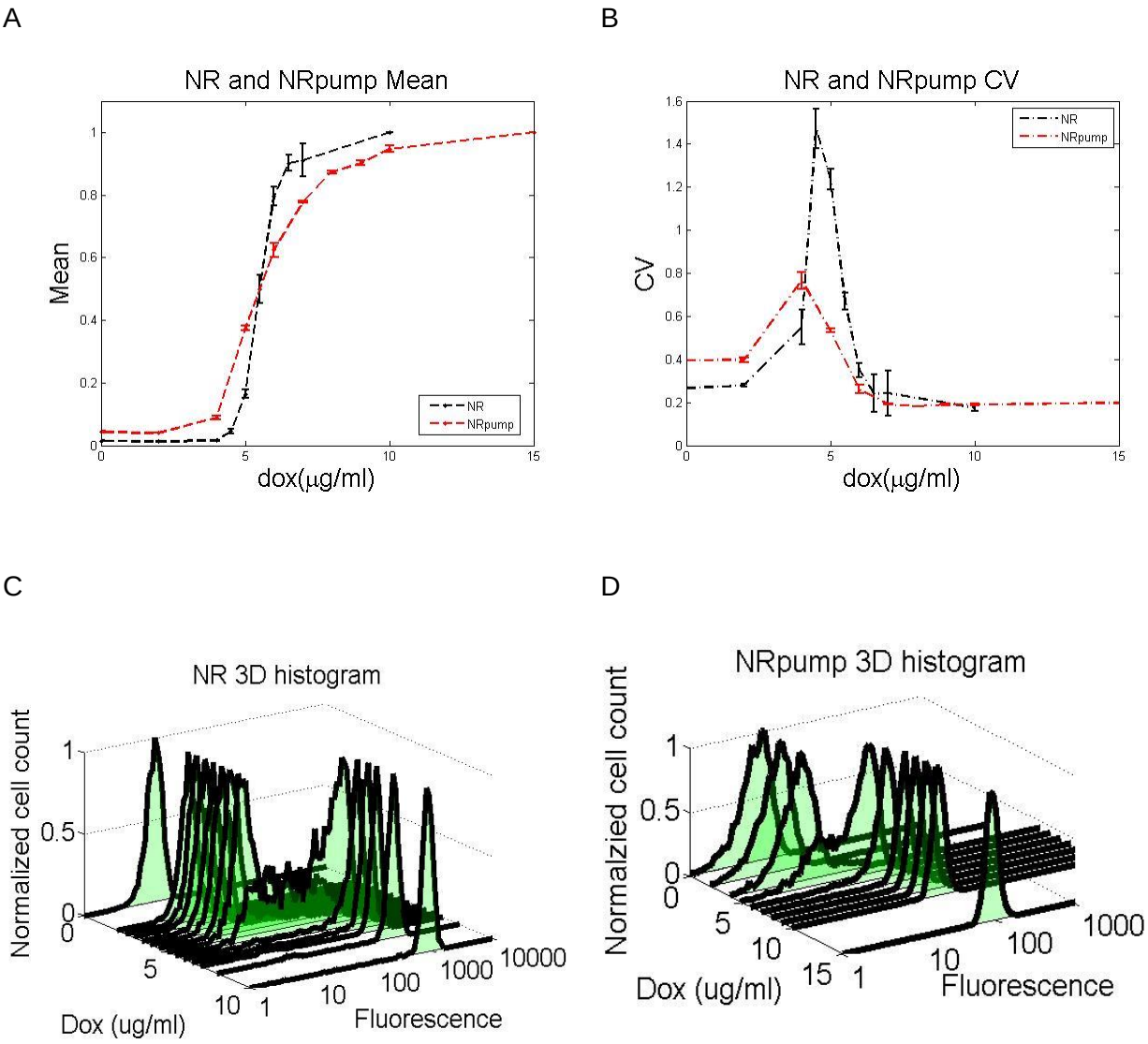

Figure 3.5 NR and NRpump mean and CV dose-response and histograms.

Doxycycline at 10 different concentrations were used to induce yEGFP::ZeoR expression in NR gene circuit: 0, 2, 4, 5, 6, 7, 8, 9, 10 and 15 μg/ml. (A) NR and NRpump Mean dose-response; (B) NR and NRpump Coefficient of Variation (CV) dose-response. (C) Histogram of NR Mean dose-response. (D) Histogram of NRpump Mean dose-response. Data shown here was average of 3 replicates. Error bar refers to the SD of the 3 replicates' mean value.

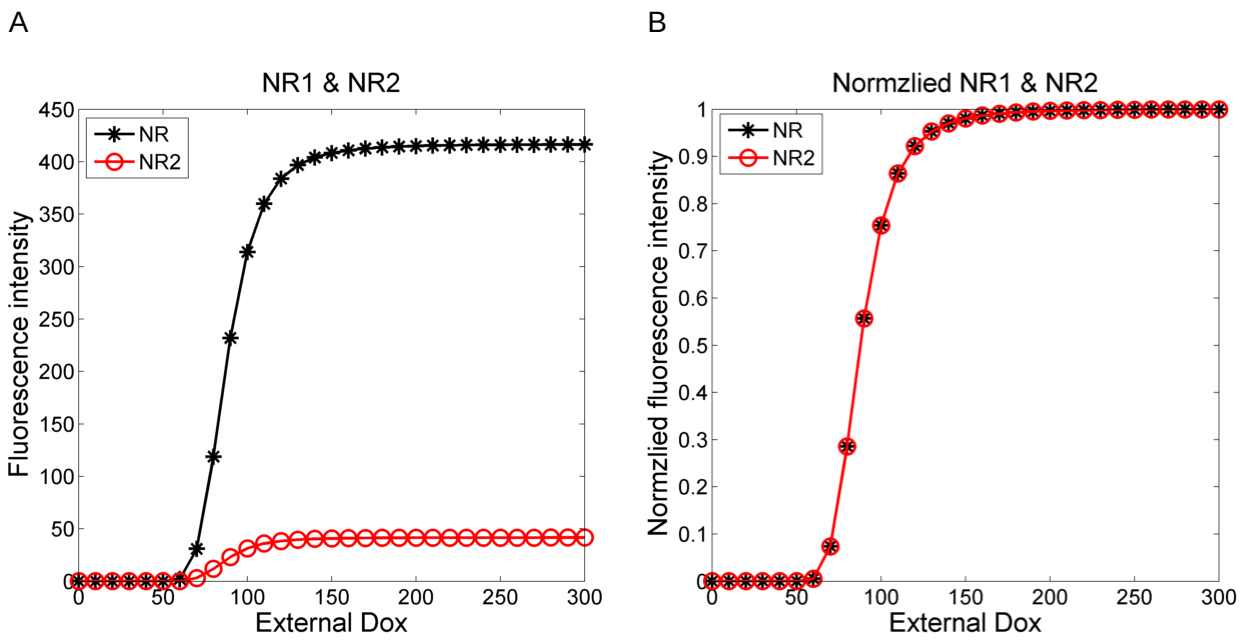

Figure 3.6 NR dose-response simulations.

(A) NR1 and NR2 Mean dose-response; (B) Normalized NR1 and NR2 Mean dose-response.

3.3 NF and NFpump gene circuits' design and dose-response in doxycycline

3.3.1 NF and NFpump gene circuit composition

Same as the NR gene circuit, the NF gene circuit is composed of two parts as well, the regulator and the reporter. It shares the same reporter with the NR gene circuit. However, the difference between NR and NF gene circuits is that the natural *GAL1* promoter driving TetR expression in the NR gene circuit was replaced by the modified *GAL1* promoter bearing TetO sites in the NF gene circuit (Figure 3.1 A and C). Therefore, both yEGFP::ZeoR and TetR genes were under the control of the same doxycycline inducible promoter. In this case, TetR is able to repress the transcription of both yEGFP::ZeoR and itself. When doxycycline appears, it binds to TetR and releases it from the TetO sites, therefore, leading to the transcription of the yEGFP::ZeoR gene in the NFpump gene circuit. The NFpump gene circuit was also composed of the regulator and the reporter. The regulator shares the same components as the NF gene circuit, namely TetR gene under the control of modified *GAL1* promoter, (*GAL1* promoter with 2 TetO sites). The *GAL1* promoter is able to transcribe the downstream gene in the presence of galactose. However, when TetR is present, it binds to the TetO sites and repress the transcription. In the report of NFpump gene circuit, *PDR5::GFP* fusion gene was used to replace the yEGFP::ZeoR fusion gene in NF gene circuit, while the promoter remained the same, modified Gal1 promoter (Figure 3.1 C and D). When doxycycline appears, it binds to TetR and releases its binding with TetO sites on the modified *GAL1* promoter, which initiated the transcription of downstream *PDR5::GFP* gene.

3.3.2 NF gene circuit dose-response

The NF gene circuit was induced with 10 doxycycline concentrations. At all doxycycline concentrations, the expression level of yEGFP::ZeoR in individual cells was uniform, meaning that there was only one peak in the fluorescence intensity histogram. At zero doxycycline concentration, yEGFP::ZeoR expression was at the basal level in the whole cell population. With gradual increase of doxycycline concentration, the expression level of yEGFP::ZeoR in each individual cell shifted to higher fluorescence intensity gradually until it reached saturation at doxycycline 4 µg/ml (Figure 3.7). After the saturation point, further increase of doxycycline concentration did not change the expression level of yEGFP::ZeoR in the cells anymore.

Then fluorescence intensity mean and CV for the histograms at each doxycycline concentration were calculated and plotted. The mean dose-response of NF was different from that of NR. Between doxycycline concentration 0 µg/ml and 4 µg/ml, the mean showed a linear dose response, and it reached saturation at 5 µg/ml (Figure 3.8 A). The data shown here was from 3 independent replicates, all the 3 replicates showed linear dose response range between 0 µg/ml and 4 µg/ml, but with slight difference in the slope of the curves, which contributed to the error bar (Figure 3.8 A). The CV dose-response was very low at all the doxycycline concentration, which corresponded well to the uniformly distributed histograms regarding yEGFP::ZeoR expression (Figure 3.8 B).

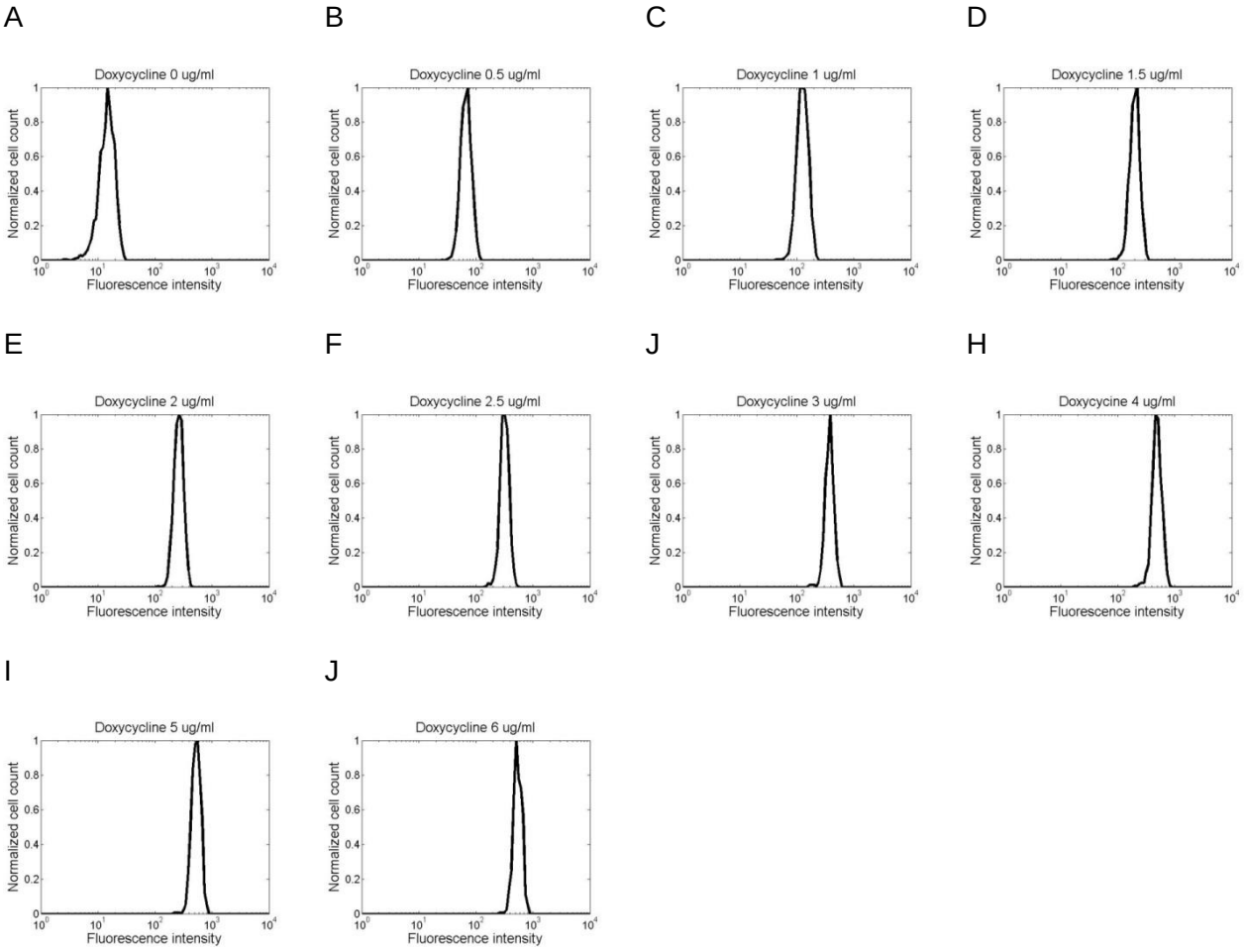

Figure 3.7 Histograms of NF dose-response.

Cells carrying NFpump gene circuit were induced at 10 doxycycline concentrations, 0, 0.5, 1, 1.5, 2, 2.5, 3, 4, 5 and 6 µg/ml; the histograms of *PDR5::GFP* expression at each doxycycline concentration were shown. In each sample, cell culture was started with 0.5 x 10^6 cells/ml, and every 12 hours, cell density was measured by Nexolum, a small amount of cell culture based on the calculation was inoculated into fresh medium to start new culture with the cell density, 0.5 x 10^6 cells/ml.

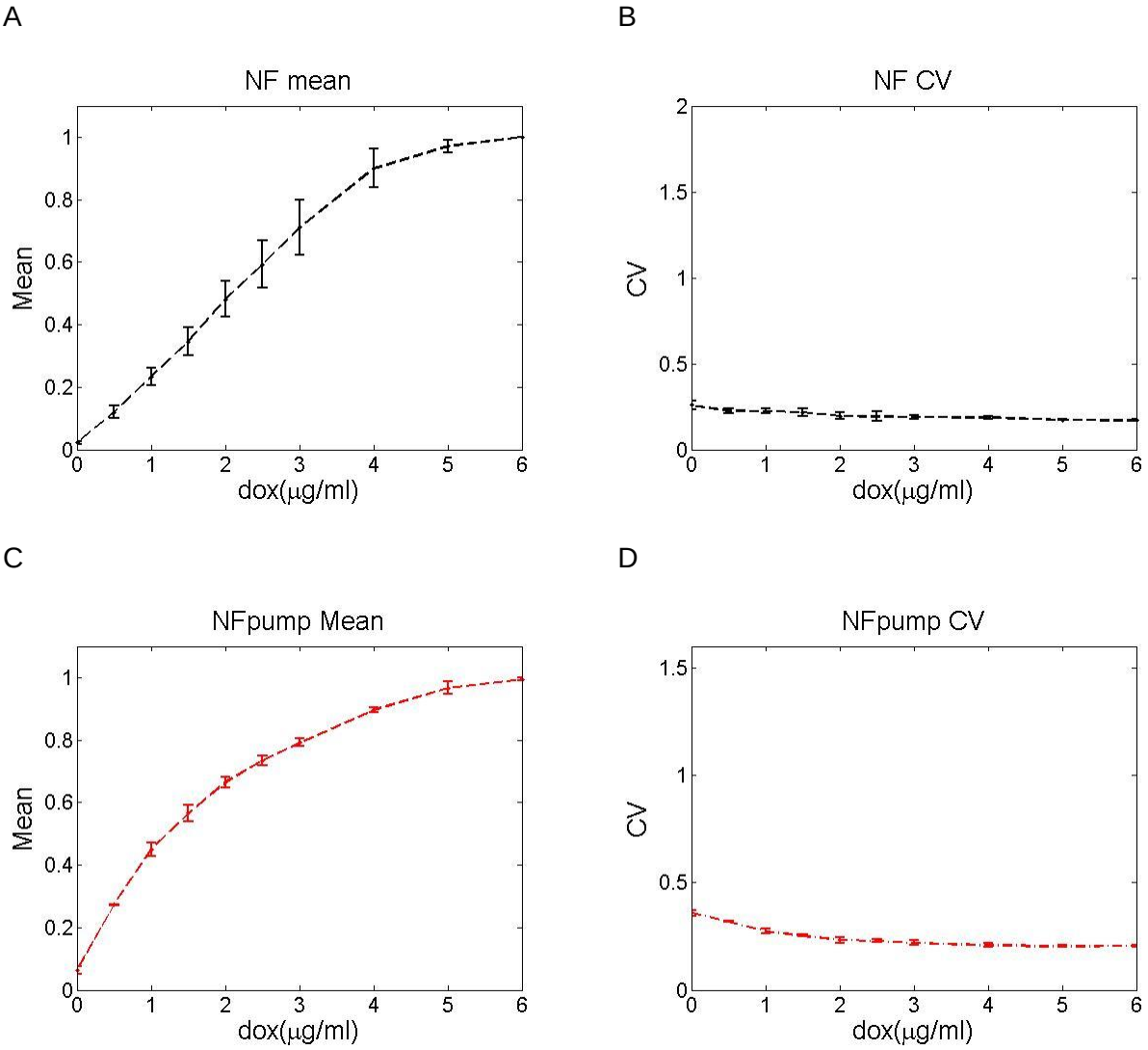

Figure 3.8 NF and NFpump mean and CV dose-responses.

Doxycycline at 10 different concentration were used to induce *yEGFP::ZeoR* or *PDR5::GFP* expression in NF and NFpump gene circuits: 0, 0.5, 1, 1.5, 2, 2.5, 3, 4, 5 and 6 μg/ml. (A) NF Mean dose-response; (B) NF Coefficient of Variation (CV) dose-response. (C) NFpump Mean dose-response; (D) NFpump Coefficient of Variation (CV) dose-response. Data shown here was average of 3 replicates. Error bar refers to the SD of the 3 replicates' mean value.

3.3.3 NFpump dose-response

After obtaining the dose response curve of the NF gene circuit, I asked if Pdr5 would be able to alter it as for NR. I followed the same experimental procedure to characterize the dose response behavior for the NFpump gene circuit. Similar to the NF gene circuit, the histograms at each of the doxycycline concentrations showed only one peak, meaning that all the cells expressed the same level of *PDR5::GFP* at every doxycycline concentration. Besides, the histogram shifted to higher expression level of *PDR5::GFP* gradually with gradual increase of doxycycline concentration, until it reached saturation at doxycycline concentration 4 µg/ml (Figure 3.9).

The fluorescence intensity mean for NFpump histograms at each doxycycline concentration was calculated. The mean increased gradually with the increasing of doxycycline concentration, and reached saturation at doxycycline concentration 4 µg/ml. The gene expression noise, CV, was calculated and plotted against the doxycycline concentration as well. It remained low at all the doxycycline concentrations, which indicated the uniform expression level of *PDR5::GFP* in the cell populations, and corresponded well to the histograms (Figure 3. C). The CV remained low during the entire range of doxycycline concentrations (the slightly higher CV at no and low doxycycline might due to the system error in FACScan flow cytometer) (Figure 3.8 D).

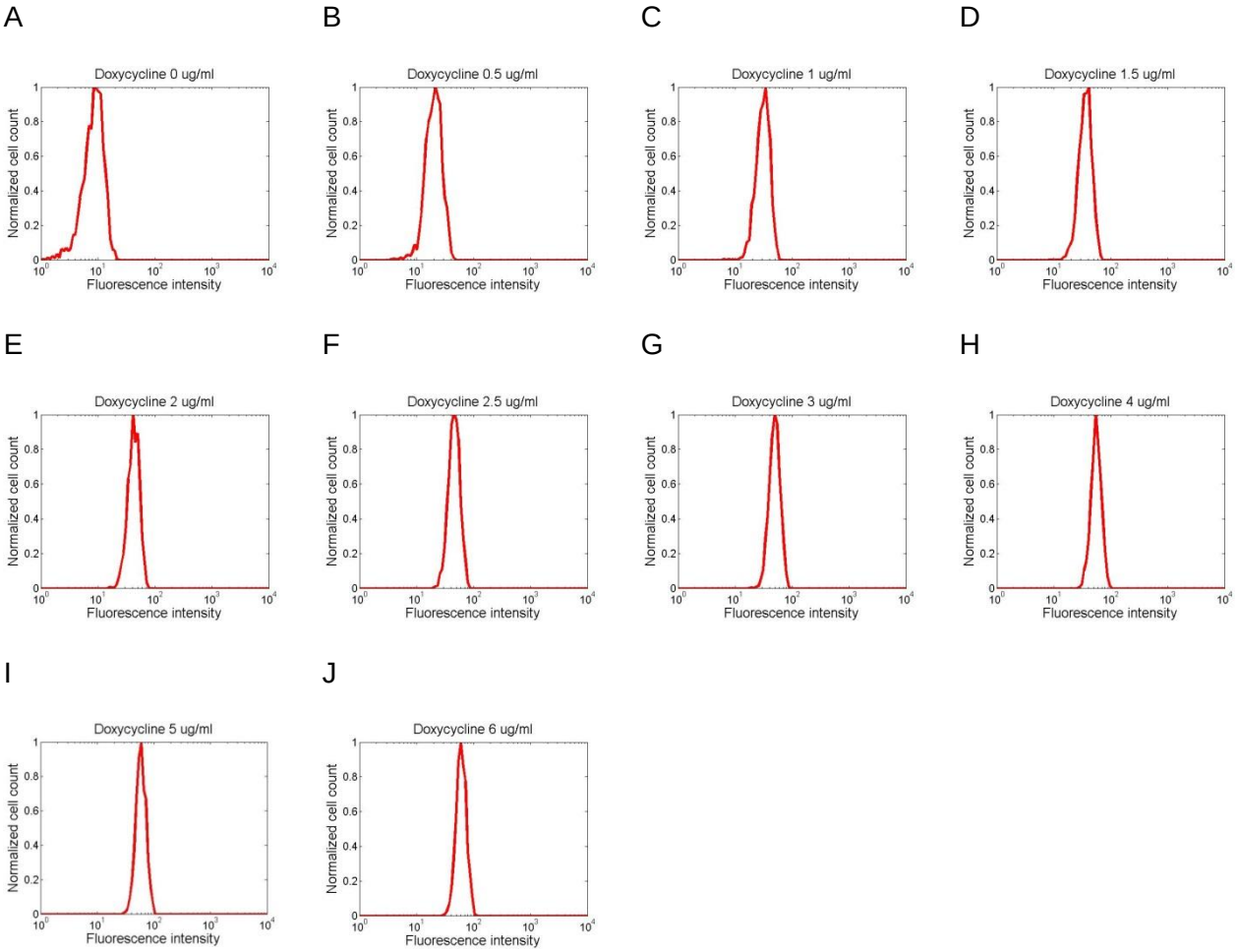

Figure 3.9 Histogram of NFpump dose-response.

Cells carrying NFpump gene circuit were induced at 10 doxycycline concentrations, 0, 0.5, 1, 1.5, 2, 2.5, 3, 4, 5 and 6 µg/ml; the histograms of *PDR5::GFP* expression at each doxycycline concentration were shown. In each sample, cell culture was started with 0.5 x 10^6 cells/ml, and every 12 hours, cell density was measured by Nexolum, a small amount of cell culture based on the calculation was inoculated into fresh medium to start new culture with the cell density, 0.5 x 10^6 cells/ml.

3.3.4 Dose-response comparison between NF and NFpump strains

In the prior section, it was shown that Pdr5 was able to change the dose-response behavior of the NR gene circuit; I was curious how it could alter the dose-response for the NF gene circuit. Since the mean and CV for NF and NFpump gene circuits were all calculated and plotted, I could compare them side by side. One obvious difference in the mean dose-response mean was that the NF gene circuit showed a linear dose response range between doxycycline concentration 0 µg/ml and 4 µg/ml, but the linear range disappeared in the dose response of the NFpump gene circuit. The dose response mean of the NFpump gene circuit had a concave curve. It had higher slope at low doxycycline concentrations compared to the NF gene circuit, which might indicate higher sensitivity to doxycycline or higher intracellular doxycycline concentration in the cells bearing NFpump gene circuit. Both the NF and NFpump gene circuits reached saturation at the same concentration of doxycycline (Figure 3.10 A). Gene expression noise, measured by the CV, was low at all the doxycycline concentrations for both NF and NFpump gene circuits (Figure 3.10 B). The slightly higher CV for NFpump gene circuit might be due to weaker GFP fluorescence of the Pdr5::Gfp protein fusion than of yEGFP in NF, causing less broad distributions when the basal expression does not change. Another reason for the lower CV could be pump-mediated negative feedback (negative feedback, known to reduce noise). The broad histograms at intermediate doxycycline concentrations indicated heterogeneous reporter expression in individual cells and are consistent with the CV peaks (Figures 3.10 C and D). In conclusion, the efflux pump, Pdr5, changed the dose response behavior for NF gene circuit as well.

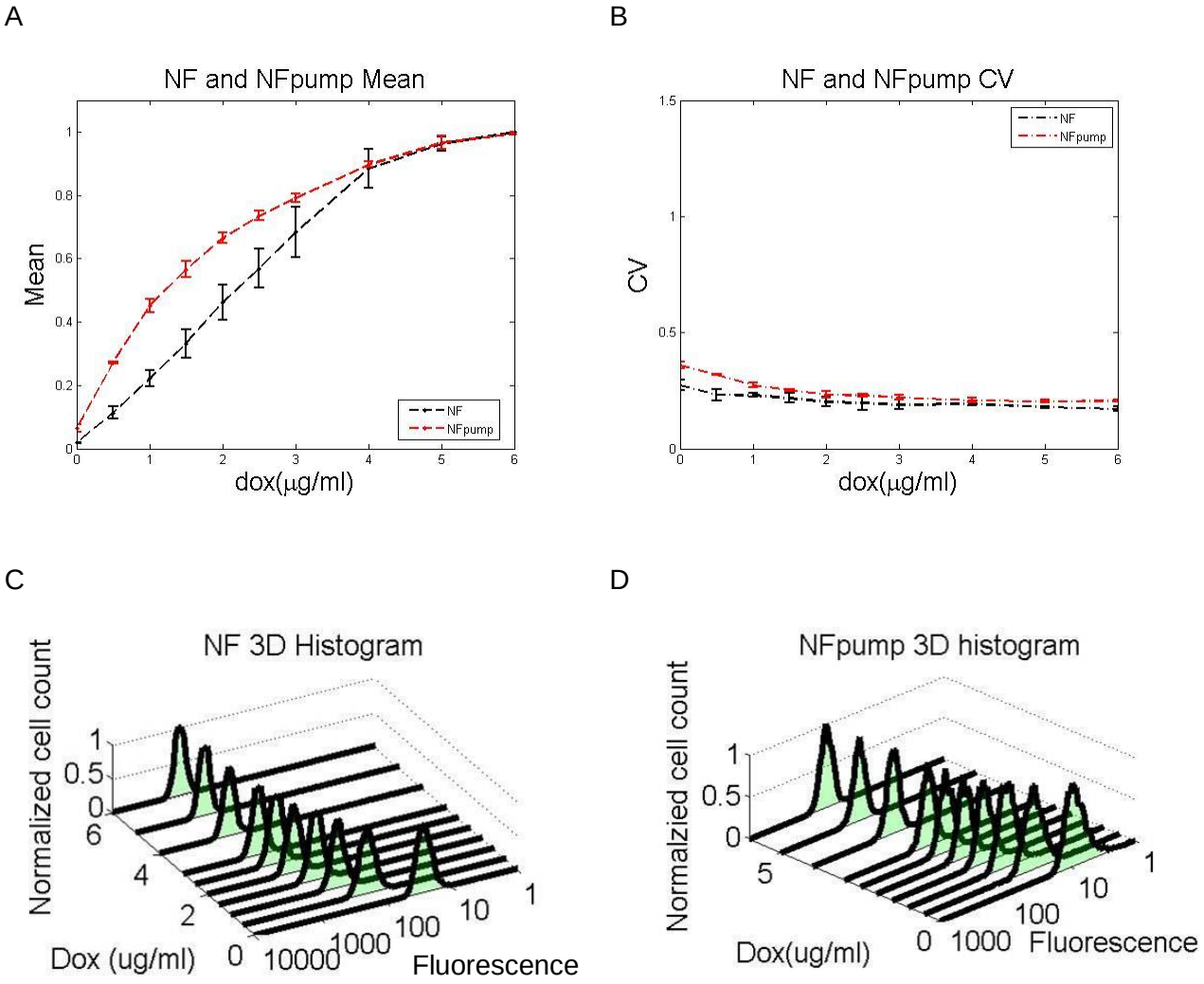

Figure 3.10 NF and NFpump mean and CV dose-responses and histograms.

(A) NF and NFpump Mean dose-responses. (B) NF and NFpump CV dose-responses. (C) NF histograms in increasing concentration of doxycycline. (D) NFpump histograms in increasing concentrations of doxycycline. Error bar refers to the SD of the 3 replicates' mean value.

3.4 NRpump mutant gene circuits and characterization of their dose-response

From the comparison between the original NR and NF gene circuits and their pump counterparts, the NRpump and NFpump gene circuits, we saw that Pdr5 changed the dose-response behavior. In order to find out if the change was because of the efflux pumping activity of Pdr5, I decided to create Pdr5 mutant with no efflux pumping function. I found two published mutations on Pdr5 that disrupt its efflux pumping activity, S558Y and G312A. It was reported that S558Y locates on the transmembrane helix 2 (TMH2) of *PDR5* gene, Pdr5 with this mutant has normal ATPase activity and drug binding capability, but has impaired coupling between ATP hydrolysis and the conformational changes in the transmembrane domains (TMDs) [143]. Therefore, it blocked the efflux pumping activity of Pdr5. Another study identified the G312A mutation in the signature region of the canonical ATP-binding site disrupted ATPase activity and therefore drug transport [144]. Strains with S558Y or G312A mutants showed hypersensitivity to drug treatment compared to the strain bearing wild type Pdr5, as the same as the strain with Pdr5 null mutant [143, 144]. Therefore, I replaced the functional *PDR5::GFP* fusion gene in the NRpump and NFpump gene circuits with the mutated *PDR5* gene fused with the GFP gene, creating the NRpump mutant and NFpump mutant gene circuits. In order to ensure that the *PDR5* mutant::GFP fusion gene has abolished efflux pumping activity, two versions of mutants were built for NRpump-mutant, NRpump-S558Y and NRpump-G312A. The same was done for NFpump-mutant.

3.4.1 NRpump-mutant gene circuit composition

Because the two mutations were both confirmed to compromise efflux pumping activity of Pdr5, two versions of mutant gene circuits were built with each one bearing one single mutation. The NRpump-mutant gene circuits share the same regulator with the NRpump gene

circuit. The only difference is in the reporter, the *PDR5::GFP* fusion gene in NRpump gene circuit was replaced by *PDR5* mutant::GFP fused gene, *PDR5*-S558Y::GFP or *PDR5*-G312A::GFP. In the presence of galactose, TetR was expressed from the Gal1 promoter, and it could bind to the TetO2 sites on the modified *GAL1* promoter on the reporter (Figure 3.11 A and B). When doxycycline was present, it associated with TetR and therefore, released its binding to the TetO sites As a result, the downstream *PDR5*-mutation::GFP gene was able to be transcribed. However, since Pdr5 mutants were not able to pump out doxycycline, the two NRpump-mutant gene circuits lose the additional negative feedback that wild type Pdr5 generated.

3.4.2 NRpump mutant gene circuits dose-response

It has been discovered that Pdr5 pumps out tetracycline family molecules including doxycycline, therefore, I asked if the efflux pumping function of Pdr5 protein was the cause of the dose-response behavior change in NRpump. In order to test that, I characterized the dose-response for NRpump-mutant gene circuits and expected the dose-response behavior would maintain that of the NR gene circuit.

First, both NRpump-312 and NRpump-558 strains were induced with the same series of doxycycline concentration as it was used for NRpump. The level of *PDR5*-G312A::GFP expression was measured by Flow Cytometry at each doxycycline concentration. At no and low doxycycline concentration, *PDR5*-G312A::GFP expression was low in the whole cell population. At intermediate doxycycline concentration, some cells in the population showed increased level of *PDR5*-G312A::GFP expression, while the majority of cells still remained at low expression level. With further increase of doxycycline concentration, more cells shifted to high *PDR5*-G312A::GFP expression with only a very small percentage of cells staying at low *PDR5*-G312A::GFP expression. At high doxycycline concentration, all the cells in the population had

high *PDR5*-G312A::GFP expression expressers, and fluorescence intensity stayed the same with further increase of doxycycline concentration, meaning that the level of *PDR5*-G312A::GFP expression reached maximum in each individual cell (Figure 3.12).

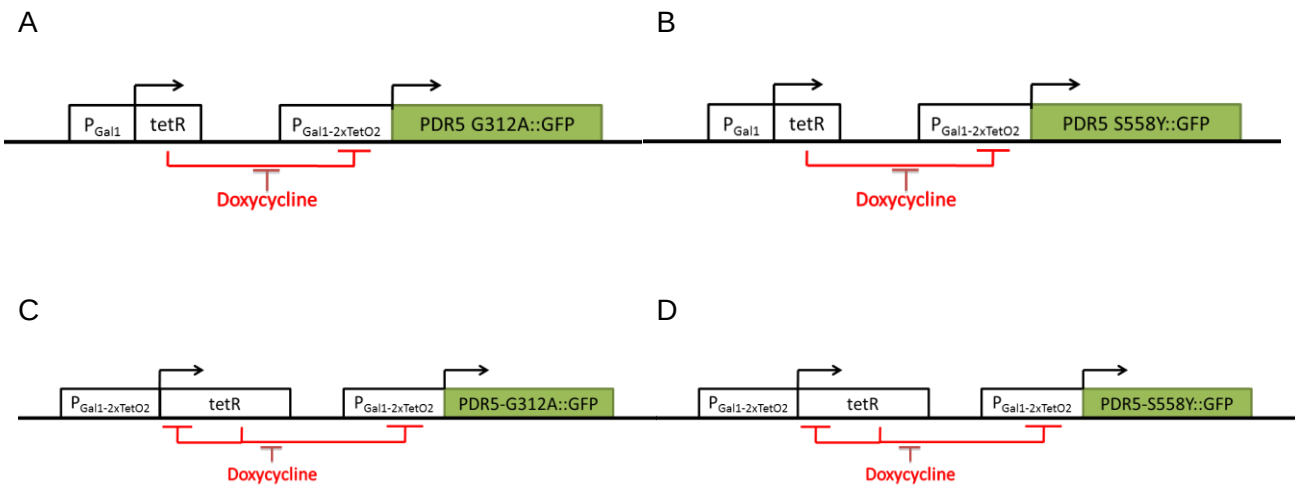

Figure 3.11. Regulation scheme for Negative Regulation pump mutant (NRpump-mutant) and Negative Feedback pump mutant (NFpump-mutant) gene circuits.

(A) NRpump-312. (B) NRpump-558. (c) NFpump-312. (D) NFpump-558.

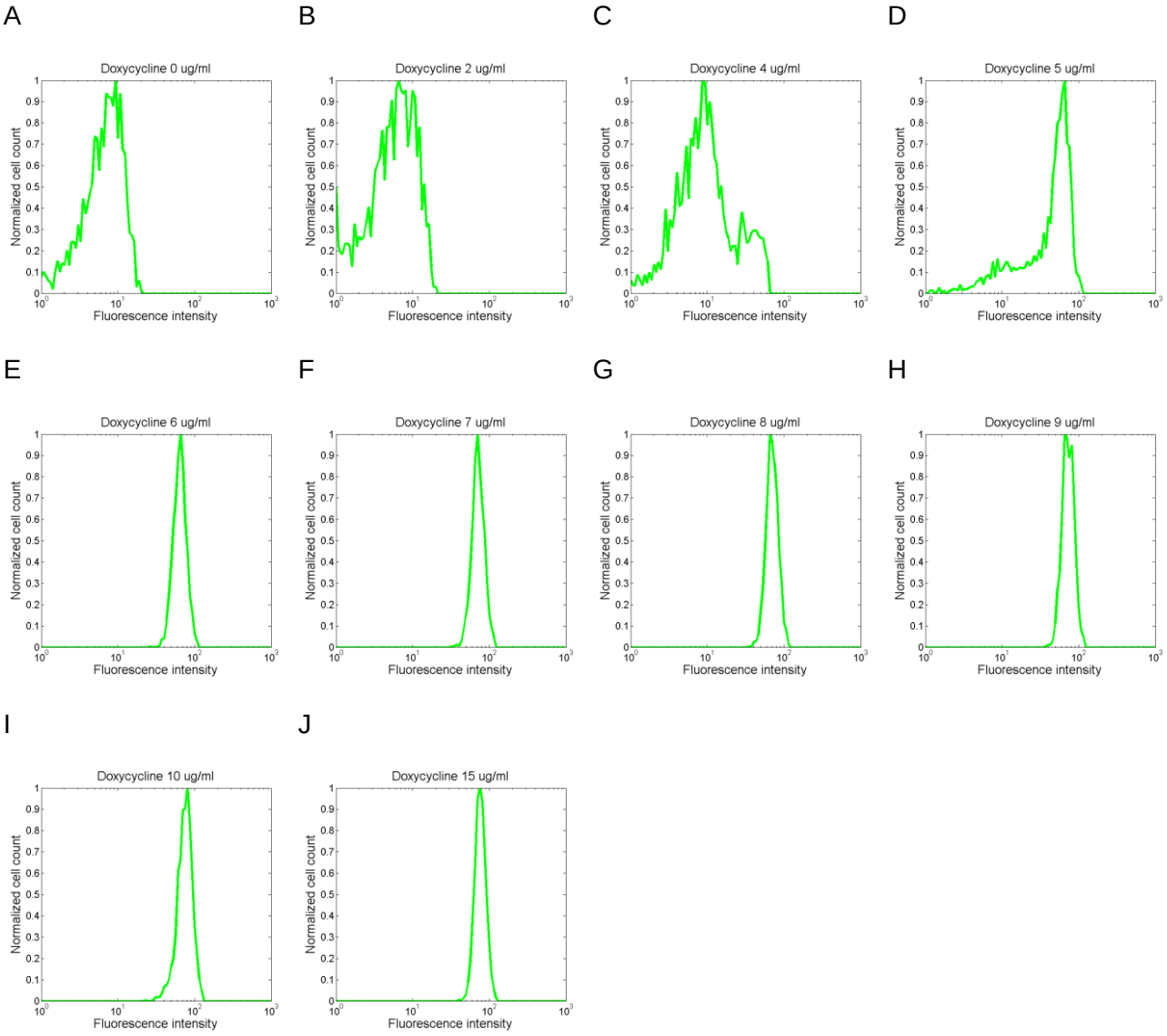

Figure 3.12 Histograms of NRpump-312 dose-response.

Cells carrying NRpump-312 gene circuit were induced at 10 doxycycline concentrations, 0, 2, 4, 5, 6, 7, 8, 9, 10 and 15 µg/ml; the histograms of *PDR5::GFP* expression at each doxycycline concentration were shown. In each sample, cell culture was started with 0.5 x 10^6 cells/ml, and every 12 hours, cell density was measured by Nexolum, a small amount of cell culture based on the calculation was inoculated into fresh medium to start new culture with the cell density, 0.5 x 10^6 cells/ml.

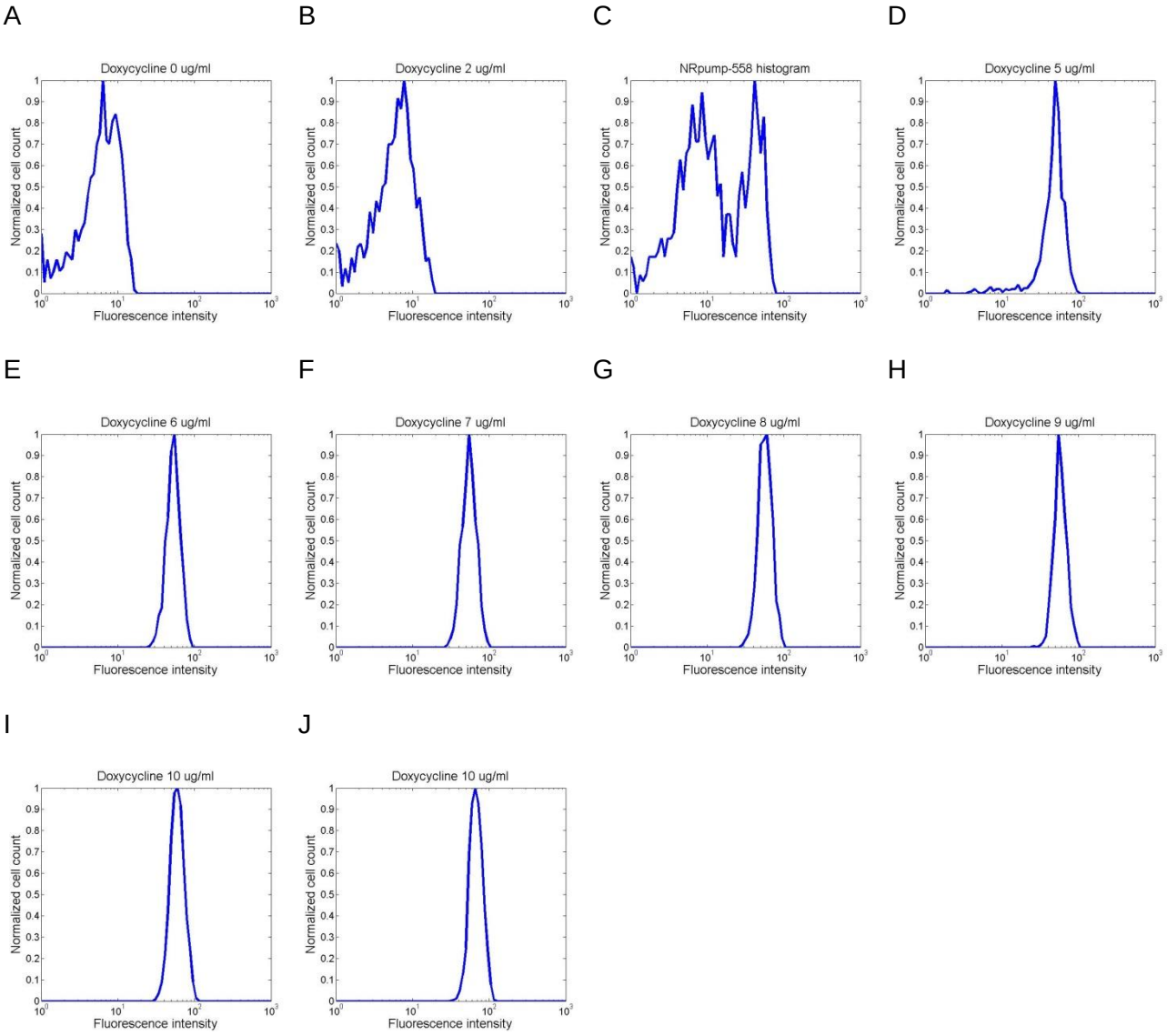

Figure 3.13 Histograms of NRpump-558 dose-response.

Cells carrying NRpump-558 gene circuit were induced at 10 doxycycline concentrations, 0, 2, 4, 5, 6, 7, 8, 9, 10 and 15 µg/ml; the histograms of PDR5::GFP expression at each doxycycline concentration were shown. In each sample, cell culture was started with 0.5 x 10^6 cells/ml, and every 12 hours, cell density was measured by Nexolum, a small amount of cell culture based on the calculation was inoculated into fresh medium to start new culture with the cell density, 0.5 x 10^6 cells/ml.

The histograms of NRpump-558 reporter expression were very similar to NRpump -312. At no and low doxycycline concentration, all the cells in the population expressed a minimum level of *PDR5*-S558Y::GFP. At intermediate doxycycline concentration (4 µg/ml), a minority of cells started to express a higher level of *PDR5*-S558Y::GFP while the rest of the cells still remained at low *PDR5*-S558Y::GFP expressers. With increasing of doxycycline concentration (5 µg/ml), around half of the cells in the population expressed high level of *PDR5*-S558Y::GFP, while the other half expressed at low level. As doxycycline concentration was further increased (6 µg/ml), the majority of cells in the population had high *PDR5*-S558Y::GFP expression, with only a small fraction of cells expressing low level of *PDR5*-S558Y::GFP. At high doxycycline concentration, all the cells expressed high level of *PDR5*-S558Y::GFP, and the level of expression would reached its maximum. Further increases of doxycycline concentration would not increase fluorescence intensity in individual cells (Figure 3.13).

Then I calculated the mean of each histogram for both NRpump-312 and NRpump-558 at each doxycycline concentration. At doxycycline concentrations of 0 µg/ml and 2 µg/ml, both NRpump-mutant strains showed minimum fluorescence intensity (Figure 3.14 A and C). Both mutant gene circuits started to respond to doxycycline at 4 µg/ml, and showed steep rise in dose response mean with increase of doxycycline concentration between 4 µg/ml and 7 µg/ml. Then the dose response mean kept rising, but with much slower pace until it reached saturation at doxycycline concentration 9 µg/ml. The error bar at middle doxycycline concentration range indicated relatively high variation, which might be due to individual variability of different colonies. The error bar would be narrow down with more dose response data from replicates. The dose response CV was also calculated for both mutant gene circuits at each doxycycline concentration. Both CVs showed a peak at doxycycline concentration 4 µg/ml, which corresponded well with the diverse gene expression shown on the histograms (Figure 3.13). The CVs were low at both low and high doxycycline concentration, because the gene

expression level in the cell population was uniform at both situations. However, the CVs at low doxycycline centration were relatively higher than CVs at high concentration, which might be due to the low dose response mean (Figure 3.14 B and D). CV was defined as standard deviation divided by the mean, even the standard deviation was the same for the histogram at both low and high doxycycline concentration, the CV at low doxycycline concentration would be higher than the CV at high concentration.

When I aligned the dose response mean together for both NRpump mutant gene circuits, the two curves showed exactly the same pattern and overlapped, which suggested that the two mutations, S558Y and G312A, altered Pdr5 function the same way, although different underlying mechanisms were proved. The CV of both mutant gene circuits showed the same pattern as well. The only difference was that the CV for Nrpump-312 was slightly higher at no and low doxycycline concentration, which suggested slightly higher expression noise of the target gene.

A

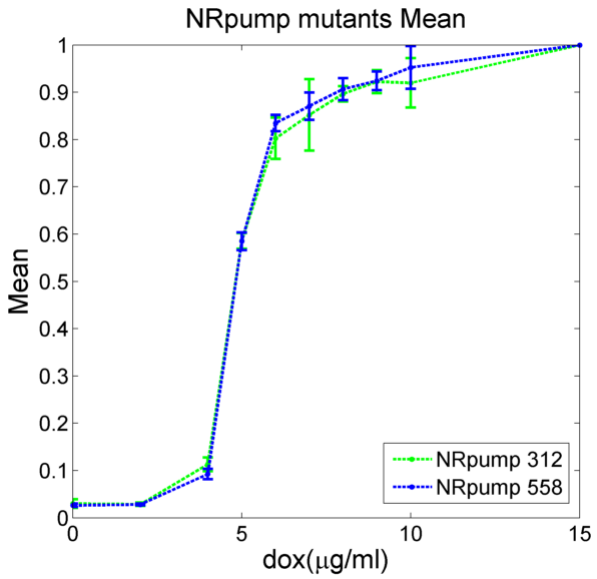

B

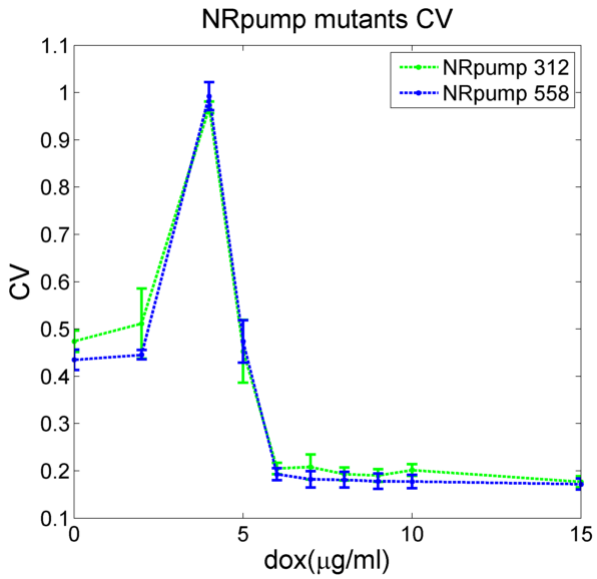

Figure3.14 NRpump mutants mean and CV dose-responses.

Doxycycline at 10 different concentration were used to induce *PDR5::GFP* expression in NR gene circuit: 0, 2, 4, 5, 6, 7, 8, 9, 10, 15 μg/ml. (A) NRpump-312 and NRpump-558 Mean dose-response; (B) NRpump-312 and NRpump-558 Coefficient of Variation (CV) dose-response. Data shown here was average of 3 replicates. Error bar refers to the SD of the 3 replicates' mean value.

3.5.1 NFpump mutant gene circuits composition

As for the NRpump mutant gene circuits, two versions of NFpump mutant gene circuits were built with one bearing S558Y mutation, and the other bearing the G312A mutation on *PDR5*. The NFpump mutant gene circuits share the same regulator with the NFpump gene circuit. The only difference is in the reporter, the *PDR5::GFP* fusion gene in NRpump gene circuit was replaced by the *PDR5* mutant::GFP fused gene*, PDR5*-S558Y::GFP or *PDR5*-G312A::GFP. In the presence of galactose, TetR was expressed under the Gal1 promoter, and it bound to the TetO2 sites on the modified *GAL1* promoter on the reporter. When doxycycline came in, it associated with TetR and therefore, released its binding to the TetO2 sites. As a result, the downstream *PDR5*-mutation::GFP gene was able to be transcribed (Figure 3.11 C and D).

3.5.2 NFpump mutants dose-response

The dose-response mean of NF gene circuit was linear from doxycycline concentration 0 µg/ml to 4 µg/ml. However, the dose-response mean of NFpump gene circuit was no longer linear. It was clear that the Pdr5 pump changed the dose-response behavior. Because it was known that Pdr5 pumps out the inducer, doxycycline, we assumed that the efflux pumping activity of Pdr5 was responsible for this change. The two mutations, S558Y and G312A, were proved to abolish the efflux pumping activity, so we expected the mutation would restore linearity of the NF gene circuit mean dose-response mean. In other words, the mean dose-responses of NFpump mutant gene circuits were expected to be linear between doxycycline concentration 0 µg/ml and 4 µg/ml.

Two NFpump mutant strains were induced by the same series of doxycycline concentration as it was used for NFpump. At all of the doxycycline concentrations, the expression level of *PDR5*-mutation::GFP in both mutants showed single peaked distribution. At

0 µg/ml doxycycline concentration, the cells in both mutant circuits showed minimum expression level of Pdr5 mutant. With gradual increase of doxycycline concentration, the expression level of Pdr5 mutant in each individual cell increased accordingly, until it reached maximum expression level at doxycycline concentration 2.5 µg/ml. Then the Pdr5 mutant expression in each cell in both mutant gene circuits remained stable, further increase of doxycycline concentration did not increase its level. (Figure 3.15, Figure 3.16).

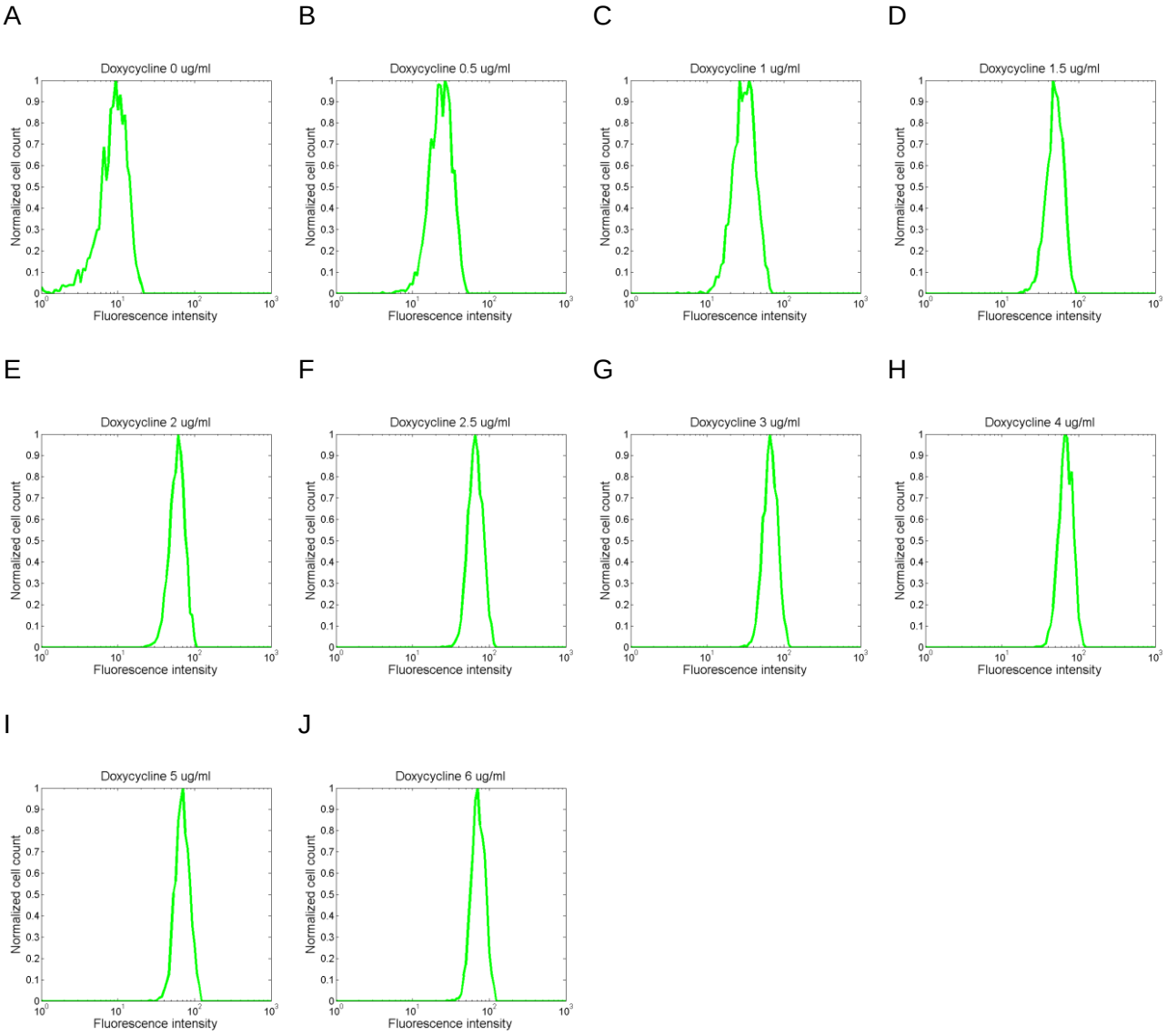

Figure 3.15 Histograms of NFpump-312 dose-response.

Cells carrying NFpump-312 gene circuit were induced at 10 doxycycline concentrations, 0, 0.5, 1, 1.5, 2, 2.5, 3, 4, 5 and 6 µg/ml; the histograms of *PDR5*::GFP expression at each doxycycline concentration were shown. In each sample, cell culture was started with 0.5 x 10^6 cells/ml, and every 12 hours, cell density was measured by Nexolum, a small amount of cell culture based on the calculation was inoculated into fresh medium to start new culture with the cell density, 0.5 x 10^6 cells/ml.

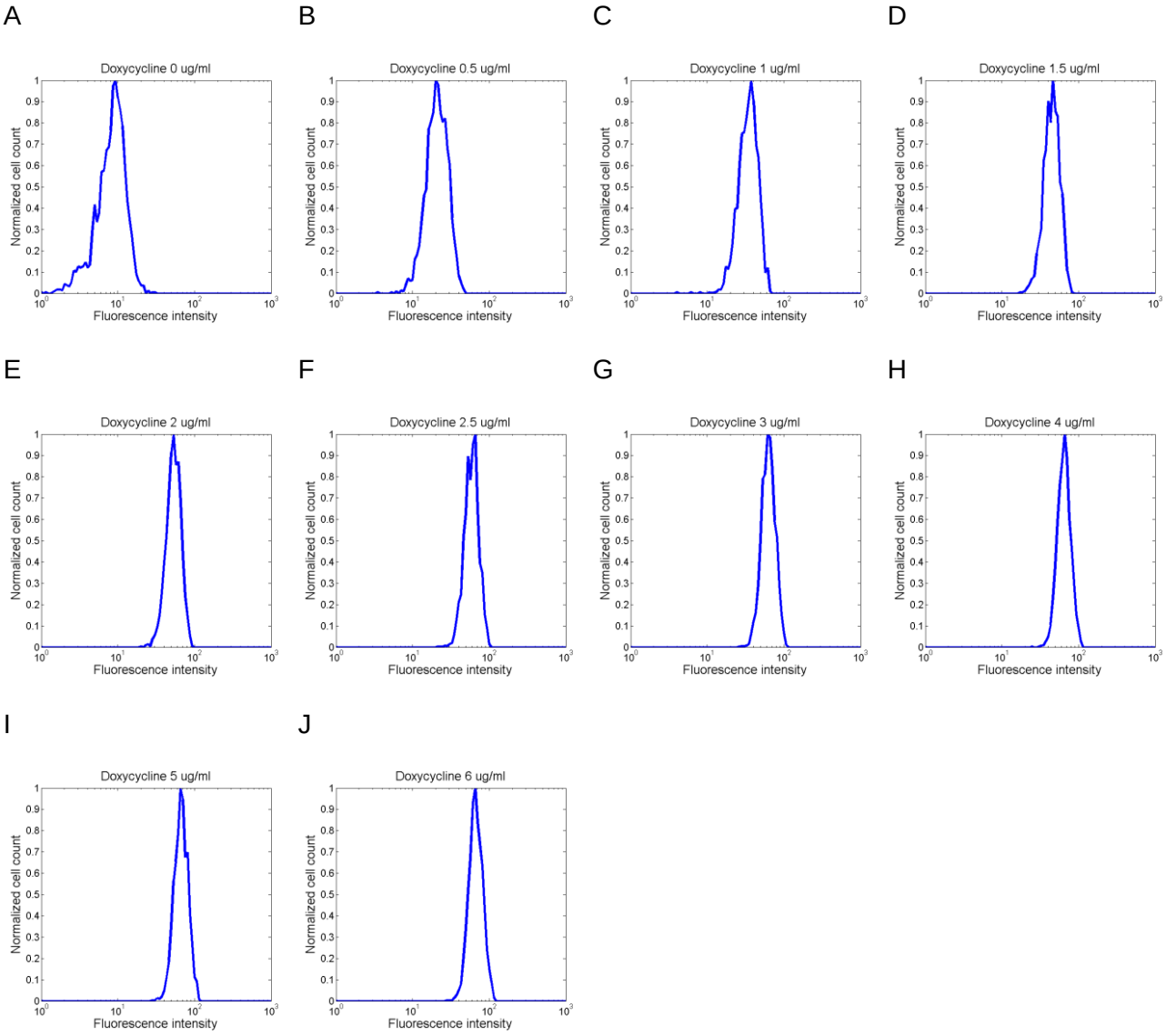

Figure 3.16 Histograms of NFpump-558 dose-response.

Cells carrying NFpump-558 gene circuit were induced at 10 doxycycline concentrations, 0, 0.5, 1, 1.5, 2, 2.5, 3, 4, 5 and 6 µg/ml; the histograms of PDR5::GFP expression at each doxycycline concentration were shown. In each sample, cell culture was started with 0.5 x 10^6 cells/ml, and every 12 hours, cell density was measured by Nexolum, a small amount of cell culture based on the calculationas inoculated into fresh medium to start new culture with the cell density, 0.5 x 10^6 cells/ml.

Then the mean of each histogram at every doxycycline concentration was calculated for both mutant gene circuits. The dose response mean for both gene circuits showed a linear range between doxycycline concentrations 0 µg/ml and 1.5 µg/ml, and then they both began to curve until they reached saturation at 3 µg/ml. Further increase of doxycycline concentration did not increase Pdr5 mutant expression level in each individual cell. The CV for both mutant gene circuits was low at all doxycycline concentrations. The slightly increased CV at no and low doxycycline concentration was due to lower mean. Next, I compared the dose-responses of the two NFpump-mutants, they showed the same dose-response curve in terms of both mean and CV (Figure 3.17).

3.6 Dose-response comparison among NR, NRpump and NRpump mutants

Knowing that the Pdr5 mutants lost efflux pumping function, I measured and compared the dose-responses of reporter expression mean and CV of NRpump and NRpump mutants. The experimental results indicated that both NRpump mutants had similar mean dose-responses as NR did at high inducer concentrations; and they were steeper compared to the mean dose-response of NRpump. However, both NRpump mutants responded to doxycycline at a lower concentration compared to NR, but similar to NRpump (Figure 3.18 A). The CV dose-responses were similar for all the 4 strains, with the CV of NR peaked at slightly higher doxycycline concentration (Figure 3.18 B). This might be due to high GFP fluorescence intensity in NR, and higher inducer sensitivity of NRpump and NRpump mutants. This result confirmed that the efflux pumping function of Pdr5 caused the dose-response change in high doxycycline concentrations in NRpump, but was not the cause for higher sensitivity at low doxycycline concentrations.

A

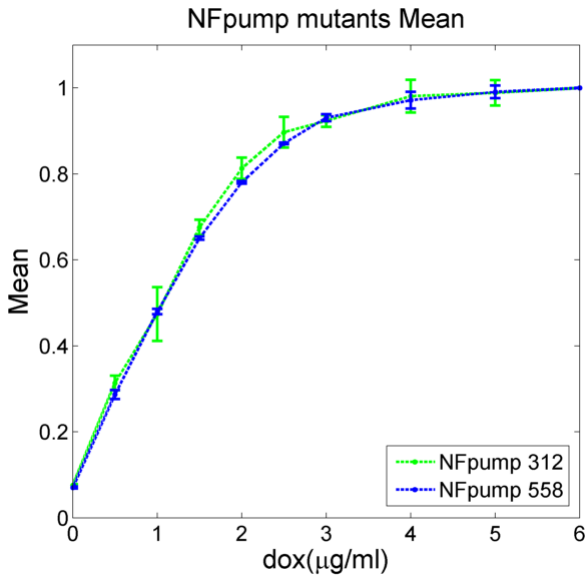

B

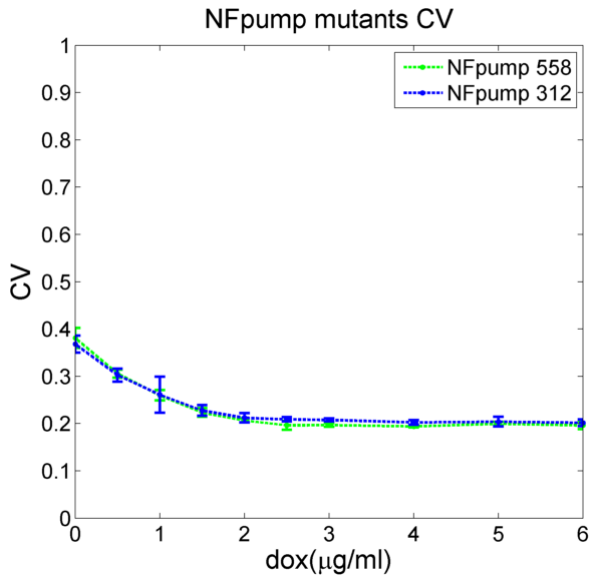

Figure 3.17 NFpump mutants mean and CV dose-response.

Doxycycline at 10 different concentrations were used to induce PDR5::GFP expression in cells carrying NFpump mutants gene circuit: 0, 0.5, 1, 1.5, 2, 2.5, 3, 4, 5 and 6 μg/ml. (A) NRpump-312 and NRpump-558 Mean dose-response; (B) NRpump-312 and NRpump-558 Coefficient of Variation (CV) dose-response. Data shown here was average of 3 replicates. Error bar refers to the SD of the 3 replicates' mean value.

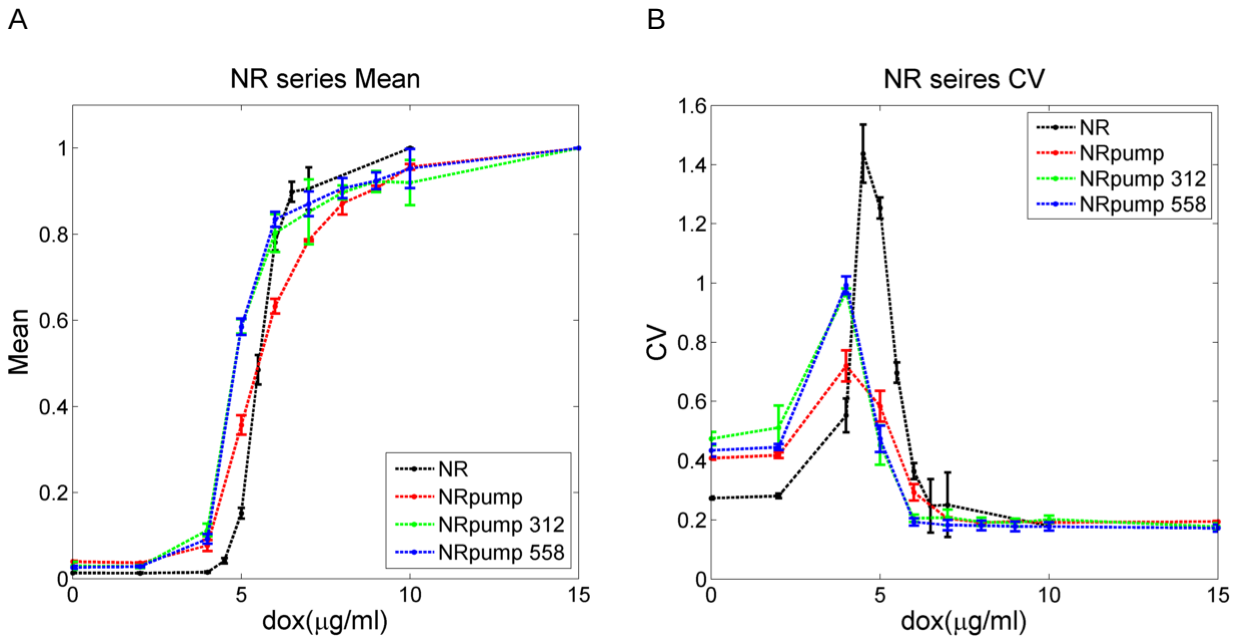

Figure 3.18 Mean and CV dose-responses comparison among NR, NRpump and NRpump-mutants.

(A) NR, NRpump and NRpump-mutant Mean dose-responses. (B) NR, NRpump and NRpump-mutant CV dose-responses. Doxycycline at 10 different concentrations were used to induce *yEGFP::ZeoR* expression in cells carrying NR gene circuit: 0, 2, 4, 4.5, 5, 5.5, 6, 6.5, 7 and 10 μg/ml. Another 10 different doxycycline concentrations were used to induce *PDR5*::GFP expression in cells carrying NRpump and NRpump mutant gene circuits: 0, 2, 4, 5, 6, 7, 8, 9, 10 and 15 μg/ml. Data shown here was average of 3 replicates for each strain. Error bar refers to the SD of the 3 replicates' mean value.

From the above comparison among the four strains in the NR series, the NRpump and two NRpump mutants were more inducer-sensitive to doxycycline than NR was at low concentration (Figure 3.18). In order to prove that, I applied one-way ANOVA at doxycycline concentration 4 µg/ml (Figure 3.19 A) to the data. The mean value of NRpump and the two NRpump mutants were all significantly higher than the mean of NR (Table 1). On the contrary, NRpump appeared lower mean value compared to the mean of other three strains (Figure 3.19 A), which was confirmed also by one way ANOVA (Table 2).

A

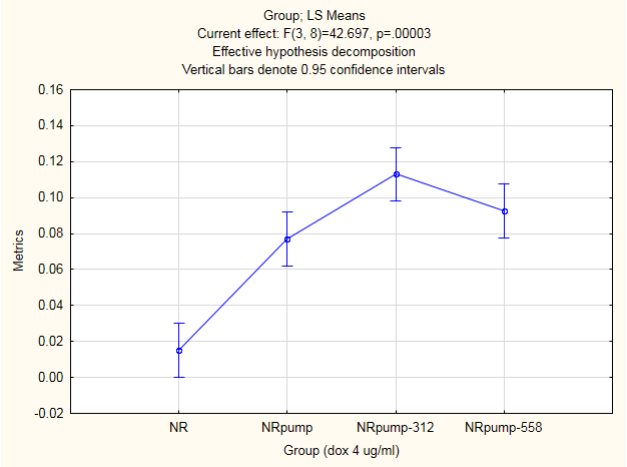

B

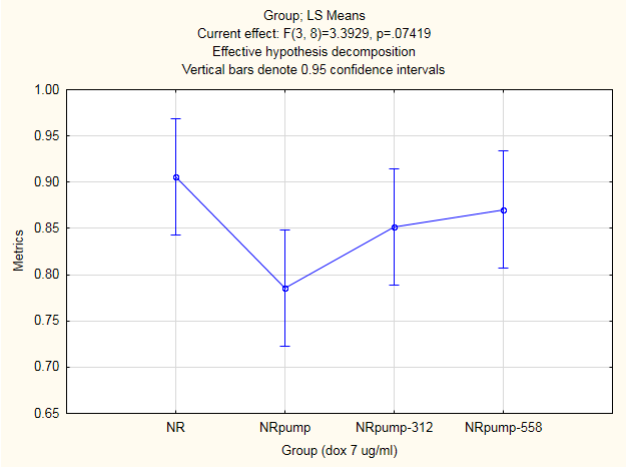

Figure 3.19 Mean dose-response among NR, NRpump and NRpump-mutant at low and high doxycycline concentration.

(A) Doxycycline concentration at 4 µg/ml. (B) Doxycycline concentration at 7 µg/ml. One-way ANOA was performed for all of the four NR related strains at the specified doxycycline concentrations.

	NR	NRpump	NRpump-312	NRpump-558
NR		0.000141	0.000005	0.000029
NRpump	0.000141		0.004280	0.126933
NRpump-312	0.000005	0.004280		0.055482
NRpymp-558	0.000029	0.126933	0.055482	

Table 1 ANOVA test for NR, NRpump and NRpump-mutants at doxycycline concentration 4 μg/ml.

Numbers showed in the table are p values calculated by ANOVA. P values less than 0.05 indicates significant difference, which were shown in red.

	NR	NRpump	NRpump-312	NRpump-558
NR		0.014598	0.199901	0.388194
NRpump	0.014598		0.126416	0.059865
NRpump-312	0.199901	0.126416		0.640887
NRpymp-558	0.388194	0.059865	0.640887	

Table 2 ANOVA test for NR, NRpump and NRpump-mutants at doxycycline concentration 7 μg/ml.

Numbers showed in the table are p values calculated by ANOVA. P values less than 0.05 indicates significant difference, which were shown in red.

3.7 Dose-response comparison among NF, NFpump and NFpump mutant strains

Compared to NFpump, the mean dose-responses of both NFpump mutant gene circuits had a linear range between doxycycline concentrations 0 µg/ml and 1.5 µg/ml, and saturated at 3 µg/ml (Figure 3.20 A). This result indicated that the deviation from linear dose-response mean curve can be attributed to the protein's efflux pumping function. However, the slopes of the linear ranges in both NFpump mutants were larger than that in NF, which suggested that the non-functional pump increased somehow the sensitivity of the NF gene circuit to the doxycycline concentration, similar to the functional pump. The gene expression noise for both NFpump-mutants was low as it was for both the NF and NFpump gene circuits, which was consistent with the narrow and uniform distributions of reporter expression, observed by single cell-level measurements (Figure 3.20 B). However, the dose-response mean curves of NFpump mutants did not completely overlap with that of NF as expected. Instead, the NFpump mutants shower higher sensitivity to doxycycline at low concentration compared to NF, and their sensitivity was at the same level as for NFpump, indicated by the slope of dose-response mean curves at low doxycycline concentration (Figure 3.20 A). This data suggested the existence of other factors beyond the efflux pumping function of Pdr5 that affected the dose-response change in NFpump compared to NF. In summary, functional Pdr5 changed the linearity of dose-response mean by efflux pumping activity, but the increased sensitivity to doxycycline was caused by other factors instead of the efflux pumping function of Pdr5.

As validated above, NF has a linear range of mean dose-response, which was lost in NFpump, and restored in NFpump mutants, but with a narrower linear range. In order to quantify the change of linear range of dose-response mean for NF, NFpump and NFpump-mutant gene circuits, I calculated the L1 norm. The idea of L1 norm was to compare the mean dose-response of the gene circuits to an 'ideal' linear curve that would produce perfectly linear dose-response.

Then the experimental data of these 4 gene circuits was compared to the perfect line, and the area between the perfect line and each dose-response curve at every doxycycline concentration was calculated. The smaller the area was, the more linear the dose-response would be. Therefore, zero area would be an indicator for perfectly linear dose-response. As a result, NF showed a linear dose-response up to 80% of saturation (Figure 3.21 A), NFpump showed linear range up to 40% saturation (Figure 3.21 B), while the linear range for both NFpump-mutants ended between 60% and 70% saturation (Figure 3.21 C and D). The results again showed that Pdr5 altered the linear dose-response of NF gene circuit, and Pdr5 mutants with compromised efflux pumping function restored part of the linear dose-response range, but not all. The four strains showed different L1 norm value when they reached 100% saturation. The actual L1 norm value at 100% saturation reflected the speed for the gene circuits to reach saturation. The higher the L1 norm value was, the less doxycycline concentration the gene circuit needs to reach saturation. For example, the L1 norm for NF at 100% was around 1, while it was above 1.5 for NFpump-mutant, meaning that NFpump-mutant reached saturation at less doxycycline concentration compared to NF.

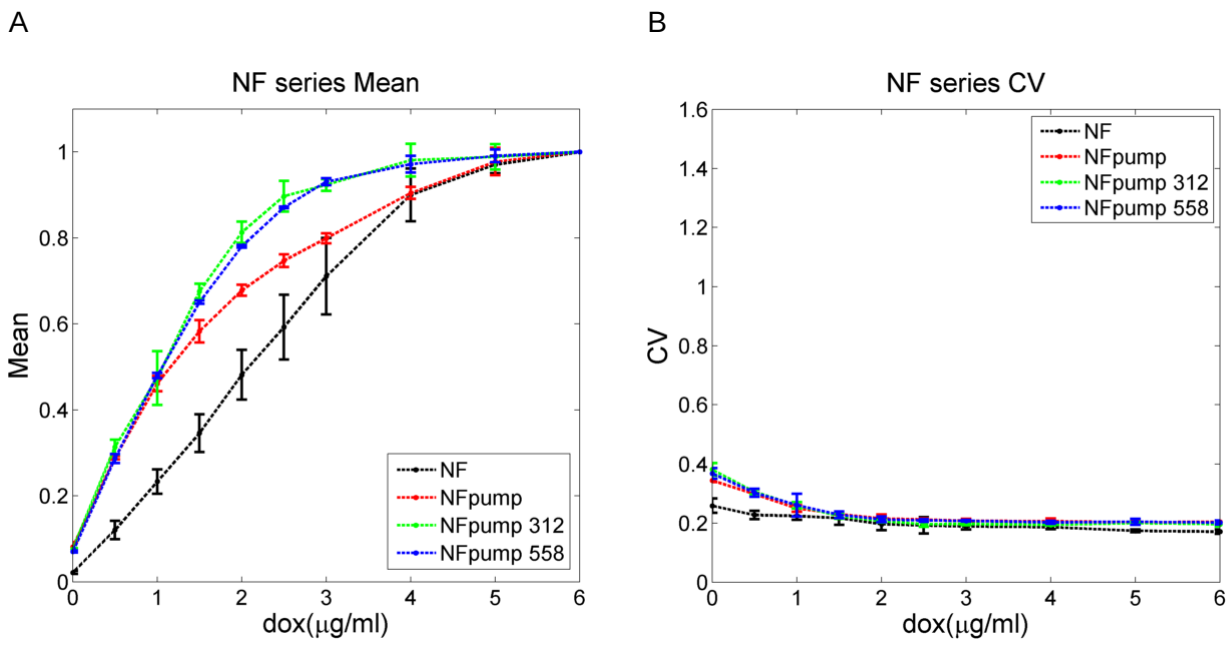

Figure 3.20 Dose-response comparison among NF, NFpump and NFpump-mutant.

(A) NF, NFpump and NFpump mutants Mean dose-responses. (B) NF, NFpump and NFpump-mutant CV dose-responses. Doxycycline at 10 different concentrations were used to induce target gene expression in NF, NFpump and NFpump mutants: 0, 0.5, 1, 1.5, 2, 2.5, 3, 4, 5 and 6 μg/ml. Data shown here was an average of 3 replicates for each strain. Error bar refers to the SD of the 3 replicates' mean value.

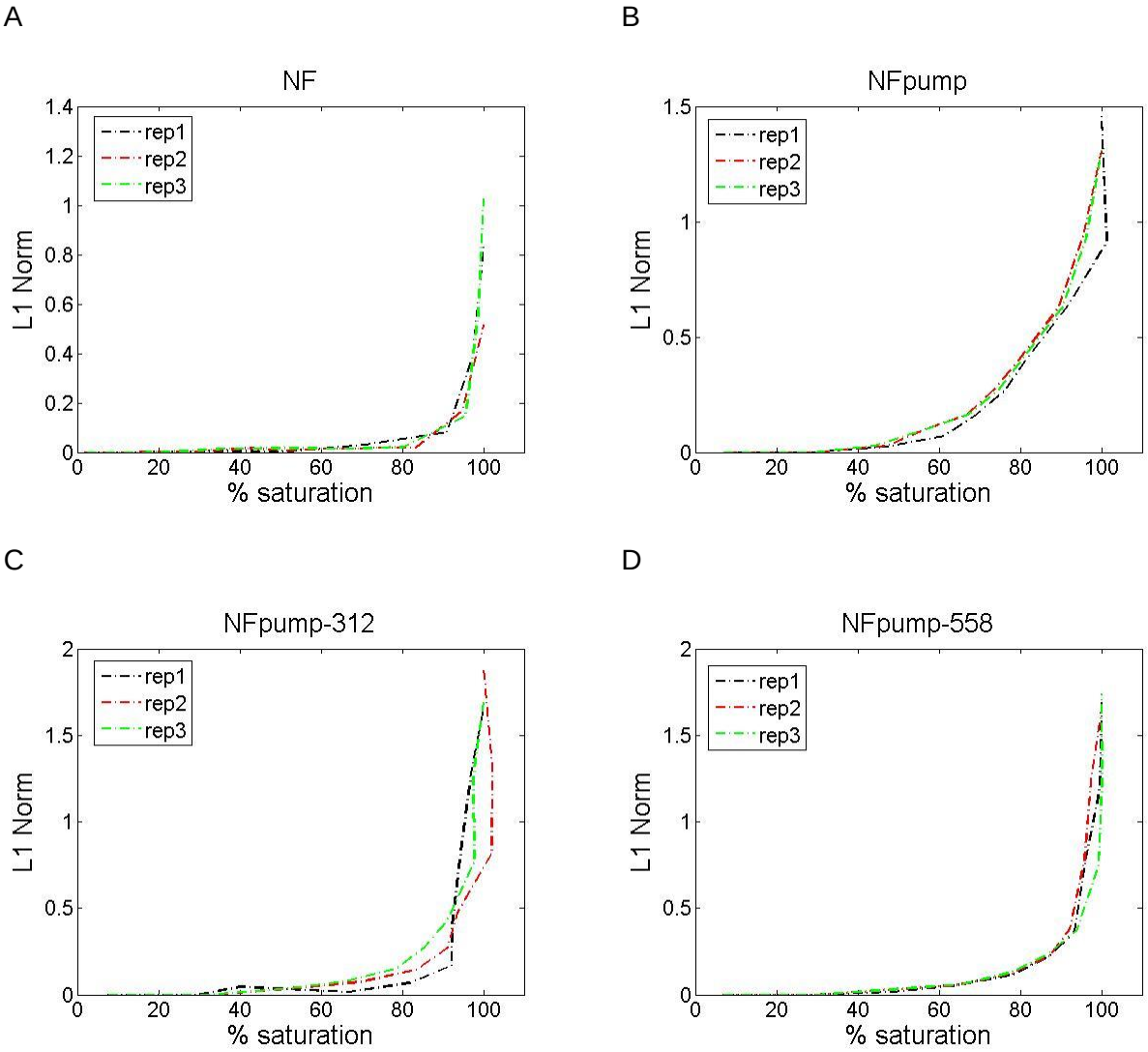

Figure 3.21 L1 norm for NF, NFpump and NFpump-mutants mean dose-responses.

(A) NF L1 norm; (B) NFpump L1 norm; (C) NFpump-312 L1 norm; (D) NFpump-558 L1 norm. L1 norm was calculated and plotted in matlab.

In order to prove that the mean dose-responses for NF, NFpump and the two NFpump-mutant gene circuits are different, I used one way ANOVA based on the L1 norm at the lowest doxycycline concentration where all four strains reached saturation, 5 µg/ml. The L1 norm for NF was the lowest among the four; NFpump-mutants showed the highest L1 norm while NFpump was in between (Figure 3.22). The ANOVA test showed that the L1 norm of both NF and NFpump were different from the other three, the L1 norms of two NFpump-mutants were not different from each other, but they were both different from NF and NFpump.

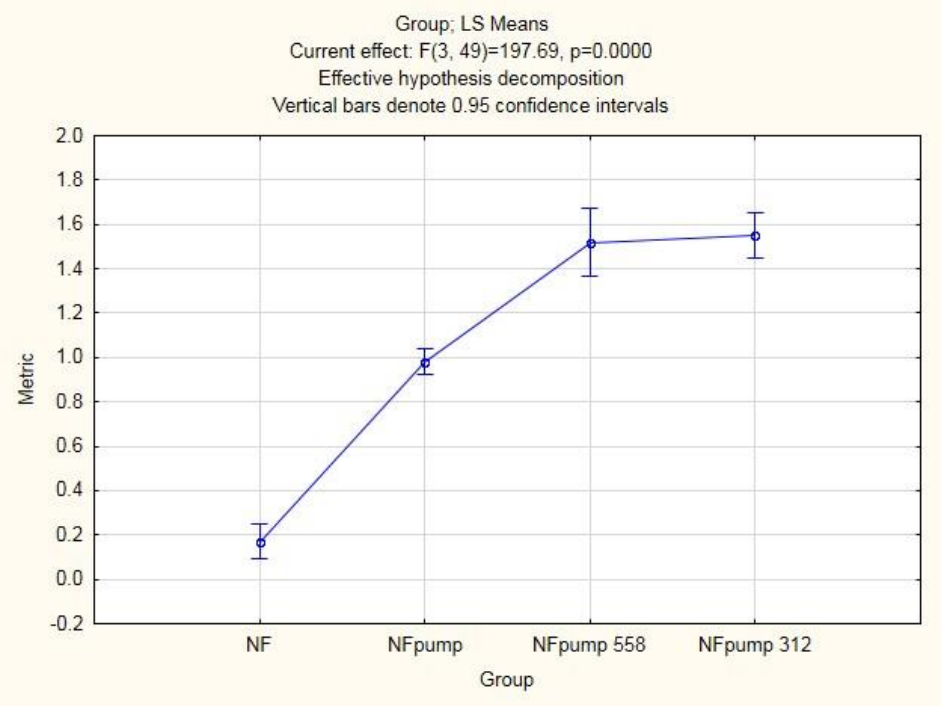

Figure 3.22 L1-norm of NF, NFpump and NFpump-mutant mean dose-responses.

One way ANOVA test was done at doxycycline concentration 5 µg/ml, where all of the four strains reached saturation.

	NF	NFpump	NFpump-312	NFpump-558
NF		0.000166	0.000166	0.000166
NFpump	0.014598		0.000166	0.000166
NFpump-312	0.000166	0.000197		0.99203
NFpymp-558	0.000166	0.000166	0.99203	

Table 3 ANOVA test for the linearity of NF, NFpump and NFpump-mutant mean dose-responses.

Numbers showed in the table are p values calculated by ANOVA. P values less than 0.05 indicates significant difference, which were shown in red.

3.8 Investigation on other factors that contribute to the dose-response mean in NFpump

The NF strain showed a linear mean dose-response ranging between doxycycline concentrations 0 µg/ml and 4 µg/ml (Figure 3.20 A). On the contrary, NFpump lost the linear dose-response; instead, it showed a concave curve of mean dose-response, which had higher sensitivity to doxycycline than NF at low doxycycline concentration (Figure 3.20 A). NFpump-mutants with compromised efflux pumping function of Pdr5 restored linear range for dose-response mean, but the linear range covered a narrower range of doxycycline concentrations (0 µg/ml to 2 µg/ml) compared to NF (0 µg/ml to 4 µg/ml). Moreover, the slope of the linear dose-response range in NFpump-mutants is higher than the slope of NF (Figure 3.20 A), which indicated higher sensitivity to doxycycline at low concentration. Interestingly, this sensitivity in NFpump-mutants is the same as NFpump. These results suggested the existence of another mechanism that also contributed to the change of dose-response mean in NFpump compared to NF, besides the efflux pumping function of Pdr5.

My collaborator created stochastic simulations of dose-response for all the NR series and NF series strains based on previous research [145], which were able to reproduce my experimental results. On the basis of these models, he performed sensitivity analysis and tested if TetR concentration was lower in pump and pump-mutant strains compared to their non-pump counterparts, then he matched the data. In order to test the hypothesis that reduced TetR expression contributes to the dose-response change in pumps trains, I created 2-color gene circuits representing all of the 8 gene circuits used before, by fusing TetR with mCherry and replacing the original TetR on these gene circuits (Figure 3.23).

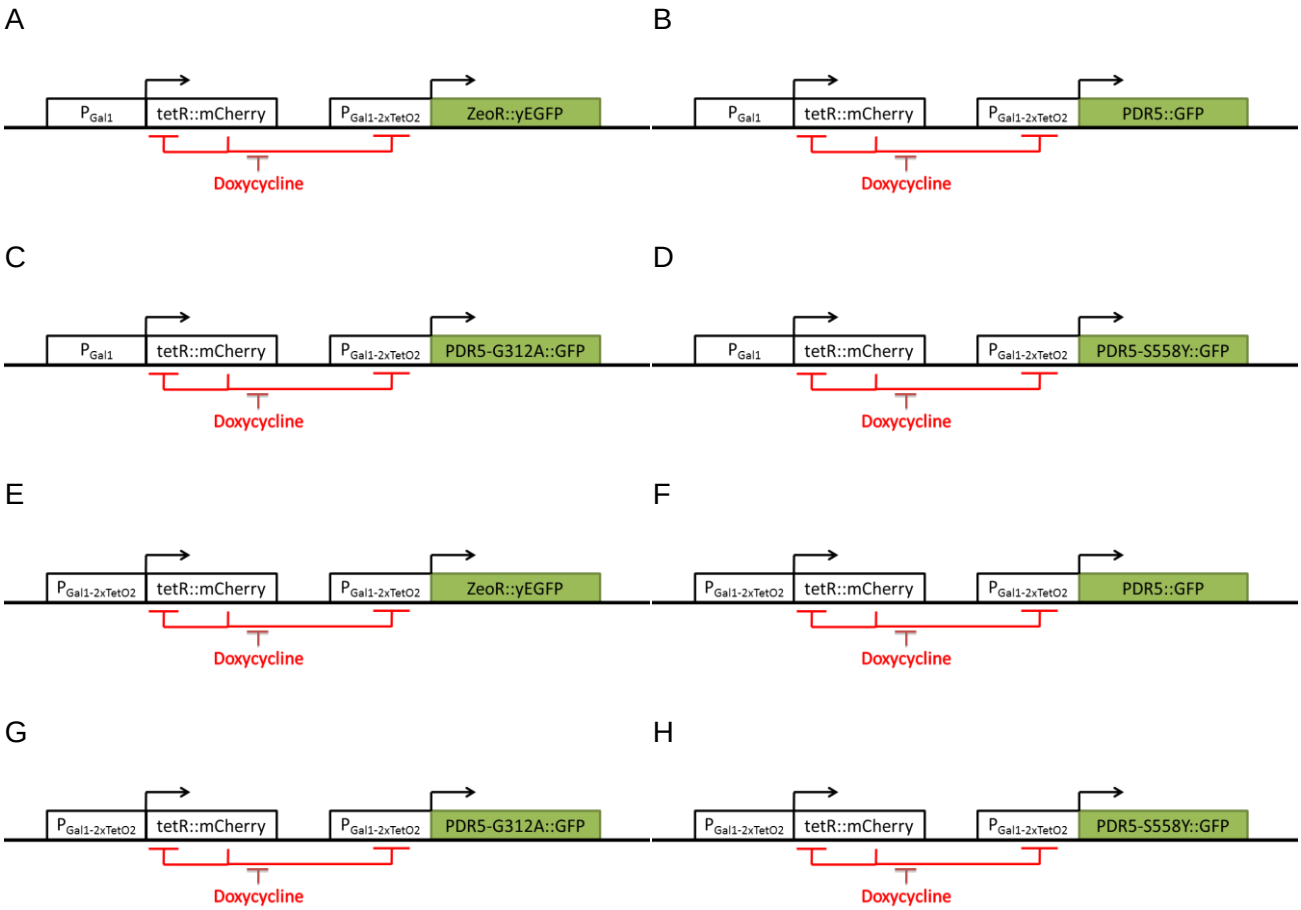

Figure 3.23 Regulation scheme for 2-color gene circuits.

(A) NR. (B) NRpump. (C) NRpump-312. (D) NRpump-558. (E) NF. (F) NFpump. (G) NFpump-312. (H) NFpump-558

3.8.1 Two-color NR and NF gene circuits and their TetR expression

2-color NR and NF strains were induced by the same concentration of doxycycline used for single color NR and NF strains respectively, and their TetR expression was measured by flow cytometry. In the NR strain, TetR expression was similar across the entire range of doxycycline concentrations, even in the absence of doxycycline (Figure 3.24 A). Because TetR was under the control of the wild type *GAL1* promoter, it was constitutively expressed in the presence of galactose. TetR expression in the NF strain was at the basal level in the absence of doxycycline, and it rose with the increase of doxycycline concentration. The increase showed a linear dose-response range between doxycycline concentrations 0 µg/ml and 2.5 µg/ml, and then the TetR expression reached saturation at doxycycline 3 µg/ml.

A

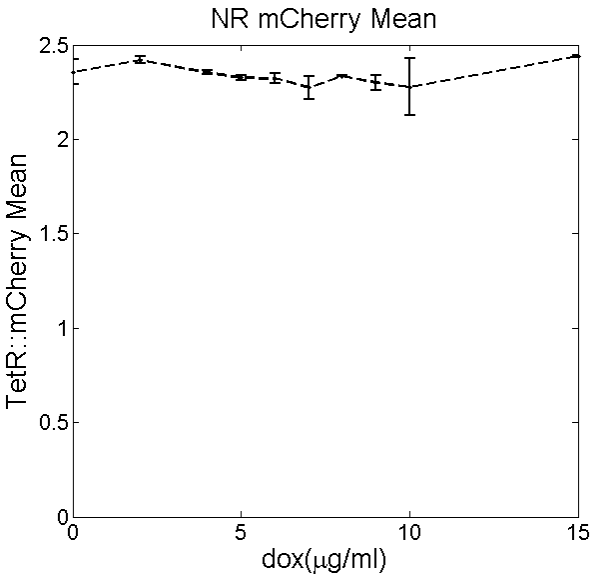

B

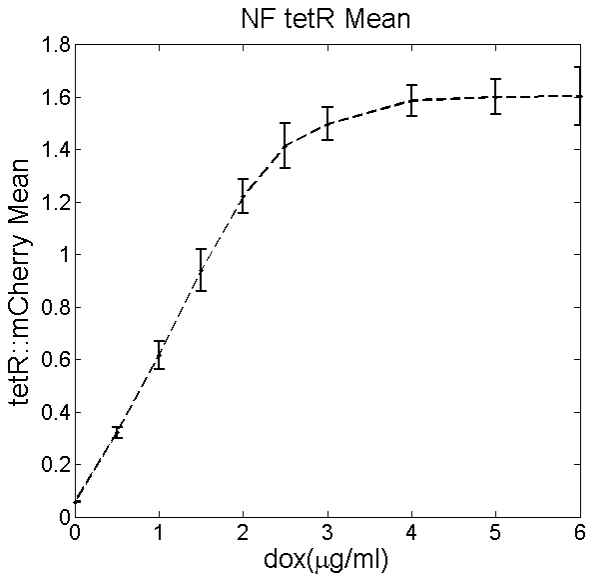

Figure3.24 TetR::mCherry expression in the NR and NF.

(A) NR. (B) NF. NR was induced by doxycycline concentration 0, 2, 4, 4.5, 5, 5.5, 6, 6.5, 7 and 10 μg/ml. NF strain was induced by doxycycline concentration 0, 0.5, 1, 1.5 2, 2.5, 3, 4, 5 and 6 μg/ml. Data shown here was average of 3 replicates. Error bar refers to the SD of the 3 replicates' mean value.

3.8.2 Two-color NRpump, NRpump mutant, NFpump and NFpump mutant gene circuits and their TetR expression

In order to monitor TetR expression in pump and pump mutant strains, 2-color pump strains were also induced by the same set of doxycycline concentration used for their single color counterparts, and their TetR expression was measured by flow cytometry. Same as NR strain, NRpump and NRpump-mutant strains all showed similar TetR expression level across the entire doxycycline concentrations. However, all the pump strains showed lower TetR expression than NR did (Figure 3.25 A). Among the three pump strains, NRpump-312 had higher TetR expression than the other two, which had the same TetR expression level (Figure 3.25 A). As expressed for NF, NFpump and NFpump-mutant strains all showed increased TetR expression with increasing doxycycline concentration. However, all the pump strains had lower TetR expression compared to NF at every doxycycline concentration above 0.5 μg/ml. Among the four NF series strains, NFpump had the lowest TetR expression; the two NFpump-mutants were in the middle, while NF had the highest TetR expression level. These results clearly indicated that pump strains had lower TetR expression than non-pump strains in both NR and NF, no matter if the pump was functional or not. The error bars indicated clone depended variation of TetR expression. According to the mathematical simulation developed by my collaborator, the TetR expression in NRpump and NRpump mutant strains were expected to be on the same level. Same applied to NF series strains. However, I noticed that although NRpump and NRpump-312 showed the same TerR expression level, NRpump-558 had a slightly higher level of expression. Besides, NFpump mutant strains both showed higher tetR expression than NFpump did. To my knowledge, the difference is highly likely due to clone variability, because strong clone dependent variation of TetR expression was observed in all the pump strains (in the figure we only showed 3 most representative replicates for each strain) (Figure 3.25 C and D). However, regardless of the variability of different clones in terms of TetR expression, all the pump clones showed lower TetR expression than the non-pump clones, which confirmed my

hypothesis that reduced TetR expression contributed to the dose-response change in pumps strains by reducing TetR repression on *PDR5* transcription and therefore increased their sensitivity to doxycycline.

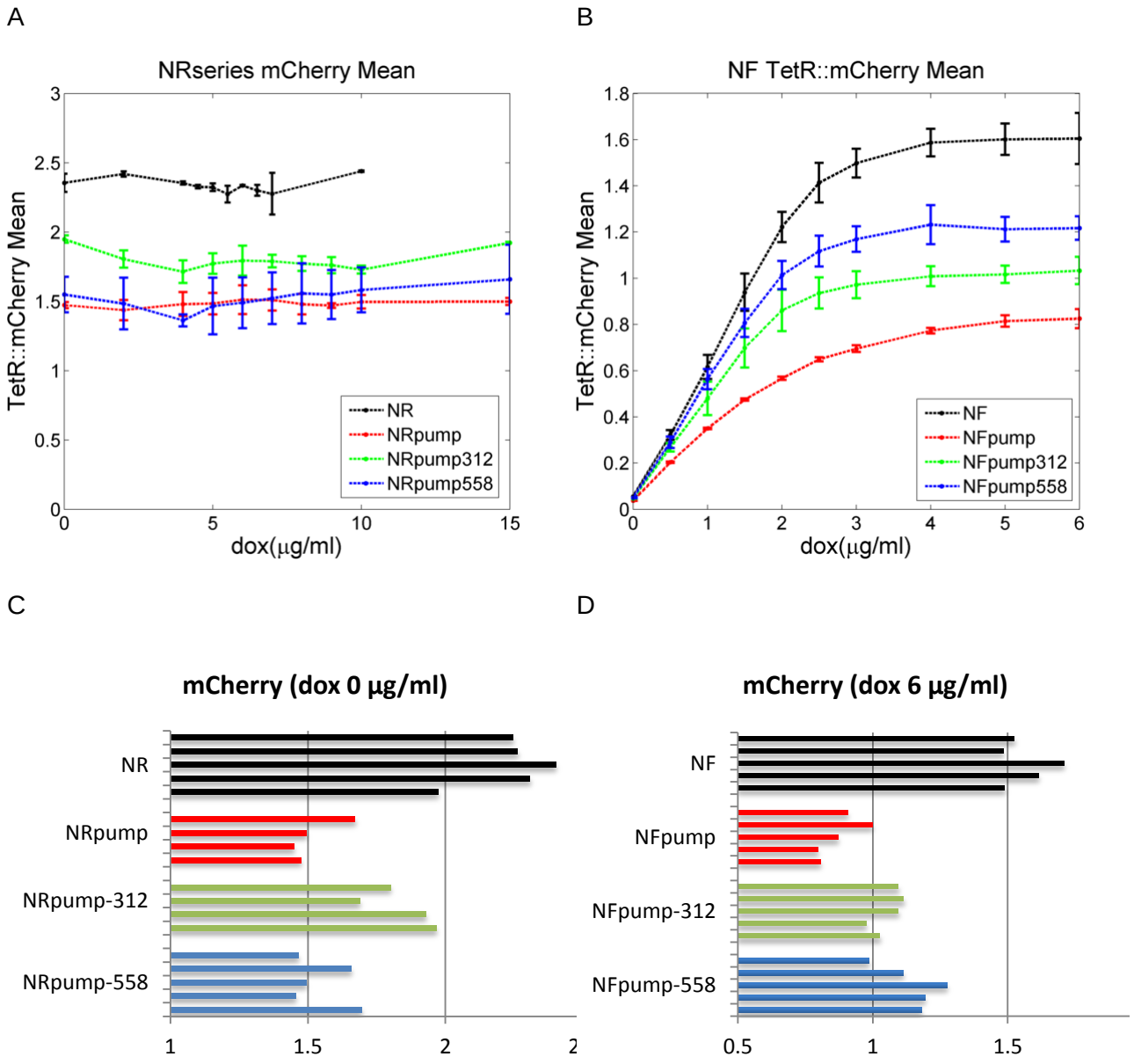

Figure 3.25 TetR::mCherry expression in all the NR related and NF related strains.

(A) NR, NRpump and NRpump-mutant. (B) NF, NFpump and NFpump-mutant. (C) mCherry expression level in different NR series clones at no doxycycline environment. (D) mCherry expression level in different NF series clones at the maximum doxycycline concentration (6 μg/ml). NR was induced by doxycycline concentration 0, 2, 4, 4.5, 5, 5.5, 6, 6.5, 7 and 10 μg/ml. NRpump and NRpump-mutant strains were induced by doxycycline concentration 0, 2, 4, 5, 6, 7, 8, 9, 10 and 15 μg/ml. NF, NFpump and NFpump-mutant strain was induced by doxycycline

concentration 0, 0.5, 1, 1.5 2, 2.5, 3, 4, 5 and 6 μg/ml. Data shown in (A) and (B) was average of 3 replicates. Error bar refers to the SD of the 3 replicates' mean value.

3.8.3 Endogenous Pdr5 expression does not affect dose-response results.

Because endogenous Pdr5 was knocked out in all the pump strains, but not in NR and NF strains, I suspected that endogenous Pdr5 would affect the dose-response behavior of NR and NF strains by removing intracellular doxycycline. If this happened, the dose-response curves for NR and NF were not comparable to their pump counterparts. In order to test this hypothesis, I knocked out endogenous Pdr5 in the NR strain and characterized its dose-response the same way I did for NR strain with endogenous Pdr5. Then the dose-response curves for the two NR strains were compared. The results showed that both NR strains exhibited sigmoidal dose-response curves, and the two dose-responses were indistinguishable (Figure 3.26). CV dose-responses for both NR strains were similar; they were low at both low and high doxycycline concentration and peaked at the same intermediate concentration (4.5 µg/ml). The higher noise in NR (*PDR5* KO) strain at low doxycycline concentration was probably background noise. Therefore, it is safe to conclude that endogenous Pdr5 expression did not affect the shape of dose-response curve for NR strain, which might be due to its extremely low level of expression in the cells, and can be neglected. Although the same experiment was not performed for NF strain, since endogenous Pdr5 did not change the dose-response curve for NR strain, it should not change it in NF strain either.

3.8.4 The two-color NF strain is more sensitive to doxycycline than the single color NF.

In my experimental data, I also noticed an interesting phenomenon. Although both 2-color and single color NF strains showed linear dose-response curve in certain doxycycline concentration range, the dose-response mean curve of 2-color NF has steeper slope compared to that of single color NF, meaning that the 2-color NF was more sensitive to doxycycline than NF and reached saturation at lower doxycycline concentration (Figure 3.27 A and B). A related observation was made in earlier research [29]. This might be due to the fusion of mCherry and TetR, which have weakened TetR's repression of target gene transcription.

3.8.5 Correlation between TetR and target gene expression in NF and NFpump strains

In NF gene circuits, the regulator, TetR, and the target gene, yEGFP::ZeoR, were constructed in symmetric positions, which meant that the expression of these two genes will correlate with each other. Previous research has shown the correlation [29]. Since the expression of yEGFP::ZeoR increases with the increase of inducer concentration, in a linear manner, TetR expression was expected to show the same dose-response curve. In order to test the hypothesis, the 2-color NF strain was induced with the same set of doxycycline concentration used for single color NF induction. As a result, TetR and yEGFP::ZeoR expression had the exactly the same dose-response curves, which overlapped (Figure 3.28 A). Similarly, NFpump was expected to show the same correlation between TetR and *PDR5::GFP* expression, because the replacement of *yEGFP::ZeoR* by *PDR5::GFP* in NFpump gene circuit did not change its topological structure. In order to test this hypothesis, 2-color NFpump strain was induced by the same set of doxycycline concentrations used for single color NFpump strain induction. However, the results were not quite as expected. *PDR5* expression showed higher sensitivity to doxycycline compared to TetR expression (Figure 3.28 B). The results indicated the existence of certain factors that changed the topological structure of NF network.

A

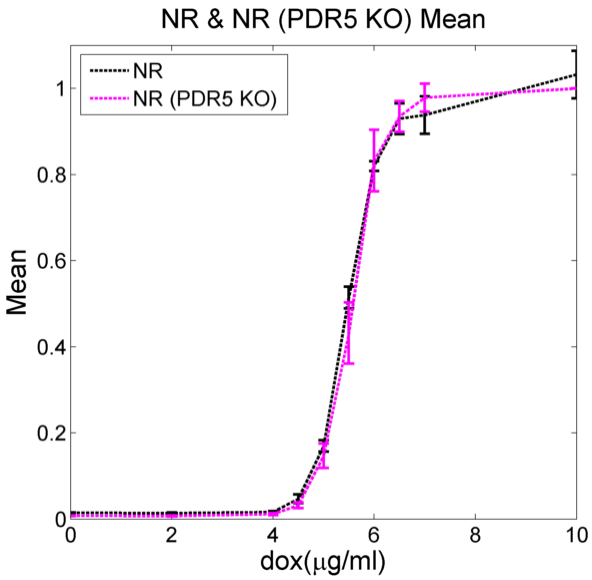

B

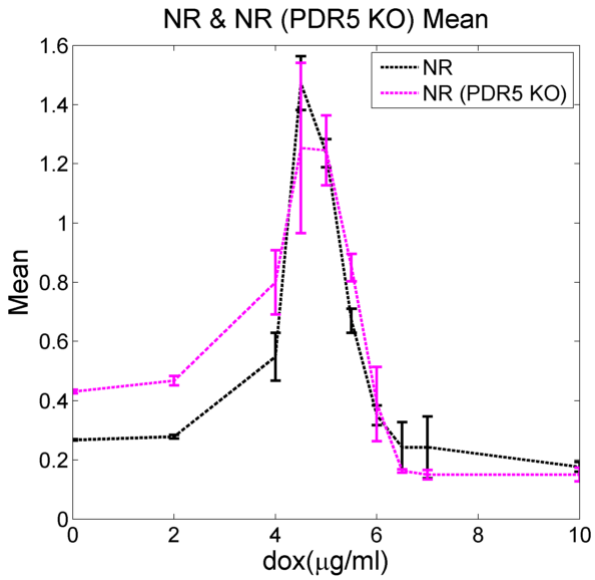

Figure 3.26 yEGFP expression in NR and NR (*PDR5* knockout) strains.

(A) Mean does-response. (B) CV dose-response. Both NR strains were induced by doxycycline concentration 0, 2, 4, 4.5, 5, 5.5, 6, 6.5, 7 and 10 μg/ml. Data shown here was average of 3 replicates for each strain. Error bar refers to the SD of the 3 replicates' mean value.

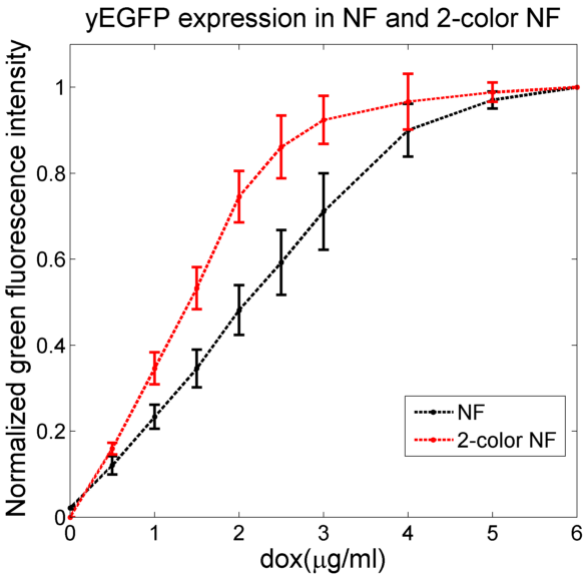

Figure 3.27 yEGFP expression in NF and 2-color NF strains.

Both NF strains were induced by doxycycline concentration 0, 0.5, 1, 1.5, 2, 2.5, 3, 4, 5 and 6 μg/ml. Data shown here was average of 3 replicates for each strain. Error bar refers to the SD of the 3 replicates' mean value.

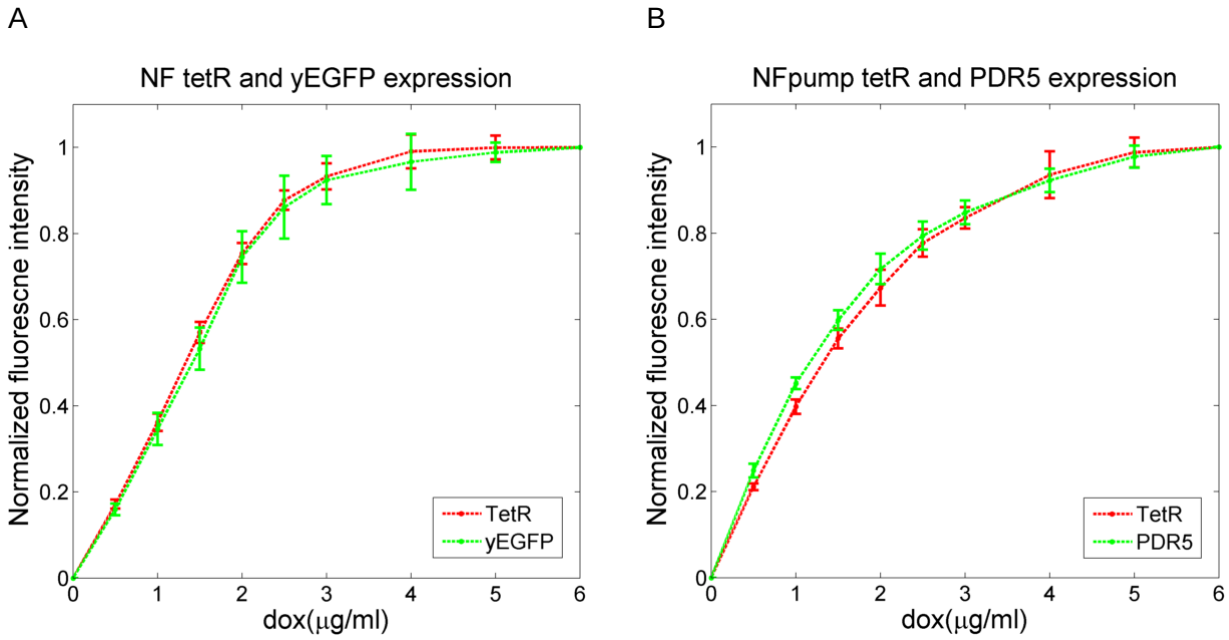

Figure 3.28 Correlation between TeR and target gene expression in NF and NFpump strains.

(A) TetR and *yEGFP::ZeoR* expression in NF. (B) TetR and *PDR5::GFP* expression in NFpump. Both NF strains were induced by doxycycline concentration 0, 0.5, 1, 1.5, 2, 2.5, 3, 4, 5 and 6 μg/ml. Data shown here was average of 3 replicates for each strain. Error bar refers to the SD of the 3 replicates' mean value.

3.9 Conclusion and discussion

Based on previously characterized inducible synthetic gene circuits in *Saccharomyces cerevasiae* [29], NR and NF, I studied the functional effect of introducing a protein pump into these networks, by creating two relevant gene circuits, NRpump and NFpump. I found that Pdr5, a multidrug resistance pump, when placed under the control of NR and NF changed the inducer sensitivity of the two gene circuits. NRpump became more inducer-sensitive than NR at low doxycycline concentration, but less sensitive at high concentration (Figure 3.18 A). On the other hand, NFpump became more sensitive to doxycycline than NF at all doxycycline concentrations before saturation (Figure 3.20 A). These observations were contradictory to my expectation that both strains (NRpump and NFpump) should be less inducer-sensitive than their non-pump counterparts, considering that Pdr5 can exclude tetracycline family molecules from the cell and thereby decrease their intracellular concentration [143, 146, 147]. These results implied the existence of an opposing force that increases inducer sensitivity in NRpump and NFpump. In order to uncover the unknown mechanism, we turned to computational modeling. Addition of the efflux pumping term to NR in our stochastic simulations was able to reproduce the mean dose-response for NRpump at high doxycycline concentration, but failed at low concentration. Stochastic simulations were performed by my collaborator, Daniel Charlebois. Based on his simulations and parameter sensitivity analysis, I found that when synthesis rate of TetR was reduced, the simulations were able to reproduce the entire dose-response shift as I observed in the experiment (Figure 3.5 A). The same parameter settings applied to NFpump simulation was able to reproduce our experimental result as well (Figure 3.10 A). Therefore, I identified two potential mechanisms that contributed in opposite manner to the change of NRpump and NFpump dose-responses. In order to confirm the effect of the efflux pumping function of Pdr5 to the change of dose-response in pump strains in the experiment, I created NRpump and NFpump strains bearing *PDR5* mutants with compromised efflux pumping function. The dose-

responses of such pump mutant strains were intermediates between those of pump strains and non-pump strains. For example, the dose-response mean of NRpump mutants were similar to NR at high doxycycline concentration, but the same as NRpump at low doxycycline concentration (Figure 3.18 A); the mean dose-response of NFpump mutants restored linearity as exhibited by NF, but maintained high sensitivity to doxycycline at low to intermediate concentration as NFpump did (Figure 3.20 A). These results showed that the efflux pumping function of Pdr5 was responsible for the decreased sensitivity to doxycycline for NRpump at high doxycycline concentration, decreased sensitivity for NFpump at low and intermediate doxycycline concentration, and linearity loss in NFpump. Next, to confirm the computationally predicted role of TetR levels, I measured TetR expression in all the NR and NF series strains by fusing mCherry to TetR. The experimental measurements showed that TetR had lower expression level in all the pump strains (whether or not Pdr5 is functional) compared to NR and NF strains respectively, which confirmed my hypothesis. Lower TetR level in pump strains reduced the repression of *PDR5* transcription, therefore, increased Pdr5 expression.
Now we are able to explain the dose-response differences between pump strains and their non-pump counterparts with the two opposing forces.

The mechanism for reduced TetR expression in pump strains is still unclear and needs further investigation. Although TetR expression was reduced in all the pump strains, it was not caused by Pdr5 protein properties by the fact that TetR level remained the same during the entire dose-response in NR series strains. It is highly possible that the integration of the *PDR5* gene upstream of the TetR promoter impaired TetR transcription. This occurred in the pump stains but not non-pump strains because the *PDR5* gene is over 5 kb while the *ZeoR* gene (in NR and NF) is around 1 kb. Another possibility is that the epigenetic modification (for example, methylation) of *PDR5* affected the downstream transcription factor binding to TetR's promoter. The assumption of impaired TetR transcription is supported by the unbalanced expression of TetR and *PDR5*-mutant in NFpump mutant strains (Figure 3.28 B).

I have proven that Pdr5 protein did not affect TetR expression. However, the expression of endogenous Pdr5 in NR and NF strains was still a concern for its influence on their dose-response curve, because Pdr5 was knocked out in all the pump strains (including single color and 2-color), but not in NR and NF strains. In order to test that, Pdr5 was knocked out in NR strain, and we found that the Pdr5 knockout NR strain showed the same dose-response curve as normal NR strain did (Figure 3.27).

Although reduced TetR expression affected the dose-response of all the pump strains, by comparing the dose-response difference between functional and non-functional pump strains, we can still see the changes caused by the efflux pumping function of Pdr5, which decreased the sensitivity to inducer.

In my experimental data, I also noticed an interesting phenomenon. The dose-response mean curve of 2-color NF had steeper slope compared to single color NF, meaning that the 2-color NF was more sensitive to doxycycline than NF and reached saturation at lower doxycycline concentration (Figure 3.28 A and B). Similar observations were made earlier [29]. This might be due to the fusion of mCherry to TetR, which might have weakened TetR's inhibition function.

Chapter 4 Effect of protein pump on Positive Feedback (PF) gene circuit and dose-respone memory change

4.1 Introduction

Multidrug resistance is a universal phenomenon that has been observed from the simplest microorganisms to the most advanced cell types. A number of mechanisms of multidrug resistance have been discovered, such as active exclusion of toxic molecules, which plays the most important role in protecting cells from adverse environment. In *Saccharomyces cerevisiae*, a complex regulatory network has evolved, in which Pdr5p plays a major role of pumping out toxic molecules. The *PDR5* gene is naturally regulated by *PDR1* and *PDR3*, both of which are transcription factors. Toxic substrates activate *PDR1* expression, which then binds to the promoter of both *PDR3* and *PDR5* and starts their transcription. Pdr3 is also able to bind to its own promoter and the promoter of *PDR5* and help transcribe the efflux pump protein. Therefore, *PDR5* is regulated by a positive feedback network in the natural system. So, why did a positive feedback regulatory network evolve? Does the positive feedback regulatory network confer advantage for yeast cells to survive compared to other regulatory systems? If this is true, in what environment does positive feedback network give this advantage? In order to answer these questions, it will be worth trying to use the negative regulation (NR), negative feedback (NF), and positive feedback (PF) synthetic gene circuits to regulate the *PDR5* gene, and compare the growth rate of cells carrying these gene circuits in different environments. For that purpose, the dose-response of PF controlling *PDR5* gene needs to be studied.

In the previous chapter, *PDR5* introduced into NR and NF gene circuits was discovered to change their dose response behavior by both efflux pumping activity and its influence on intracellular TetR concentration. Besides NR and NF, another gene circuit, Positive Feedback (PF) was also constructed and studied in our laboratory before. The PF gene circuit had a different dose-response pattern than either NR or NF gene circuits, showing bimodality. Since Pdr5 had been proved to pump out the intracellular inducer, doxycycline, it introduced negative feedback loops into the NR and NF regulatory networks. Therefore, I wanted to find out if Pdr5 introduced into the PF gene circuit would change its behavior and if so, how it would change it. Inconstant to NR and NF, there are two stable steady states in PF cells, giving rise to two subpopulations and cells that switch from one to another. Previous research has identified the growth rate and cellular memory of these two subpopulations. The introduction of *PDR5* will be highly likely to change these, and it will be interesting to find out now.

4.2 PF gene circuit and characterization of its dose response

Similar to the NR and NF gene circuits, the positive feedback (PF) gene circuit has two parts, the target gene (reporter) and the regulator. The target gene was the gene fusion ZeoR::yEGFP under the control of a modified *CYC1* promoter, which bears two TetO sites. The reporter was the rtTA gene under the control of the same modified *CYC1* promoter. rtTA is a transactivator that is able to bind to TetO sites only when bound by tetracycline compounds, such as doxycycline and ATc. In the presence of galactose and tetracycline, rtTA expressed at basal level could bind to tetracycyline, and this complex bound to TetO sites on the promoters driving both the reporter and the regulator, could activate the transcription of both yEGFP::ZeoR and

rtTA forming a positive feedback loop. The PFpump gene circuit shared most parts with PF, the only difference being that the yEGFP::ZeoR fusion in PF was replaced by *PDR5::GFP* gene in PFpump (Figure 4.1).

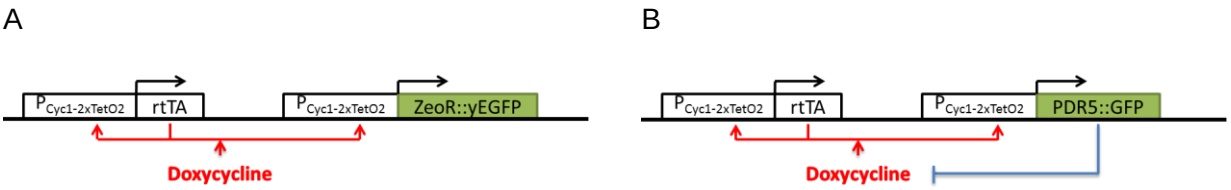

Figure 4.1 Regulation scheme for Positive Feedback (PF) and Positive Feedback pump (PFpump mutant) gene circuits.

(A) PF. (B) PFpump.

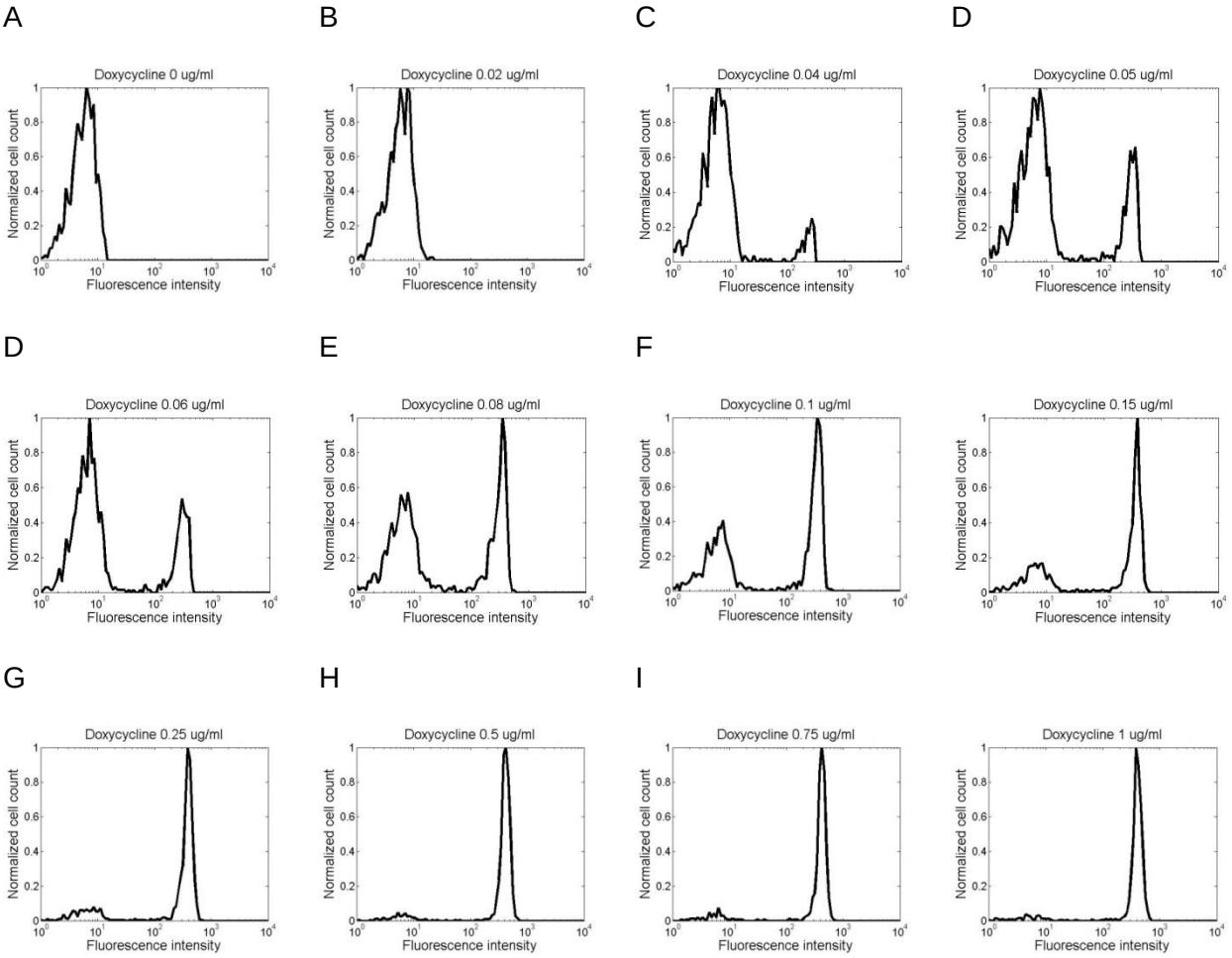

Figure 4.2 Histograms of PF dose-response.

The PF gene circuit was induced at 12 doxycycline concentrations, 0, 0.02, 0.04, 0.05, 0.06, 0.08, 0.1, 0.15, 0.25, 0.5, 0.75 and 1 µg/ml; the histograms of yEGFP::ZeoR expression at each doxycycline concentration are shown. In each sample, cell culture was started with 0.5 x 10^6 cells/ml, and every 12 hours, cell density was measured by Nexcelom, and a small amount of cell culture was inoculated into fresh medium aiming to start new culture with the cell density of 0.5 x 10^6 cells/ml.

First, PF cells were induced with 12 different doxycycline concentrations, and flow cytometry was used to measure yEGFP::ZeoR expression in individual cells. At doxycycline concentrations 0 and 0.02 µg/ml, cells in the whole population showed minimal level of yEGFP::ZeoR expression. Starting at a doxycycline concentration of 0.04 µg/ml, a group of high yEGFP::ZeoR expressers appeared, making the fluorescence intensity histogram bimodal. With increased doxycycline concentration, the high peak grew while the low peak shrank. At a doxycycline concentration of 0.08 µg/ml, the majority of cells in the population already expressed a high level of yEGFP::ZeoR. When doxycycline concentration reached 0.5 µg/ml, the low peak almost disappeared and the histogram remained the same with further increase of doxycycline concentration until it reached 1 µg/ml (Figure 4.2).

Then the mean for the cell population at each doxycycline concentration was calculated, and plotted against doxycycline concentration. It had a sharp rise starting from doxycycline concentration 0.04 µg/ml until doxycycline reached 0.1 µg/ml, after which the increase of the mean slowed down compared to the beginning. The mean reached saturation when doxycycline concentration reached 0.5 µg/ml, which agreed well with the histogram (Figure 4.3 A). Next, the CV was calculated. It started low, and showed a very sharp increase starting at doxycycline concentration 0.04 µg/ml and reached a high peak at doxycycline concentration 0.08 µg/ml, where the bimodal distribution had two peaks of similar height. After reaching the peak, the CV showed a sharp decrease until doxycycline concentration reached 0.25 µg/ml, and then it flattened down at doxycycline concentration of 1 µg/ml.

A

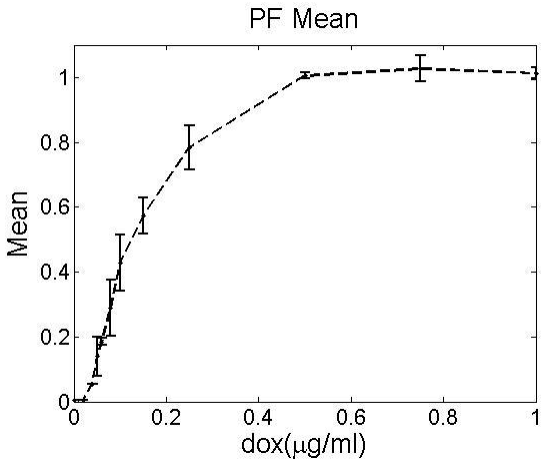

B

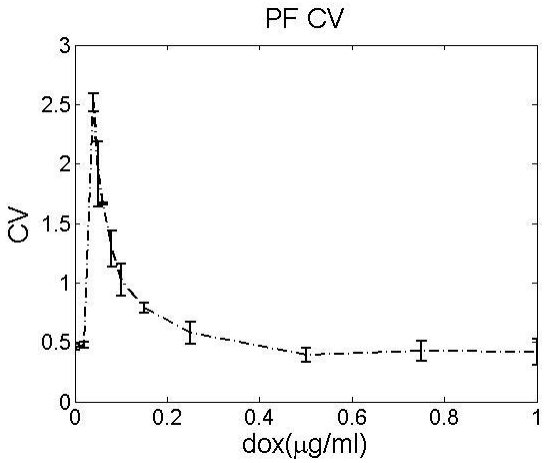

Figure 4.3 PF mean and CV dose-responses.

(A) Mean dose-response. (B) CV dose-response. Cells carrying PF gene circuit was induced by 12 doxycycline concentrations: 0, 0.02, 0.04, 0.05, 0.06, 0.08, 0.1, 0.15, 0.25, 0.5, 0.75 and 1 μg/ml. The plots show the average of 3 replicates. Error bars indicate the SD of the 3 replicates' mean value.

4.3 PFpump gene circuit and characterization of its dose-response

After obtaining the dose-response for the PF gene circuit, I wondered how the *PDR5* gene would change its dose-response. Therefore, the dose-response for the PFpump gene circuit was characterized with the same experimental procedure as for the PF gene circuit. In no doxycycline environment, all the cells in the population expressed uniformly low level of *PDR5::GFP*. When doxycycline concentration was increased to 0.02 µg/ml, a high *PDR5::GFP* expresser peak appeared, although the low expressers were the majority of the population. When doxycycline concentration reached 0.04 µg/ml, low expressers and high expressers showed almost equal peaks, meaning that the number of low expressers roughly equaled the number of high expressers. With further increase of doxycycline concentration, more cells switched to the high *PDR5::GFP* expression level from the low level, until it reached the concentration of 0.25 µg/ml, where all cells in the population became high expressers, and the histogram did not change with further increase of doxycycline (Figure 4.4).

Next, the mean and CV were calculated at each doxycycline concentration. From doxycycline 0.02 µg/ml to 0.1 µg/ml, the dose-response curve showed a steep rise, and then it slowed down with further increase of doxycycline concentration. The curve reached saturation around a doxycycline concentration of 0.25 µg/ml (Figure 4.5 A). The *PDR5::GFP* expression noise or CV peaked at doxycycline concentration 0.04 µg/ml, which corresponded well to the almost equal peaks in the reporter expression histogram with bimodal distribution. The CV was low at low and high doxycycline concentrations because all or majority of cells expressed either low or high *PDR5::GFP* in either case (Figure 4.5 B).

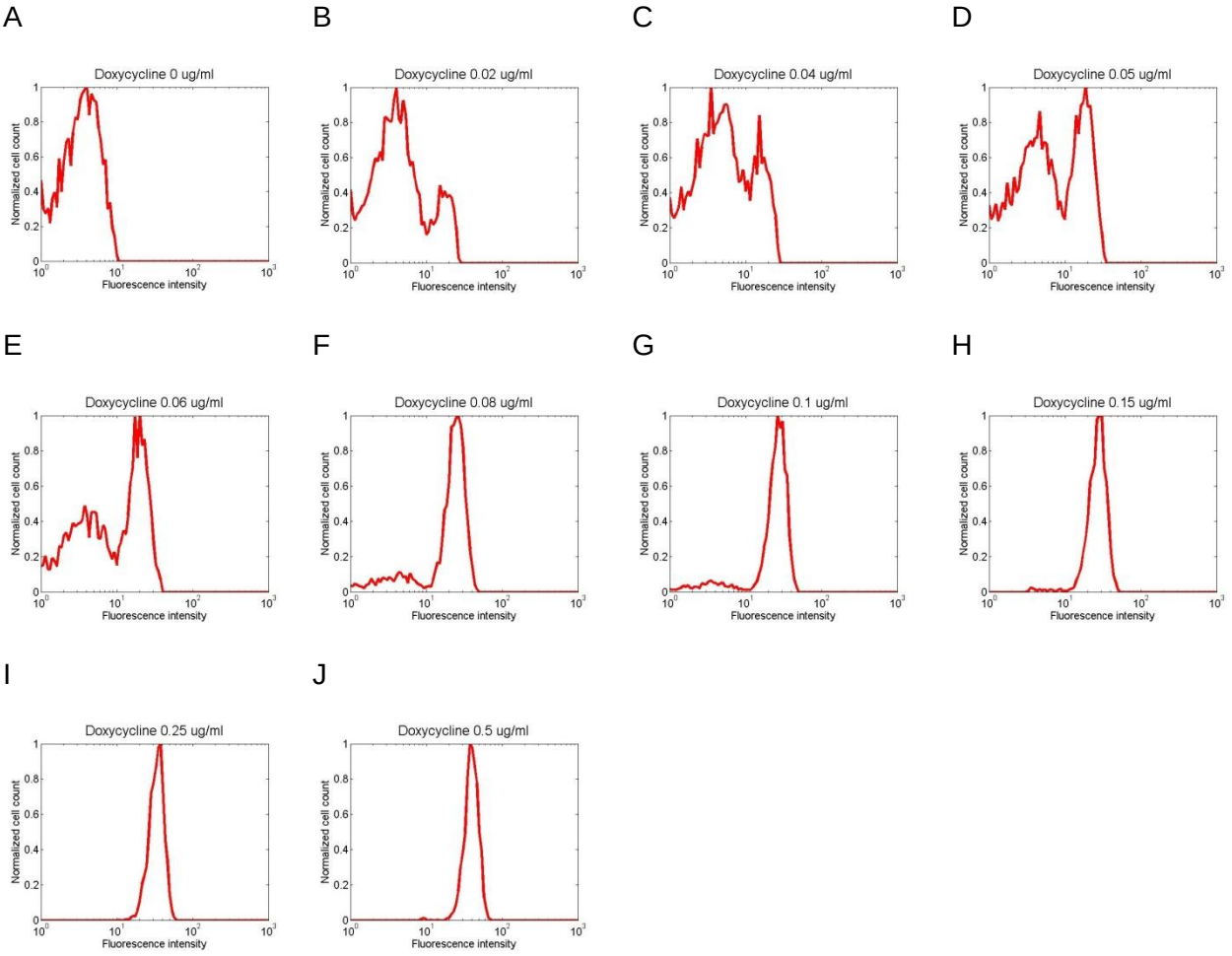

Figure 4.4 Histograms of PFpump dose-response.

The PF gene circuit was induced at 10 doxycycline concentrations, 0, 0.02, 0.04, 0.05, 0.06, 0.08, 0.1, 0.15, 0.25 and 0.5 µg/ml; the histograms of *PDR5::GFP* expression at each doxycycline concentration were shown. In each sample, cell culture was started with 0.5 x 10^6 cells/ml, and every 12 hours, cell density was measured by Nexcelom, a small amount of cell culture was inoculated into fresh medium aiming to start new culture with the cell density of 0.5 x 10^6 cells/ml.

A

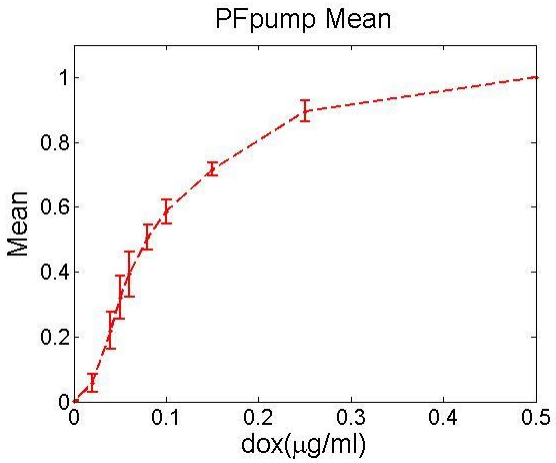

B

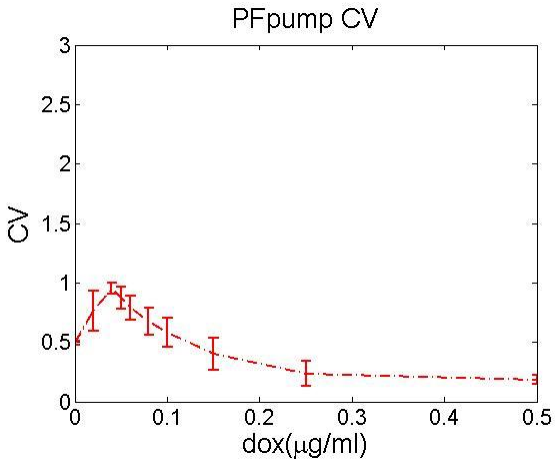

Figure 4.5 PFpump mean and CV dose-response.

(A) Mean dose-response. (B) CV dose-response. Cells carrying PFpump gene circuit were induced by 10 doxycycline concentrations: 0, 0.02, 0.04, 0.05, 0.06, 0.08, 0.1, 0.15, 0.25 and 0.5 μg/ml. The plots show the average of 3 replicates. The plots show the average of 3 replicates. Error bars indicate the SD of the 3 replicates' mean value.

A

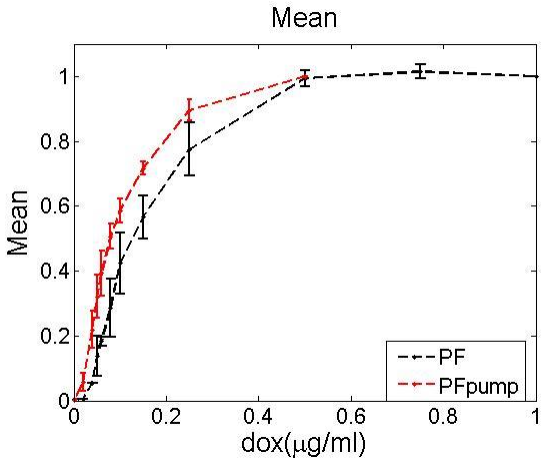

B

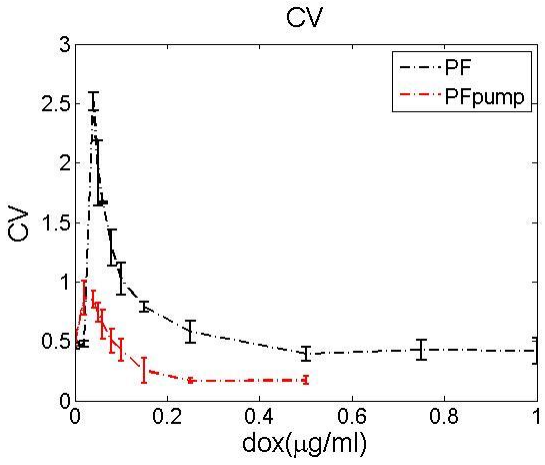

Figure 4.6 PF and PFpump mean and CV dose-response.

(A) Mean dose-responses. (B) CV dose-responses. The plots show the average of 3 replicates for each strain. Error bar indicate the SD of the 3 replicates' mean value.

Although the dose-response behaviors of PF and PFpump were similar, they had differences as well. The mean dose-response of PFpump was more sensitive to doxycycline compared to PF (Figure 4.6 A), which was consistent with the results from NR-NRpump and NF-NFpump comparison. The CV peak of PFpump appeared earlier than for PF, which might be due to the higher sensitivity of PFpump to doxycycline (Figure 4.6 B). The CV peak of PF was much higher than that of PFpump, probably because the GFP fluorescence intensity was higher in PF (Figure 4.6 B), or because PFpump incorporated negative feedback that lowers noise.

Comparing the histograms of PF and PFpump, I found that PF and PFpump differ at identical doxycycline concentration (Figure 4.7). For example, at doxycycline concentration 0.05 µg/ml, PFpump had higher percentage of high expressers compared to PF. First, I thought that the pump actively excludes doxycycline from the cells, so it would take higher doxycycline concentration for PFpump to reach the same percentage of high expressers as PF does (Figure 4.7). However, the experimental observation was quite contradictory. In order to explain the discrepancy, we decided to measure the growth rate and cellular memory of both low and high expressers in PFpump. Cellular memory was defined by the average time for each individual cell to stay in one gene expression state. Previous work showed that PF cells switch between the two subpopulations in the histogram. The cell growth rate and cellular memory was calculated for each subpopulation, and differed [81]. Since PFpump had bimodal expression as well, I wanted to determine its growth rate and cellular memory.

A

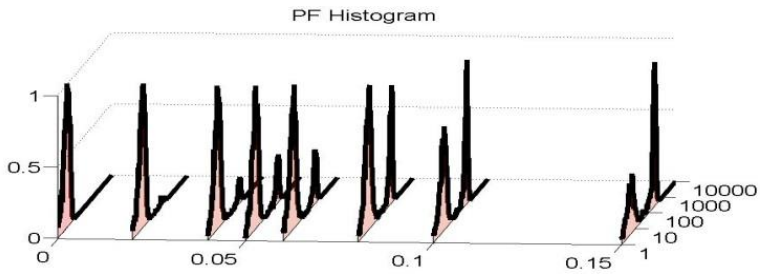

B

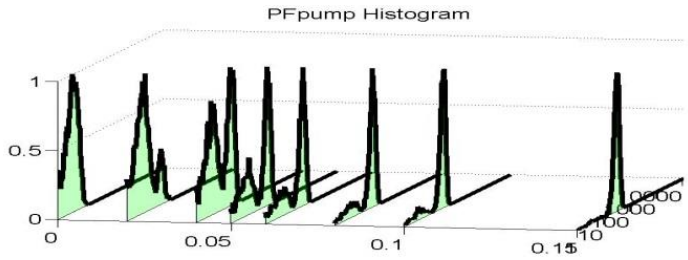

Figure 4.7 Histograms of target gene expression in PF and PFpump.

(A) PF cells induced in doxycycline. (B) PFpump cells induced in doxycycline. PF cells were induced by doxycycline concentrations 0, 0.02, 0.04, 0.05, 0.06, 0.08, 0.1, 0.15, 0.25, 0.5, 0.75 and 1 µg/ml. PFpump cells were induced by 10 doxycycline concentrations: 0, 0.02, 0.04, 0.05, 0.06, 0.08, 0.1, 0.15, 0.25 and 0.5 µg/ml.

4.4 Measurement of PFpump growth rate

First of all, I measured the growth rate for the two PFpump subpopulations. In order to do so, I induced the PFpump strain in SD medium with a doxycycline concentration of 0.05 µg/ml until gene expression became stable. Then the cell culture was sorted into high expressers and low expressers, the threshold used for the separation was the valley point on the histogram (Figure 4.4 C). Cell densities were measured every 2 hours for 24 hours and then every 12 hours for 96 hours for each of the subpopulations. The growth rate of PFpump cells induced at the same doxycycline concentration without cell sorting (mixed population) was measured as well. At the same time, PDR::GFP expression in each subpopulation was measured every 12 hours. Because the two subpopulations switch to each other, they should return to the original histogram before cell sorting. That was where the experiment ended. Data gathered through the experiments was used for computational estimation of growth rate. The growth rate for the two subpopulations and the mixed population were all decreasing with increasing doxycycline concentrations. However, the growth rate of high expressers decreased the most, while the growth rate of low expressers only showed slight decrease. The growth rate of the mixed population was intermediate, closer to the low expresser growth rate in low doxycycline concentration, but closer to high expresser growth rate once doxycycline concentration reached 0.05 µg/ml and beyond (Figure 4.8).

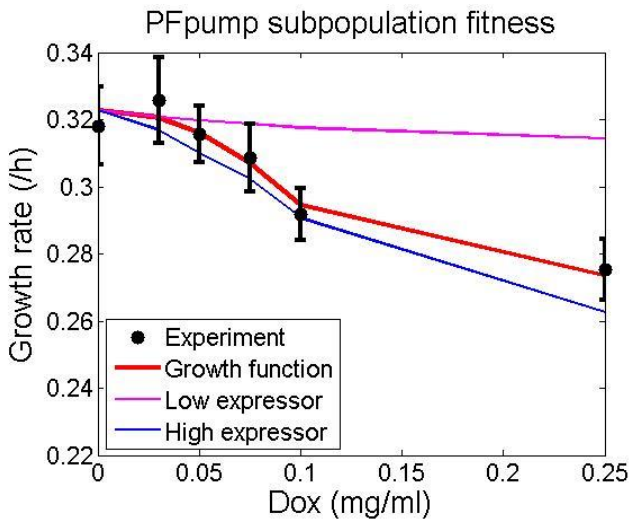

Figure 4.8 Growth rate properties of PFpump.

Computational estimation of the growth rate for low and high subpopulations. Parameters were obtained from experiments. Low and high subpopulations were separated by cell sorting, and grown in separate tubes containing SD mediums. Growth rate of cells in each tube and the whole cell population were measured every 2 hours until the reporter expression histogram recovered to the same as before sorting. The growth rate of the whole cell population was shown here, the growth rate for sorted cells were used to estimate the low and high expressors' growth rate.

A

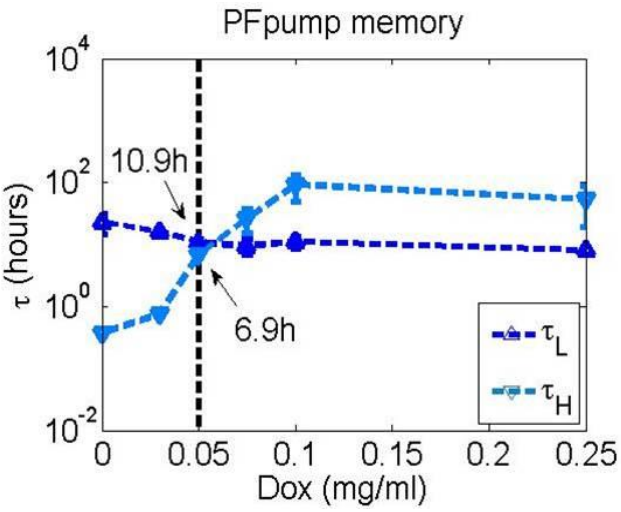

B

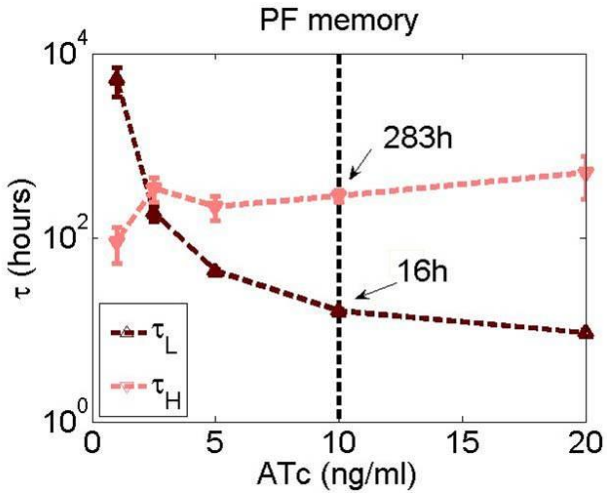

Figure 4.9 Cellular memories of the two subpopulations of PFpump and PF.

(A) PFpump cellular memory. (B) PF cellular memory [81]. The black dotted line in both figures indicated where the high expresser and low expresser plots were equal in the histogram.

4.5 Comparison of memory between PF and PFpump strains

Next, I investigated the cellular memory of PFpump. Computational estimation showed that the memory for the low expressers was 10.9 hours at doxycycline concentration 0.05 μg/ml, while that for the high expresser was 6.9 hours (figure 4.9). The memory of the low expressers remained relatively constant over the entire doxycycline concentration range, but the memory of high expressers increased from doxycycline concentration 0 to 0.1 μg/ml an remained constant afterwards (Figure 4.9). After obtaining the cellular memory of PFpump, we decided to compare it with PF and see if the efflux pump, Pdr5, would cause memory change. With data from previous work, I found that the cellular memory of low expressers was 16 hours at ATc concentration 10 ng/ml, at which the two subpopulations showed almost equal number of cells. However, the memory for high expressers was extremely high, 283 hours, at the same ATc concentration. Therefore, although low expressers and high expressers were in the same amount of cells in the population, the difference between their memories differed tremendously in PF and PFpump.

4.6 Conclusion and discussion

Here, I characterized the dose-response for PFpump for the first time. Although the dose-response of PF had been measured, it was induced by ATc. Since ATc is sensitive to light, and is not as stable as doxycycline, I re-characterized the PF dose response with doxycycline as inducer. Both PF and PFpump showed bimodal distribution at intermediate doxycycline concentrations, which suggested that the negative feedback loop introduced by Pdr5 did not interfere with a key fracture from positive feedback loop, bimodality. It is interesting to note that although negative feedback was shown to reduce the variability of steady states, PFpump still showed bimodality. Compared to the dose-response curves of NR and NF gene circuits, the

doxycycline concentrations used for PF and PFpump were much lower, indicating higher sensitivity of PF gene circuits. The PF and PFpump mean and CV dose-responses were similar. The mean dose-response increased sharply between low and intermediate doxycycline concentration, and then slowed down until the curves reached saturation at high doxycycline concentration, which was 0.25 μg/ml. Both CVs both had a single peak at intermediate doxycycline concentration, indicating diverse expression of target genes in individual cells in the population. However, PFpump cells were more sensitive to doxycycline than PF cells, proved by the fact that PFpump had higher mean than PF at the same doxycycline concentration (Figure 4.6). When I looked at the histograms for both strains, I found that higher percentage of PFpump cells became high expresser than PF cells at the same doxycycline concentration (Figure 4.7). This result was completely opposite to my expectation, because Pdr5 was an efflux pump, and it has been shown to pump out doxycycline [143, 146, 147]. Therefore, Pdr5 was expected to reduce intracellular doxycycline concentration and, as a result, PFpump cells were expected to have less high expresser than PF at the same doxycycline concentration. This contradictory discovery led us to think about previous work published in our lab about growth rate and cellular memory of the two subpopulations in PF strain. Growth rate referred to the cell growth rate, cellular memory was the average time an individual cell stayed in one stable steady state. The research showed that the two subpopulations grew at different rates, and their cellular memory differed tremendously. Therefore, I wondered if Pdr5 changed either the growth rate or cellular memory of the two subpopulations, or both. In order to answer this question, I measured the growth rate and cellular memory of the two subpopulations and mixed populations in PFpump. All of the three populations growth rate decreased with increasing of doxycycline concentration, which suggested that doxycycline caused the reduction of growth rate of PFpump cells. Low expressers only showed a slightly decrease of growth rate with increasing doxycycline concentration, which was the lowest reduction among the three populations. On the contrary, high expressers showed the highest reduction, which suggested that the expression of

PDR5::GFP reduced the cells' growth rate. Since the growth rate of PF cells had been characterized in our lab before, I wondered if Pdr5 changed the growth rate of cells bearing PF gene circuits. In order to test that, I compared my data from PFpump growth rate with previous data of PF growth rate. Because previous work on PF growth rate was done with ATc as inducer, here I needed to find the corresponding doxycycline concentration for ATc concentration used in previous work. In order to do that, I compared the histogram of PF induced by both ATc and doxycycline. When the PF cells were induced to show two equal peaks on the histogram, 10 ng/ml ATc or 0.08 µg/ml doxycycline was required (Figure 4.6 C and D). Therefore, we considered 10 ng/ml ATc and 0.08 µg/ml doxycycline to be equivalent. At an ATC concentration of 10 ng/ml, the overall growth rate of PF cells was reduced to 80% of the maximum growth rate, meaning the growth rate of cells without any inducer. More dramatically, the growth rate of high expressers was reduced to 70% of the maximum growth rate. Comparably, at doxycycline 0.08 µg/ml, the overall growth rate was above 90% of the maximum growth rate, while the growth rate for high expressers showed slightly slower than the overall growth rate (Figure 4.10 A and B). In summary, introduction of Pdr5 partially recovered the growth rate in PF high expressers. There are several possible explanations. According to previous research, the growth rate of PF cells was 0.22 division per hour in no induction condition, while the growth rate of PFpump was 0.32 division per hour in my study, and the absolute value of growth rate reduction to ATC 10 ng/ml or doxycycline 0.08 µg/ml for the two strains were both 0.015 division per hour. Therefore, it is possible that the reduction of growth rate was not relevant to what gene was expressing, meaning that the protein expression itself would reduce growth rate because it took more resources and utilize more energy in the cells. Second possibility was relevant to the efflux pumping activity of Pdr5. It has been discovered that yeast cells with endogenous Pdr5 knockout showed decreased growth rate compared to cells with normal native Pdr5 expression. The reason was that yeast cells generated metabolic wastes during their growth, and Pdr5 was able to pump out those toxic molecules. Thus, it was

possible that the expression of Pdr5 in PFpump cells reduced intracellular toxic molecules and gave PFpump cells an advantage for growth.

After obtaining the growth rate for the two subpopulations of PFpump cells, cellular memory of the two subpopulations were also calculated, because growth rate and cellular memory were the two factors that contributed to the bimodal histograms of PF and PFpump cells. Previous research had identified the cellular memory for the two subpopulations of PF cells. Here I measured the cellular memory of PFpump cells and discovered that the memory for low expressers was close to that of PF cells. However, the memory for high expressers in PFpump cells was much shorter compared to their counterparts in PF cells. One possible explanation was the efflux pumping activity of Pdr5. Since Pdr5 was able to pump out doxycycline, which was supposed to lower intracellular doxycycline concentration and therefore facilitated the back switch of high expressers to low expressers. Second explanation might be that Pdr5 affected the concentration of rtTA. In Chapter 3, I discovered the correlation that the presence of Pdr5 lowered tetR concentration. rtTA used here in PF and PFpump cells was a fusion protein composed of tetR and VP16 transactivation domain, so it is possible that Pdr5 still affects the concentration rtTA.

4.7 Future direction

First of all, since Pdr5 was shown to lower TetR concentration in NR-NRpump and NF-NFpump dose-response comparison, it will be interesting to know if Pdr5 also affected rtTA concentration in PFpump cells, because rtTA is tetR protein fused with the transactivation domain of VP16. Construction of PF and PFpump strains with fluorescence labeled rtTA will be necessary for the investigation. If Pdr5 was proved to affect rtTA concentration, immune-

precipitation assay will be done to detect if there is direct interaction between Pdr5 and rtTA. Second, stochastic simulation will be done to reproduce experimental dose-response data.

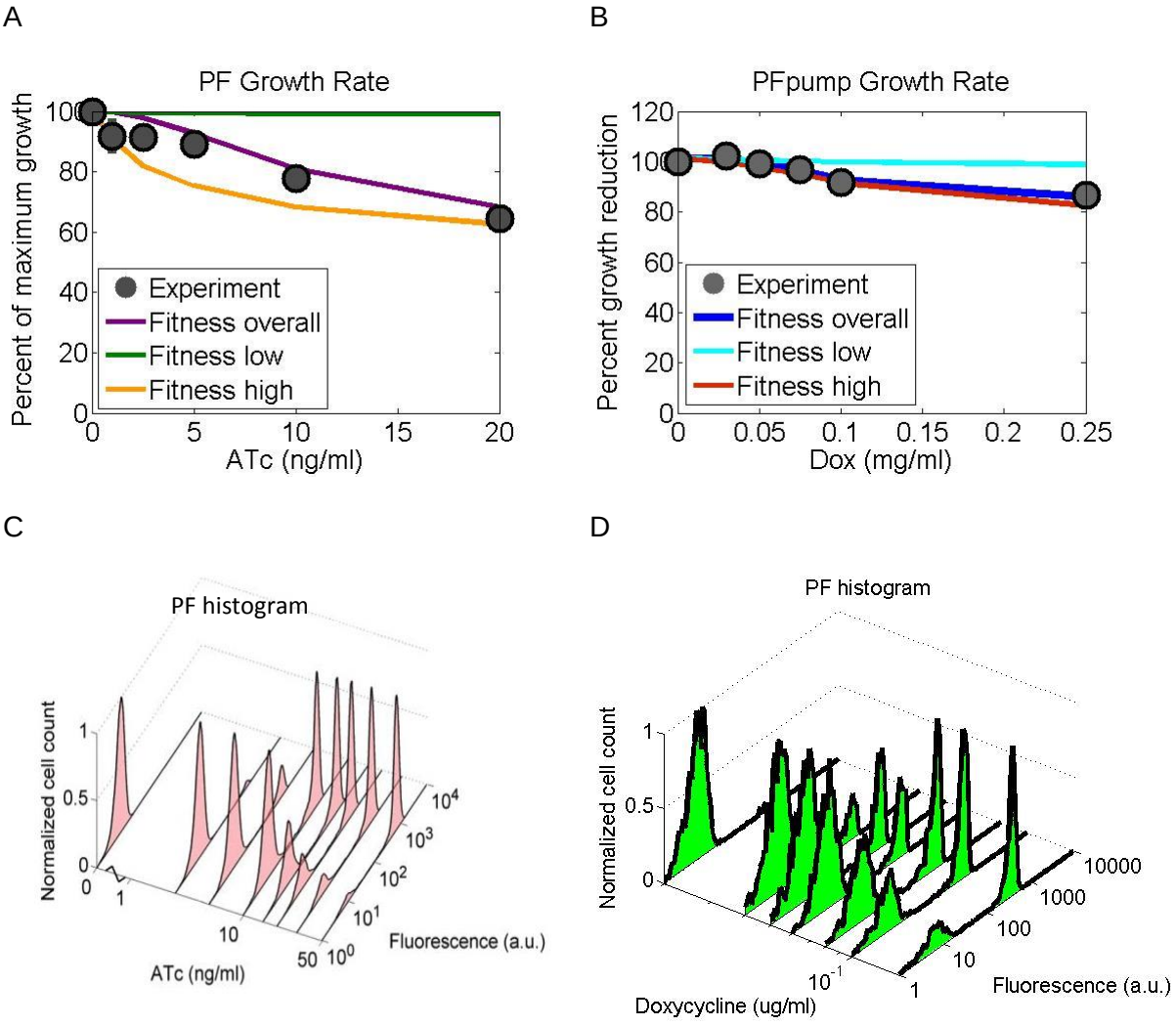

Figure 4.10 Growth rate comparisons between PF and PFpump.

(A) Growth rate of PF strain. Fitness overall refers to the PF population without cell sorting, mixture of low and high expressers. Fitness low refers to the growth rate of low expressers. (C) Fluorescence intensity histograms of PF induced by ATc. (D) Fluorescence intensity histograms of PF induced by doxycycline.

Chapter 5 Molecular evolution of NRpump, NFpump and PFpump strains

5.1 Introduction

PDR5 encodes a multidrug resistance protein, which functions as an efflux pump on the cell membrane in *Saccharomyces cerevisiae*. The natural *PDR5* gene transcription is under the control of Pdr1 and Pdr3 proteins. *PDR1* gene encodes a transcription factor that binds to the promoter of both *PDR3* and *PDR5* genes, and initiates their transcription after the binding. *PDR3* also encodes a transcription factor which is able to activate the transcription of itself and *PDR5* gene. Thus, Pdr3 forms a positive feedback loop to regulate *PDR5* transcription in the natural system. The presence of toxic molecules or drugs activates the expression of *PDR1*, which consequently leads to the transcription of both *PDR3* and *PDR5*; more *PDR3* expression will amplify the expression level of itself and *PDR5*, which form a positive feedback network. Once toxic molecules are pumped out by the Pdr5 protein, PDR1 returns to the normal level and as a consequence reduces Pdr3 and Pdr5 in the cells. Since the dose-response of the three gene circuits controlling *PDR5*, NRpump, NFpump and PFpump have been characterized, and were very different (shown in the previous chapters), I wondered if the three gene circuits would have different protection for the cell population in adverse environment. The result might be able to explain the evolution and natural selection of positive feedback loop in the regulation of *PDR5* transcription.

5.2 Pdr5 confers cells protection from fluconazole treatment

It has been shown that Pdr5 can pump out fluconazole and confer protection to the cells by the fact that the Δpdr5 strain was hypersensitive to fluconazole treatment [94]. Here I wanted to

confirm that the *PDR5::GFP* fused protein expressed in the gene circuits used in my study was able to confer resistance to fluconazole treatment as well. YPH500 and RFpump strains (Reference strain) were used for the test. YPH500 was the parental strain, on which all of the other strains were constructed based, by inserting specific synthetic gene circuits into its *HIS3* locus on the genome. Similarly, the RFpump strain was constructed by the integration of the RFpump gene circuit into the genome of the YPH500 strain. Similar to other pump gene circuits, the RFpump gene circuit also contains 2 parts, the regulator and the reporter. The regulator has a TetR gene under the control of wild type *GAL1* promoter, while the reporter has *PDR5::GFP* fused gene under control of the same wild type *GAL1* promoter (Figure 5.1). Therefore, no TetR binding sites were introduced in any of the promoter regions in RFpump gene circuit. As a result, PDR5::GFP will be expressed at a constant rate in the presence of galactose.

Next, survival of YPH500 and RFpump strains in fluconazole environment was tested. Six different fluconazole concentrations were used (0 µg/ml, 2 µg/ml, 4 µg/ml, 6 µg/ml, 8 µg/ml and 10 µg/ml) to treat both strains, while no fluconazole cultures were used as negative control. All of the cell cultures were resuspended every 12 hours to maintain their growth in exponential phase. When the YPH500 strain was cultured in 0 µg/ml fluconazole environment, its growth curve remained linear on semi log scale, because the cells kept growing in exponential phase during the entire experiment (Figure 5.2 A). However, in the presence of fluconazole, the YPH500 strain grew at a rate slightly slower than in no fluconazole environment in the first 12 hours, then the growth curve became flat, indicating a complete growth arrest (Figure 5.2 A). In contrast, the RFpump strain showed the same growth rate in all fluconazole concentrations and the negative control, indicated by the linear growth curves in all of the 6 conditions (Figure 5.2 B). In conclusion, *PDR5::GFP* was able to confer cells complete resistance to fluconazole concentration up to 10 µg/ml.

Figure 5.1 Composition of RFpump gene circuit.

In the PFpump gene circuit, both the TetR and the *PDR5::GFP* fusion gene were under control of the wild type Gal1 promoter, which was expressed constitutively in the presence of galactose. Therefore, RFpump expression was not doxycycline dependent.

A

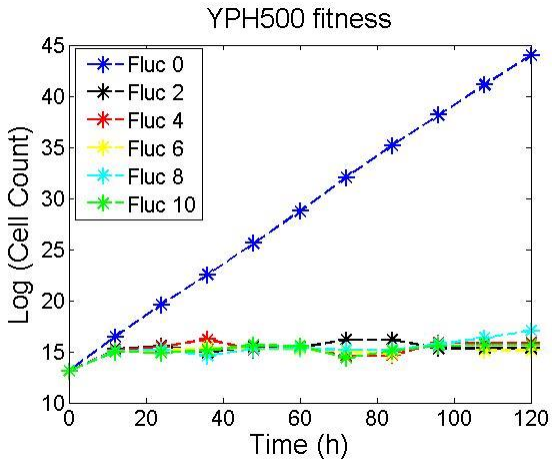

B

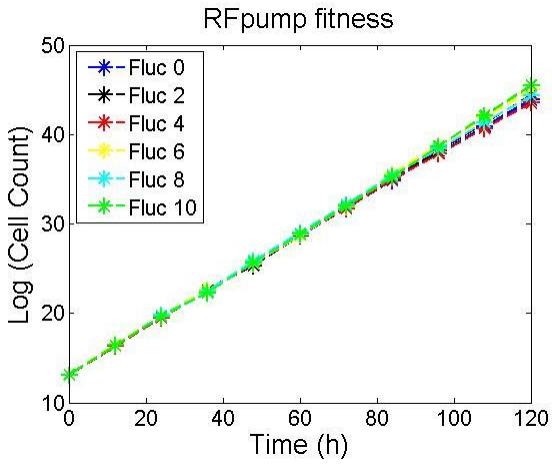

Figure 5.2 YPH500 and RFpump growth rate in the fluconazole concentrations of 0 – 10 µg/ml.

(A)YPH500 strain. (B) RFpump strain. Both strains were treated with 6 fluconazole concentrations: 0, 2, 4, 6, 8 and 10 µg/ml. In each sample, cell culture was started with 0.5 x 10^6 cells/ml, and every 12 hours, cell density was measured by Nexcelom, a small amount of cell culture based on the calculation was inoculated into fresh medium to start new culture with the cell density, 0.5 x 10^6 cells/ml. Cell count was plotted with the natural log as base.

5.3 NRpump and NFpump gene circuits evolved resistance to fluconazole treatment without induction

PDR5::GFP expression in the RFpump gene circuit was able to protect cells from fluconazole treatment in the previous experiment. Next I asked if Pdr5 under the control of NR, NF and PF gene circuits would give cells different survival advantages in the fluconazole environment. I have shown that NRpump, NFpump and PFpump gene circuits showed different distribution of Pdr5 expression under induction as discovered in the prior two chapters. However, the first step was to know how each synthetic gene circuit survives in the fluconazole environment without induction. Therefore, NRpump, NFpump and PFpump strains were treated with the same set of fluconazole concentrations as it was used for YPH500 and RFpump strains, but no doxycycline was added into the cell culture, meaning that only basal level Pdr5 in the gene circuits was expressed. The results of the three strains were all similar to YPH500 strain in the first 12 hours of fluconazole presence: the growth rate was slightly slowed down compared to no fluconazole cell culture (Figure 5.3). It has been found that fluconazole entered into the cells by diffusion, and it took at least 8 hours for the cells to respond (Data not shown). After the first 12 hours, the three strains showed different response patterns to fluconazole. Moreover, the three strains had different growth rates after 36 hours in fluconazole environment. The growth rate of NRpump first slowed down and became flat, suggesting the growth was completely ceased. Then the growth rate of the NRpump strain started to recover, and gradually went back to a level comparable to the cell culture in no fluconazole environment. This conclusion was supported by the fact that the growth rate curves of the 6 cell cultures became parallel after 48 hours (Figure 5.3 A). The curve of NFpump growth rate was similar to NRpump in that it first slowed down to flat after 24 hours culturing in fluconazole environment, and then recovered back to normal after 48 hours presence in fluconazole (including the no fluconazole control). Similar to NRpump cells, the growth rate of NFpump also recovered after a period of

fluconazole presence. However, differences remain. Unlike NRpump cells that had the same growth rate curve at different fluconazole concentration, NFpump cells responded differently. NFpump responded to lower fluconazole concentration (2 μg/ml) slower than NRpump did, indicated by the data that the growth rate of NFpump cells went flat after 24 hour in the fluconazole treatment, while it only took NRpump cells 12 hours to stop growing (Figure 5.3 A and B). No significant difference was observed for the response to fluconazole concentration higher than 2 μg/ml between NFpump cells and NRpump cells. On the contrary, the growth rate of PFpump cells became flat after 12 hours in all fluconazole concentrations (except 0 μg/ml), and the growth rate remained extremely low during the entire time with treatment.

Since the growth rates of NRpump and NFpump went back to normal after 48 hours presence in the fluconazole environment, I wondered if the recovery was caused by Pdr5 expression from the synthetic gene circuits. In order to test that, I measured PDR::GFP expression in the NRpump and NFpump cells by flow cytometry. The histograms showed that 48 hours after fluconazole treatment, Pdr5 was expressed at high level in every cell in the NRpump population at all the fluconazole concentrations, compared to basal expression of Pdr5 in the no fluconazole treatment control group (Figure 5.4 A). The histograms for NFpump showed similar pattern. The only difference was that at a fluconazole concentration of 2 μg/ml, NFpump showed bimodal distribution in the histogram with most of the cells in the population expressing high level of Pdr5 while only a small fraction remained Pdr5 low expressers (Figure 5.4 B). Since negative feedback loop has been proved to reduce gene expression noise, the bimodal distribution was highly likely due to two distinct subpopulations. This result suggested three possibilities for the fluconazole resistant cells. 1) The bimodal distribution was due to stochastic switching of cells. Even in the NF strains, there is a very small amount cells expressing high level of Pdr5, which could have taken over the whole cell population in the fluconazole treatment. 2) A single mutation might have occurred that made cells switch back

and forth in two Pdr5 expression states as PF and PFpump cells do. A mutation that weakened TetR function will lead to this stochastic switching. 3) The existence of a fluconazole resistant NFpump subpopulation without Pdr5 expression, which suggested the involvement of other factors in fluconazole resistance appeared in NFpump strains.

A

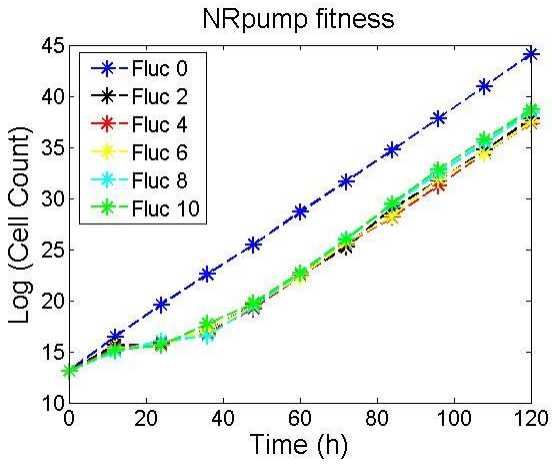

B

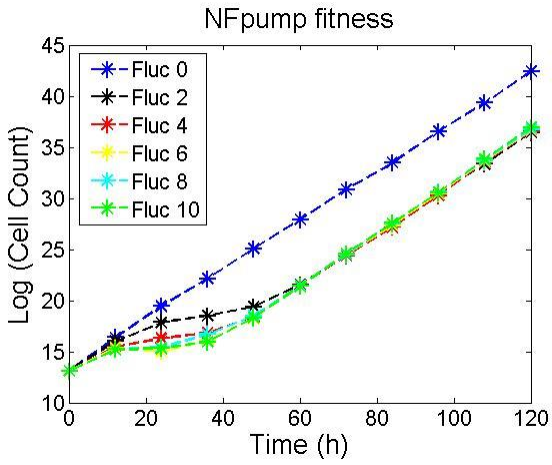

C

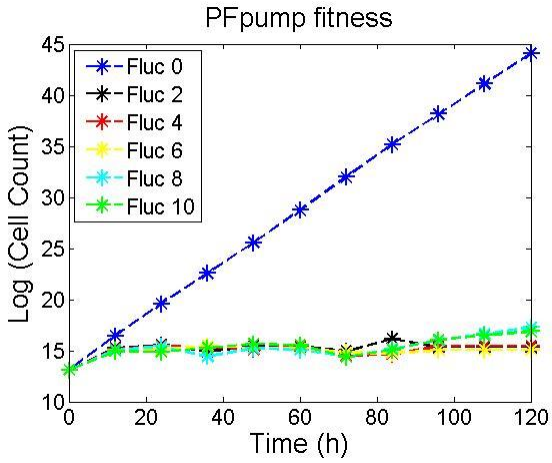

Figure 5.3 NRpump, NFpump and PFpump growth rate in the fluconazole concentrations of 0 – 10 µg/ml.

(A) NRpump strain. (B) NFpump strain. (C) PFpump strain. All the three strains were treated with 6 fluconazole concentration: 0, 2, 4, 6, 8 and 10 µg/ml. In each sample, cell culture was started with 0.5 x 10^6 cells/ml, and every 12 hours, cell density was measured by Nexcelom, a small amount of cell culture based on the calculation was inoculated into fresh medium to start new culture with the cell density, 0.5 x 10^6 cells/ml. Cell growth rate was then calculated and plotted. Cell count was plotted with the natural log as base.

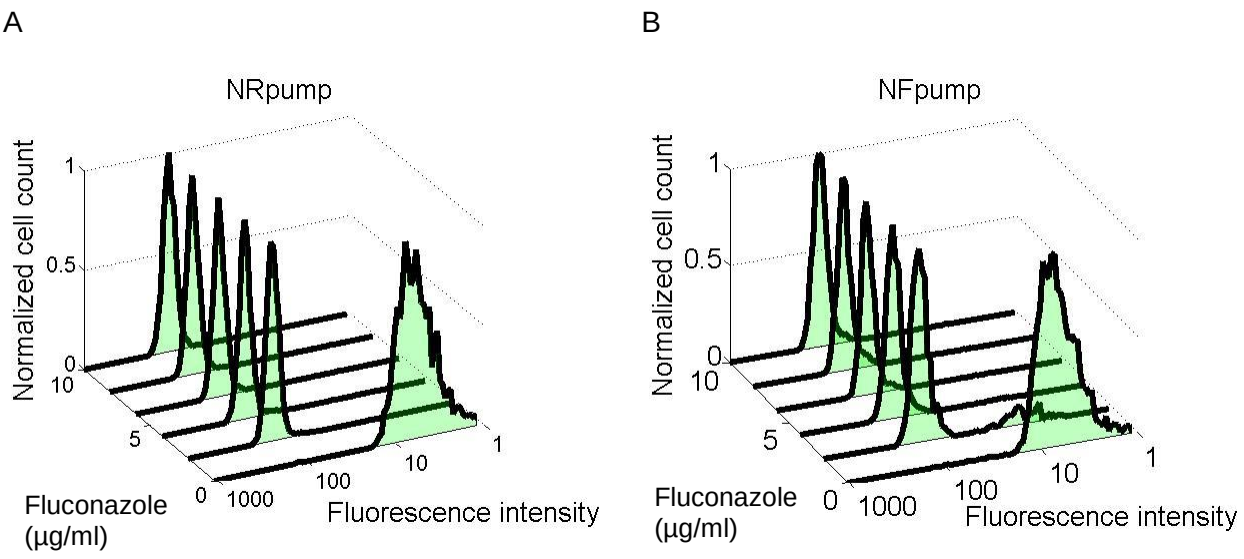

Figure 5.4 PDR5 expression histograms of NRpump and NFpump at 48th hour in the fluconazole concentrations of 0 – 10 µg/ml.

(A) NRpump strain. (B) NFpump strain. Both strains were treated with 6 fluconazole concentration: 0, 2, 4, 6, 8 and 10 µg/ml. In each sample, cell culture was started with 0.5 x 10^6 cells/ml, and every 12 hours, cell density was measured by Nexcelom, a small amount of cell culture based on the calculation was inoculated into fresh medium to start new culture with the cell density, 0.5 x 10^6 cells/ml. PDR5::GFP expression was measured by flow cytometry every 24 hours.

A

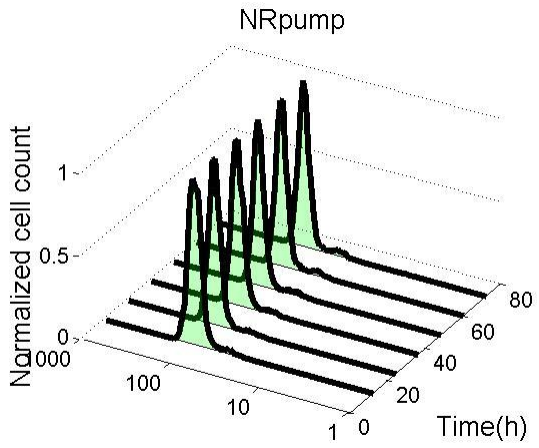

B

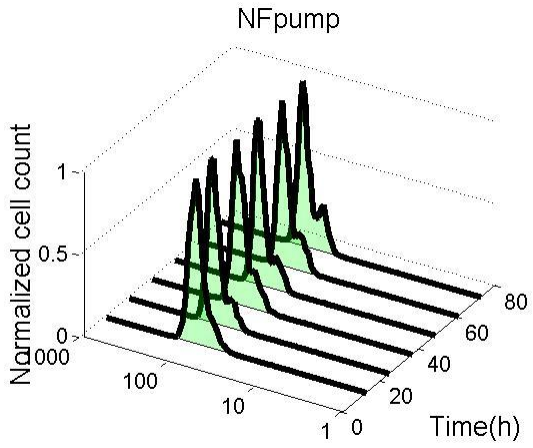

Figure 5.5 PDR5 expression histograms of NRpump and NFpump after the fluconazole removal.

(A) NRpump strain. (B) NFpump strain. Both strains were first cultured in SD medium with a fluconazole concentration of 10 µg/ml until *PDR5::GFP* expression was confirmed from the gene circuits by flow cytometry. Then the NRpump and NFpump cells cultured in SD medium without fluconazole for 72 hours. In each sample, cell culture was started with 0.5 x 10^6 cells/ml, and every 12 hours, cell density was measured by Nexcelom, a small amount of cell culture based on the calculation was inoculated into fresh medium to start new culture with the cell density, 0.5 x 10^6 cells/ml. *PDR5::GFP* expression was measured by flow cytometry every 24 hours.

It was unexpected to discover that *PDR5::GFP* from NRpump and NFpump gene circuits was expressed in the fluconazole environment in the absence of any tetracycline family inducer. Two possibilities existed. First, could cause cells to switch from low Pdr5 expression status to high Pdr5 expression status without changing their genomes. The bimodal distribution of NFpump in a fluconazole concentration of 2 µg/ml confirmed existence of two sub-populations, so I wondered if these two subpopulations would switch to each other as PF and PFpump strains showed in the last chapter. Second possibility for Pdr5 expression from the NRpump and NFpump gene circuits was the breakdown of the two gene circuits. *PDR5* was under the control of modified a *GAL1* promoter in both NRpump and NFpump gene circuits, so that *PDR5* transcription was repressed by TetR unless tetracycline family molecules were present. If TetR lost its repression capacity by genetic mutation or the modified *GAL1* promoter changed the sequence of TetO sites, which TetR protein binds, the transcription of *PDR5::GFP* would have no repression, and as a consequence, Pdr5 would be expressed in the absence of doxycycline. In order to test these two possibilities, both NRpump and NFpump strains were first treated with 10 µg/ml fluconazole for 48 hours, and then they were switched to the no fluconazole environment and cultured in the same condition for 84 hours. As expected, the histograms of NRpump showed high *PDR5::GFP* expression after 48 hours (data not shown). Moreover, the histograms remained the same at every time point after fluconazole removal until the 84th hour (Figure 5.5 A). Similarly, the histograms of NFpump did not show significant change either after fluconazole removal. They only showed a small peak that was slightly lower than the original high Pdr5 expression peak. The new peak grew higher over time, but it was still a small fraction compared to the majority of the cells that expressed higher Pdr5 than the basal levl (Figure 5.5 B). These results suggested that the expression of *PDR5::GFP* form NRpump and NFpump gene circuits were possibly due to the gene circuits' breakdown. DNA sequence data is still needed for confirmation.

After identification of fluconazole response curves for NRpump and NFpump, I noticed that even cells treated with the lowest fluconazole concentration, 2 μg/ml, showed full resistance, which made me to wonder if lower fluconazole concentration would induce a different response, such as NFpump cells in a fluconazole concentration of 2 μg/ml (Figure 5.4). Therefore, a new set of fluconazole concentrations were used to treat NRpump and NFpump strains. For NRpump strain, fluconazole concentrations below 0.6 μg/ml did not cause distinguishable difference on its growth rate compared to cells growing in no fluconazole environment. NRpump cells treated with a fluconazole concentration of 0.8 μg/ml showed a reduced growth rate starting at the 48th hour after fluconazole presence, but their growth rates recovered back to normal level after 120 hours in the fluconazole treatment. The growth rate of NRpump cells growing in fluconazole concentrations of 1.0 μg/ml and 1.5 μg/ml both slowed down after 24 hours treatment, cells in the fluconazole concentration of 1.0 μg/ml recovered their growth rate after 60 hours in the treatment, while it took cells in the fluconazole concentration of 1.5 μg/ml additional 12 hours to recover its growth rate back to the normal level (Figure 5.6 A). The growth rate of NFpump cells did not show distinguishable difference up to fluconazole concentration 1.0 μg/ml. Cells in a fluconazole concentration of 1.5 μg/ml showed decreased growth rate after 60 hours in the fluconazole environment, which was similar to NRpump in a fluconazole concentration of 0.8 μg/ml. The reduced growth rate recovered back to normal after 84 hours in the treatment (Figure 5.6 B). The comparison between NRpump and NFpump suggested that NRpump cells had higher sensitivity to fluconazole than NFpump cells did, which might relate to their different basal expression. Because it has been shown that NF has higher basal reporter expression than NR does in the previous research in our lab, and this higher expression was able to confer significant difference in cells' resistance to drug treatment.

Besides measuring the growth rate of NRpump and NFpump cells in the new set of fluconazole concentrations (0 μg/ml to 1.5 μg/ml), I also measured their *PDR5::GFP* expression

at each fluconazole concentration from 48 hours to 120 hours in the fluconazole treatment. From the fluconazole concentrations 0 µg/ml to 0.6 µg/ml, all the NRpump cells in the population expressed at basal level Pdr5 at all the time points. However, from fluconazole concentrations 0.8 µg/ml to 1.5 µg/ml, the histograms showed bimodal distribution, indicating a fraction of cells in the population became Pdr5 high expressers. The fraction of high expressers increased with the increase of fluconazole concentrations (Figure 5.7). By contrast, cells treated with a fluconazole concentration of 1.5 µg/ml showed an increased fraction of low expressers in the histograms with time passing by (Figure 5.7. This result suggested other resistance mechanism to fluconazole existed along with increased Pdr5 expression from the gene circuit in NRpump cells.

A

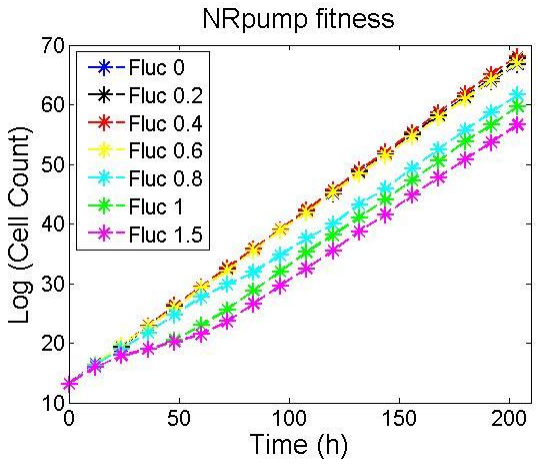

B

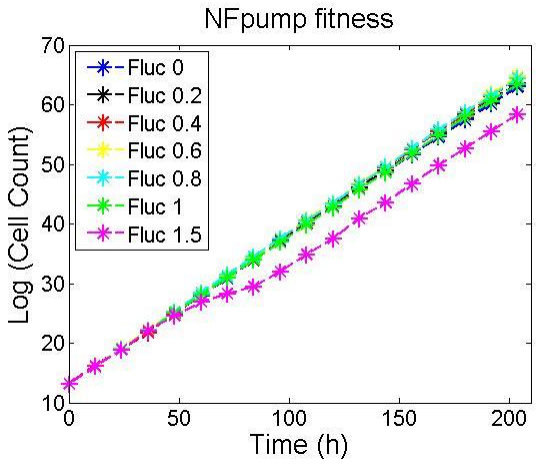

Figure 5.6 NRpump and NFpump Growth rate in the fluconazole concentrations of 0 – 1.5 µg/ml.

(A) NRpump strain. (B) NFpump strain. Both strains were cultured in 7 different fluconazole concentrations: 0, 0.2, 0.4, 0.6, 0.8, 1 and 1.5 µg/ml. In each sample, cell culture was started with 0.5 x 10^6 cells/ml, and every 12 hours, cell density was measured by Nexcelom, a small amount of cell culture based on calculated was inoculated into fresh medium to start new culture with the cell density, 0.5 x 10^6 cells/ml. Cell growth rate was then calculated and plotted. *PDR5::GFP* expression was measured by flow cytometry every 24 hours. Cell count was plotted with the natural log as base.

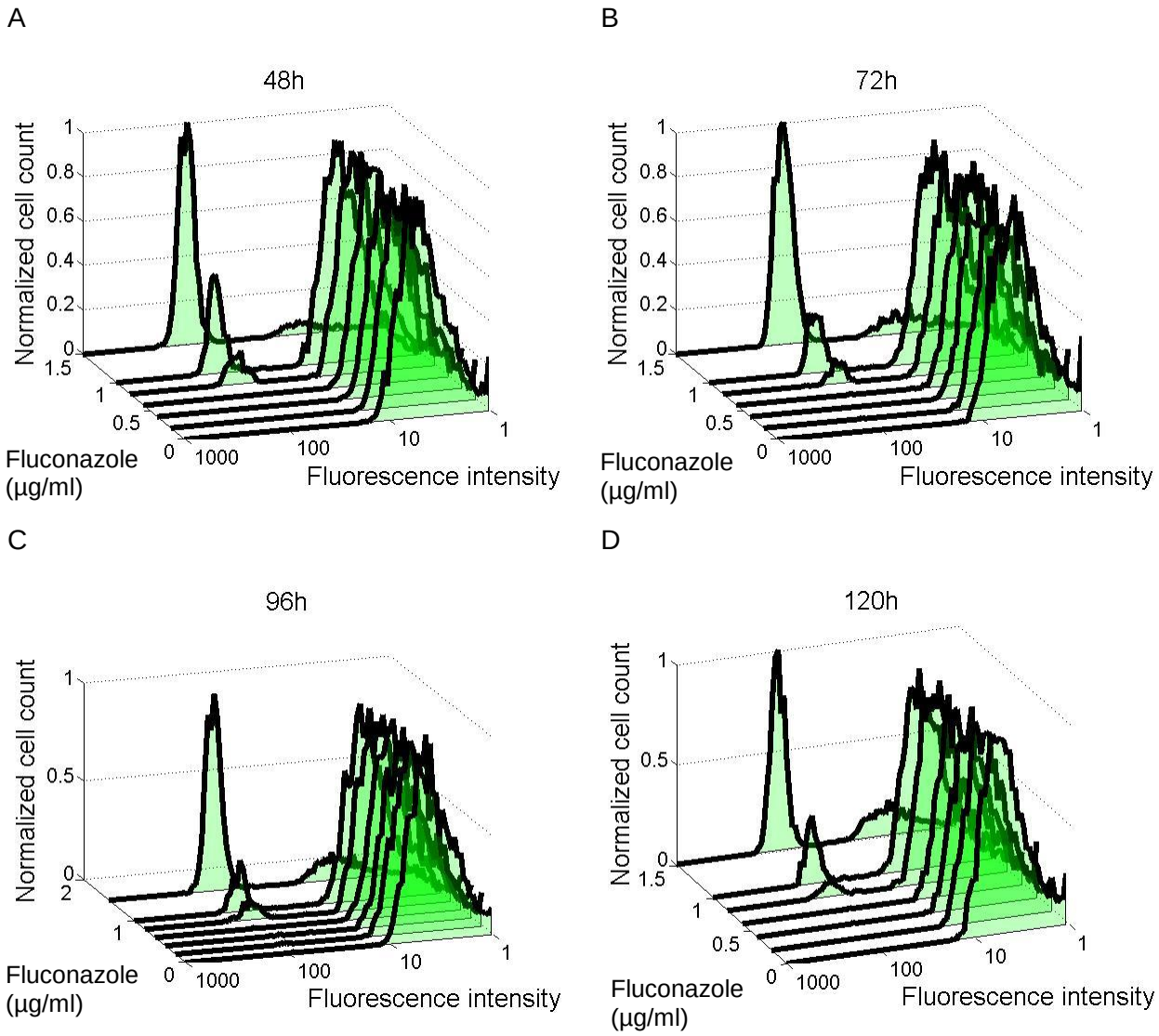

Figure 5.7 NRpump histograms in fluconazole concentrations of 0 – 1.5 µg/ml.

(A) 48 hours after the fluconazole treatment. (B) 72 hours after the fluconazole treatment. (C) 96 hours after the fluconazole treatment. (D) 120 hours after the fluconazole treatment. NRpump cells were cultured in 7 different fluconazole concentrations: 0, 0.2, 0.4, 0.6, 0.8, 1 and 1.5 µg/ml. In each sample, cell culture was started with 0.5 x 10^6 cells/ml, and every 12 hours, cell density was measured by Nexolum, a small amount of cell culture based on the calculation was inoculated into fresh medium to start new culture with the same cell density, 0.5 x 10^6 cells/ml. Cell growth rate was then calculated and plotted. *PDR5::GFP* expression was measured by flow cytometry every 24 hours.

PDR5:GFP expression was also measured in the new set of fluconazole concentration treatment in NFpump cells. From fluconazole concentrations 0 µg/ml to 0.8 µg/ml, the histograms only showed one peak composed of low Pdr5 expressers, indicating only basal Pdr5 expression in the whole population. At a fluconazole concentration of 1 µg/ml, a small peak showed up in the high fluorescence intensity zone, indicating small fraction of cells expressing high level of Pdr5. When fluconazole concentration reached 1.5 µg/ml, the vast majority of cells became high Pdr5 expressers with only a very small percentage of cells remaining as low expressers. When the fluconazole dose-responses of NRpump and NFpump were compared, differences were revealed. For example, from fluconazole concentrations 1.0 µg/ml to 1.5 µg/ml, the gradually increased fraction of low expressers in NRpump cells did not show up in NFpump cells. Instead, NFpump cells jumped to entirely high Pdr5 expressers from the distribution with majority of low Pdr5 expressers. The results suggested a gap between fluconazole concentrations 1.0 µg/ml and 1.5 µg/ml that might be able to induce bimodal distribution in NFpump cells.

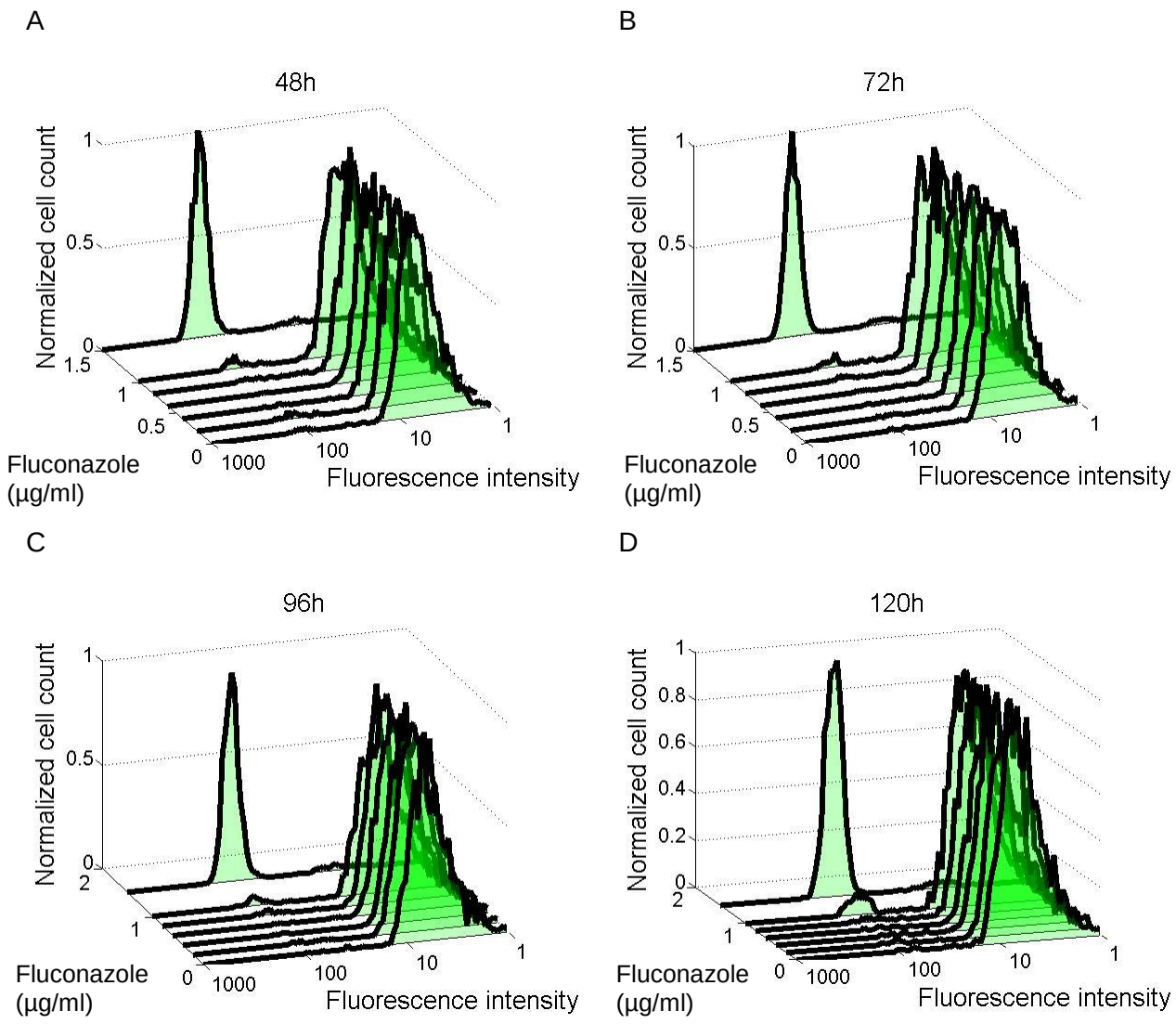

Figure 5.8 NFpump histograms in the fluconazole concentrations of 0 – 1.5 µg/ml.

(A) 48 hours after the fluconazole treatment. (B) 72 hours after the fluconazole treatment. (C) 96 hours after the fluconazole treatment. (D) 120 hours after the fluconazole treatment. NFpump cells were cultured in 7 different fluconazole concentrations: 0, 0.2, 0.4, 0.6, 0.8, 1 and 1.5 µg/ml. In each sample, cell culture was started with 0.5 x 10^6 cells/ml, and every 12 hours, cell density was measured by Nexcelom, a small amount of cell culture based on the calculation was inoculated into fresh medium to start new culture with the same cell density, 0.5 x 10^6 cells/ml. Cell growth rate was then calculated and plotted. *PDR5::GFP* expression was measured by flow cytometry every 24 hours.

So far, I identified the range of fluconazole concentrations to induce Pdr5 expression in NRpump and NFpump, but there was a gap in the histogram between fluconazole 1 μg/ml and 1.5 μg/ml, especially in NFpump cells. I wanted to further narrow down the concentrations to characterize the fluconazole dose-response change by fluconazole. Therefore, another set of fluconazole concentrations (0, 0.8, 1.0, 1.1, 1.2, 1.3, 1.4, 1.5, 1.7 and 2.0 μg/ml) was used to treat NRpump and NFpump cells. In the first 12 hours after treatment, NRpump cells in all the fluconazole concentrations expressed low level of Pdr5 and the expression was uniform, indicated by single peak in the histogram. Starting at 24 hours after treatment, NRpump cells in the fluconazole concentrations of 1 μg/ml and above showed slightly higher Pdr5 expression, and the cell number decreased compared to cells in the fluconazole concentrations of 0 and 0.8 μg/ml, indicating decreased growth rate. With longer fluconazole treatment, more cells at the fluconazole concentrations of 1 μg/ml and above turned into high Pdr5 expressers. During this transition, cells showed bimodal expression of Pdr5. NRpump cells treated with a fluconazole concentration of 0.8 μg/ml showed low Pdr5 expression level at the beginning of this experiment, but a portion of cells started to turn into high Pdr5 expressers after 60 hours in the treatment, the process lasted until 324 hours after fluconazole addition. This result showed that a fluconazole concentration of 1 μg/ml was also able to elicit Pdr5 expression from NRpump gene circuit, but at a much slower pace compared to cells treated with higher fluconazole concentrations. In this experiment, I noticed one very interesting phenomenon; cells treated with a fluconazole concentration of 1.1 μg/ml first turned from low expressers to high expressers, then they switched back to low expressers after 156 hours in the treatment. Then at 252^{th} hour after treatment, the low expressers started to switch to high expressers again until the whole population became completely high expresser at 348^{th} hour in the treatment, then the cells stayed as high expressers until the end of experiment, which was 396 hours in the fluconazole environment.

A

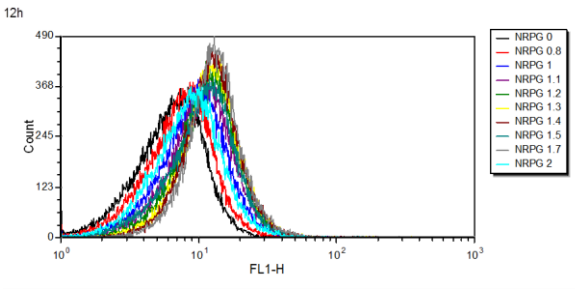
12h
Count
FL1-H
NRPG 0
NRPG 0.8
NRPG 1
NRPG 1.1
NRPG 1.2
NRPG 1.3
NRPG 1.4
NRPG 1.5
NRPG 1.7
NRPG 2

B

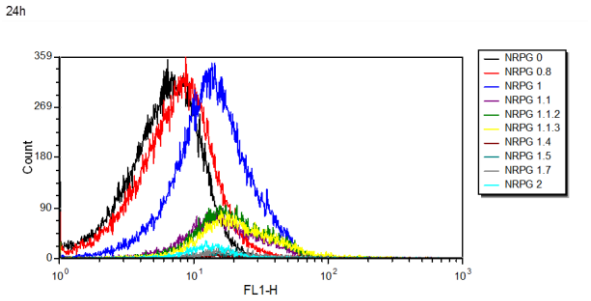
24h
Count
FL1-H
NRPG 0
NRPG 0.8
NRPG 1
NRPG 1.1
NRPG 1.1.2
NRPG 1.1.3
NRPG 1.4
NRPG 1.5
NRPG 1.7
NRPG 2

C

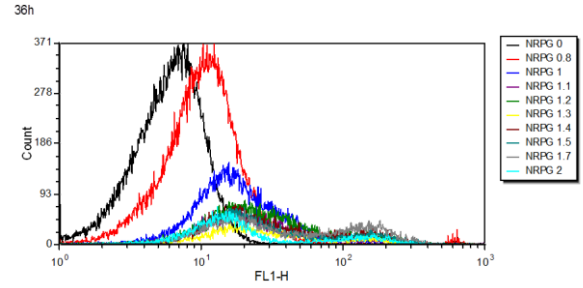
36h
Count
FL1-H
NRPG 0
NRPG 0.8
NRPG 1
NRPG 1.1
NRPG 1.2
NRPG 1.3
NRPG 1.4
NRPG 1.5
NRPG 1.7
NRPG 2

D

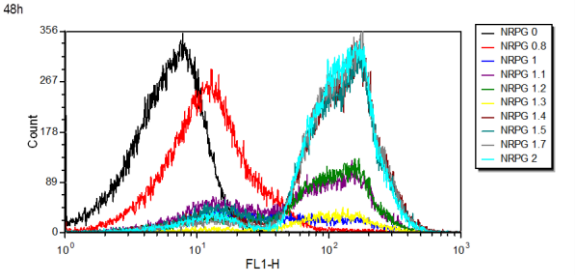
48h
Count
FL1-H
NRPG 0
NRPG 0.8
NRPG 1
NRPG 1.1
NRPG 1.2
NRPG 1.3
NRPG 1.4
NRPG 1.5
NRPG 1.7
NRPG 2

E

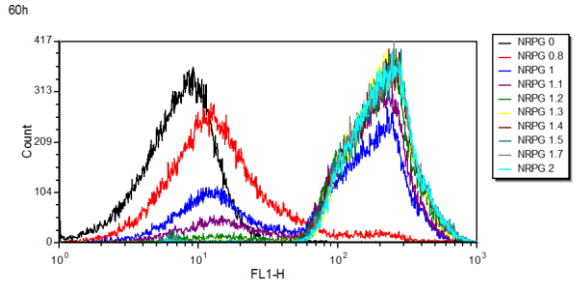
60h
Count
FL1-H
NRPG 0
NRPG 0.8
NRPG 1
NRPG 1.1
NRPG 1.2
NRPG 1.3
NRPG 1.4
NRPG 1.5
NRPG 1.7
NRPG 2

F

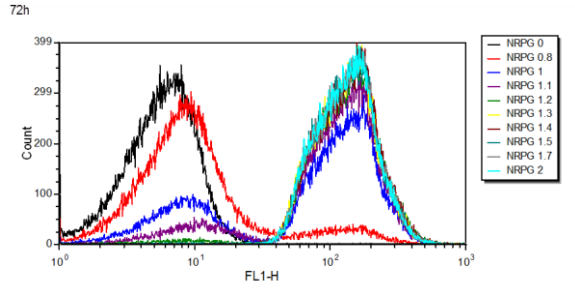
72h
Count
FL1-H
NRPG 0
NRPG 0.8
NRPG 1
NRPG 1.1
NRPG 1.2
NRPG 1.3
NRPG 1.4
NRPG 1.5
NRPG 1.7
NRPG 2

G

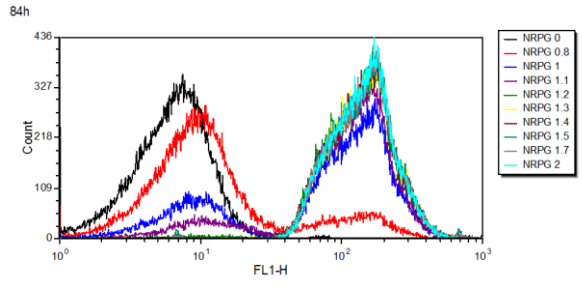
84h
Count
FL1-H
NRPG 0
NRPG 0.8
NRPG 1
NRPG 1.1
NRPG 1.2
NRPG 1.3
NRPG 1.4
NRPG 1.5
NRPG 1.7
NRPG 2

H

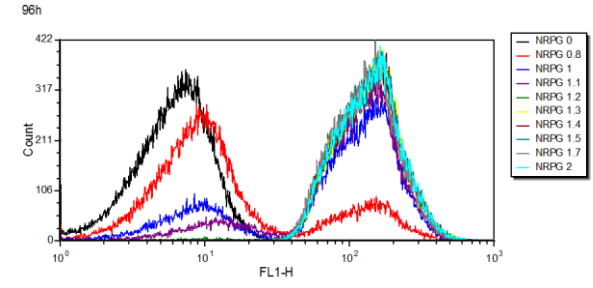
96h
Count
FL1-H
NRPG 0
NRPG 0.8
NRPG 1
NRPG 1.1
NRPG 1.2
NRPG 1.3
NRPG 1.4
NRPG 1.5
NRPG 1.7
NRPG 2

I

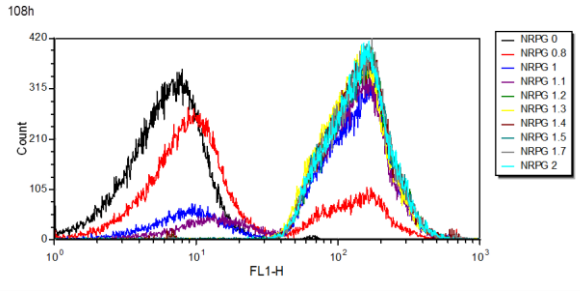
108h
Count
FL1-H
NRPG 0
NRPG 0.8
NRPG 1
NRPG 1.1
NRPG 1.2
NRPG 1.3
NRPG 1.4
NRPG 1.5
NRPG 1.7
NRPG 2

J

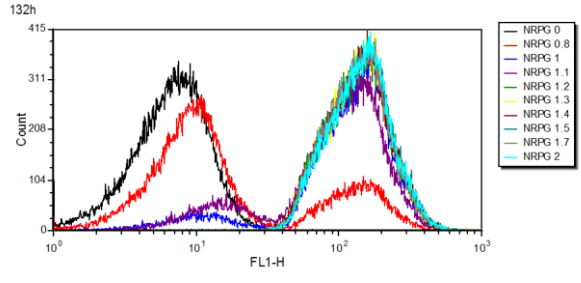
132h
Count
FL1-H
NRPG 0
NRPG 0.8
NRPG 1
NRPG 1.1
NRPG 1.2
NRPG 1.3
NRPG 1.4
NRPG 1.5
NRPG 1.7
NRPG 2

K

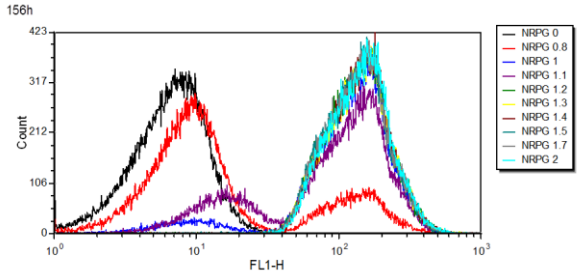
156h
Count
FL1-H
NRPG 0
NRPG 0.8
NRPG 1
NRPG 1.1
NRPG 1.2
NRPG 1.3
NRPG 1.4
NRPG 1.5
NRPG 1.7
NRPG 2

L

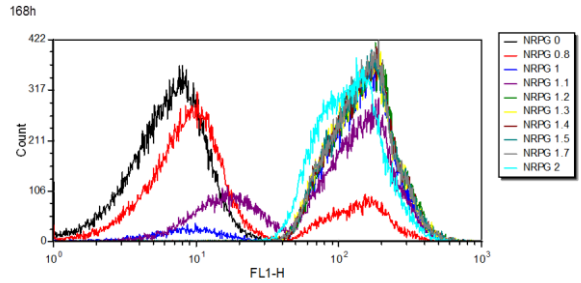
168h
Count
FL1-H
NRPG 0
NRPG 0.8
NRPG 1
NRPG 1.1
NRPG 1.2
NRPG 1.3
NRPG 1.4
NRPG 1.5
NRPG 1.7
NRPG 2

M

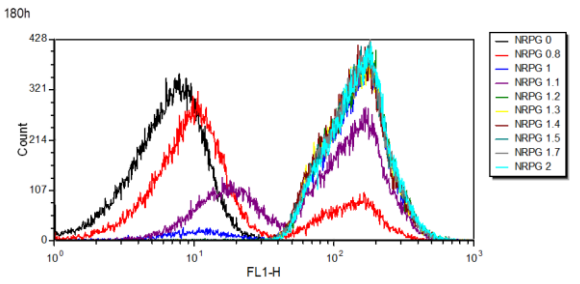
180h
Count
FL1-H
NRPG 0
NRPG 0.8
NRPG 1
NRPG 1.1
NRPG 1.2
NRPG 1.3
NRPG 1.4
NRPG 1.5
NRPG 1.7
NRPG 2

N

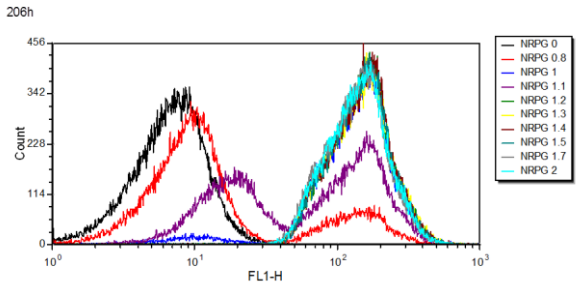
206h
Count
FL1-H
NRPG 0
NRPG 0.8
NRPG 1
NRPG 1.1
NRPG 1.2
NRPG 1.3
NRPG 1.4
NRPG 1.5
NRPG 1.7
NRPG 2

O

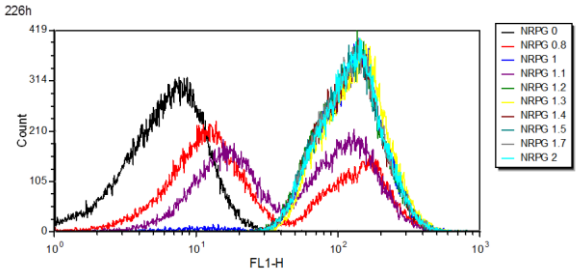
226h
Count
FL1-H
NRPG 0
NRPG 0.8
NRPG 1
NRPG 1.1
NRPG 1.2
NRPG 1.3
NRPG 1.4
NRPG 1.5
NRPG 1.7
NRPG 2

P

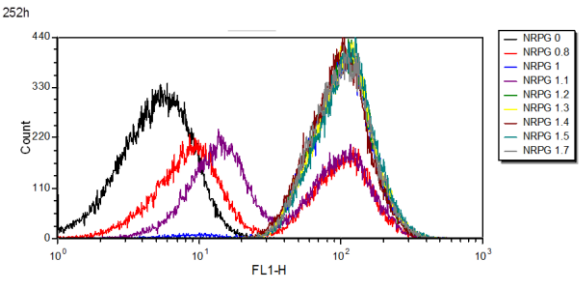
252h
Count
FL1-H
NRPG 0
NRPG 0.8
NRPG 1
NRPG 1.1
NRPG 1.2
NRPG 1.3
NRPG 1.4
NRPG 1.5
NRPG 1.7

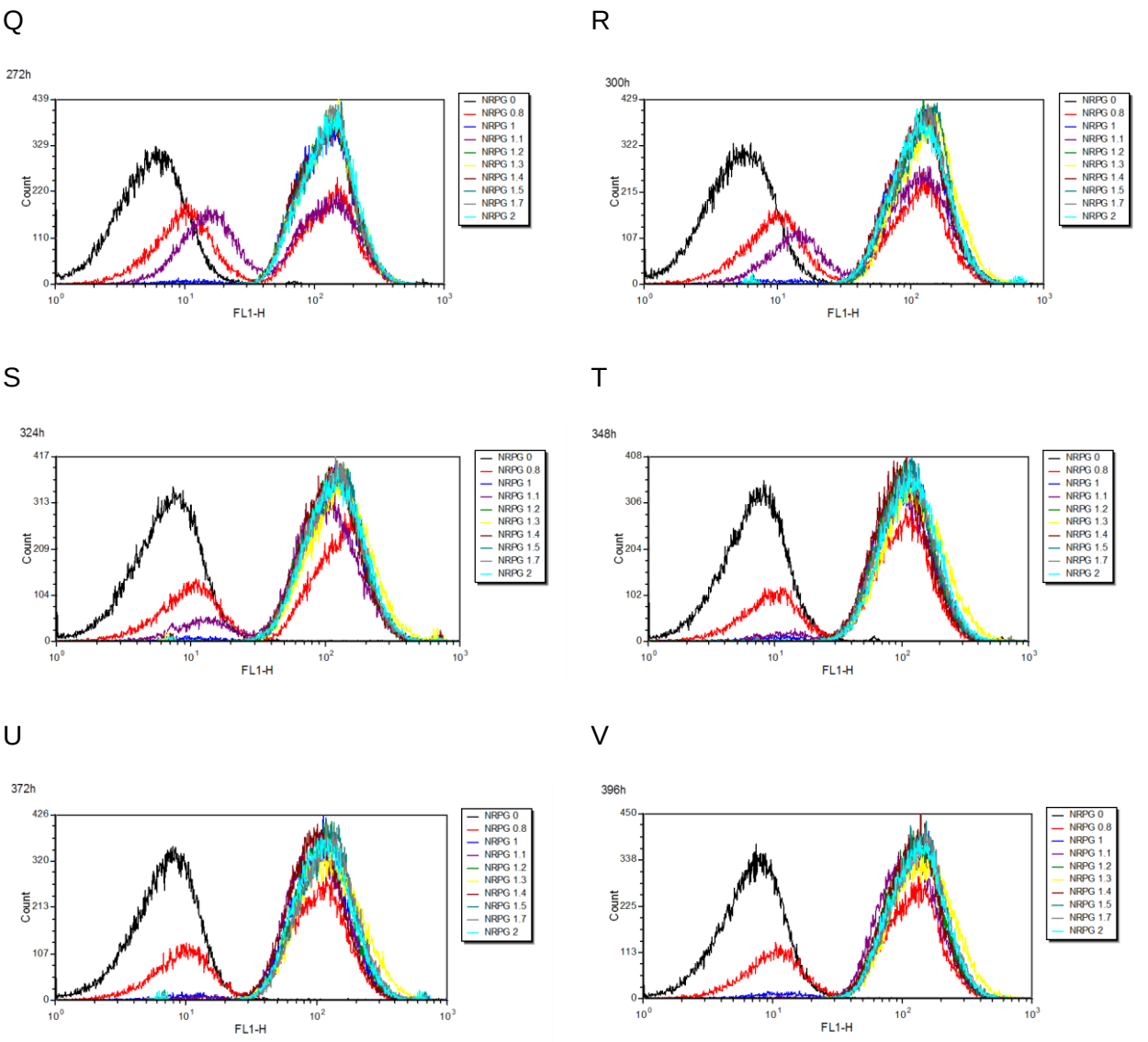

Figure 5.9 NRpump histograms in the fluconazole concentrations of 0 – 2 µg/ml.

(A) to (V) 12 hours after the fluconazole treatment to 396 hours after the treatment. Fluconazole concentrations used here were: 0, 0.8, 1, 1.1, 1.2, 1.3, 1.4, 1.5, 1.7 and 2 µg/ml. In each sample, cell culture was started with 0.5 x 10^6 cells/ml, and every 12 hours, cell density was measured by Nexolum, a small amount of cell culture based on the calculation was inoculated into fresh medium to start new culture with the same cell density, 0.5 x 10^6 cells/ml. Cell growth rate was then calculated and plotted. *PDR5::GFP* expression was measured by flow cytometry every 24 hours.

Next, I wanted to see if NFpump cells would show the same pattern in the new set of fluconazole treatment as NR did. The data showed that it took longer for NFpump cells to reposed to fluconazole compared to NRpump (Figure 5.10), and this result matched well with previous fluconazole treatment result, in which NFpump was more resistant to fluconazole than NRpump naturally (Figure 5.3). With longer fluconazole treatment, NFpump cells showed the same pattern as NRpump did: NFpump cells treated with fluconazole concentration 1 µg/ml and above gradually became high Pdr5 expressers from low expressers. However, cells treated with a fluconazole concentration of 0.8 µg/ml only began to show high Pdr5 expressers by 396 hours after the treatment, this took much longer compared to NRpump cells, which confirmed that NFpump was naturally more resistant to fluconazole than NRpump cells because of its high basal expression. Similar to NRpump cells, I also noticed that NFpump cells cultured in certain fluconazole concentration also switch forth and back and NRpump cells did, but the fluconazole concentration that induced this switch was different from NRpump. NFpump cells treated with 1.2 µg/ml switched from low Pdr5 expressers to high expressers with longer fluconazole treatment. Then the high expressers started to turn back to low expressers after 252 hours after the treatment, and the low expressers switched to high expressers again at 396th hour during fluconazole treatment. For NRpump and NFpump strains evolved in all these experiments above, frozen stocks were saved.

A

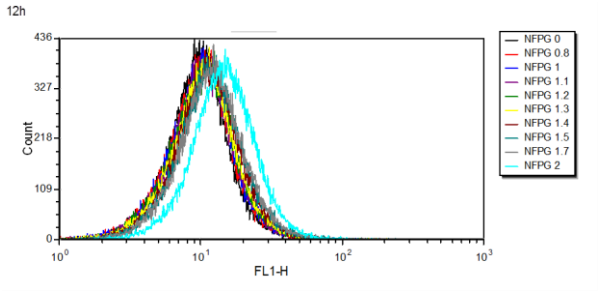
12h
Count
FL1-H
NFPG 0
NFPG 0.8
NFPG 1
NFPG 1.1
NFPG 1.2
NFPG 1.3
NFPG 1.4
NFPG 1.5
NFPG 1.7
NFPG 2

B

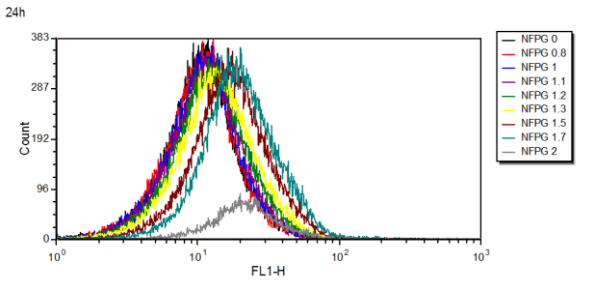
24h
Count
FL1-H
NFPG 0
NFPG 0.8
NFPG 1
NFPG 1.1
NFPG 1.2
NFPG 1.3
NFPG 1.5
NFPG 1.7
NFPG 2

C

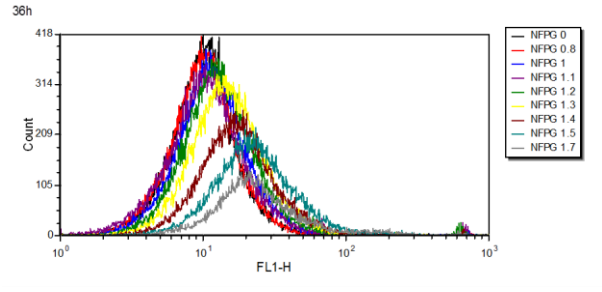
36h
Count
FL1-H
NFPG 0
NFPG 0.8
NFPG 1
NFPG 1.1
NFPG 1.2
NFPG 1.3
NFPG 1.4
NFPG 1.5
NFPG 1.7

D

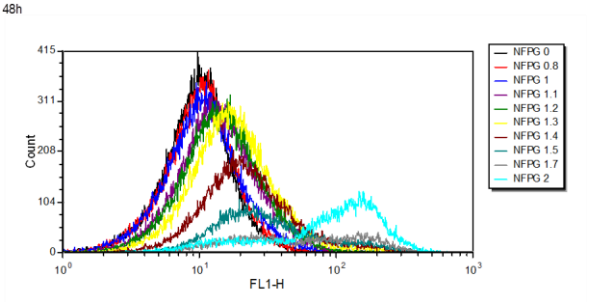
48h
Count
FL1-H
NFPG 0
NFPG 0.8
NFPG 1
NFPG 1.1
NFPG 1.2
NFPG 1.3
NFPG 1.4
NFPG 1.5
NFPG 1.7
NFPG 2

E

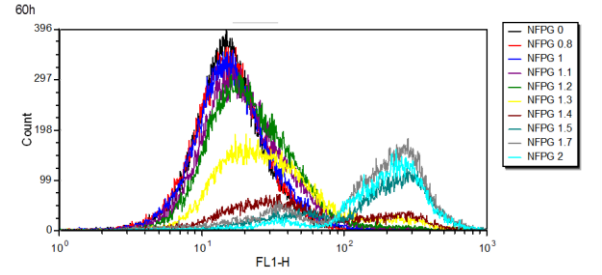
60h
Count
FL1-H
NFPG 0
NFPG 0.8
NFPG 1
NFPG 1.1
NFPG 1.2
NFPG 1.3
NFPG 1.4
NFPG 1.5
NFPG 1.7
NFPG 2

F

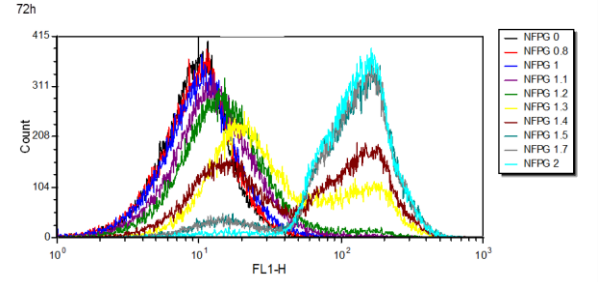
72h
Count
FL1-H
NFPG 0
NFPG 0.8
NFPG 1
NFPG 1.1
NFPG 1.2
NFPG 1.3
NFPG 1.4
NFPG 1.5
NFPG 1.7
NFPG 2

G

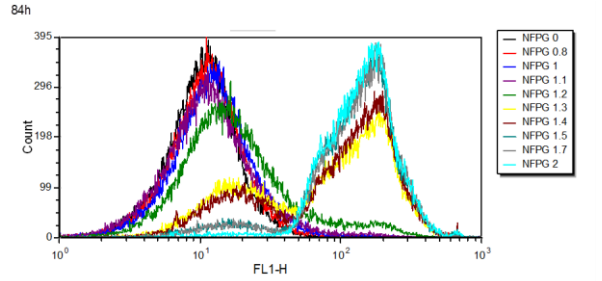
84h
Count
FL1-H
NFPG 0
NFPG 0.8
NFPG 1
NFPG 1.1
NFPG 1.2
NFPG 1.3
NFPG 1.4
NFPG 1.5
NFPG 1.7
NFPG 2

H

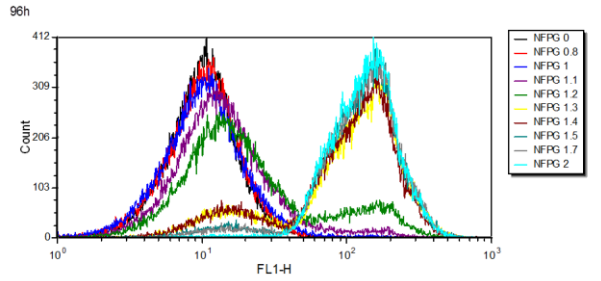
96h
Count
FL1-H
NFPG 0
NFPG 0.8
NFPG 1
NFPG 1.1
NFPG 1.2
NFPG 1.3
NFPG 1.4
NFPG 1.5
NFPG 1.7
NFPG 2

I

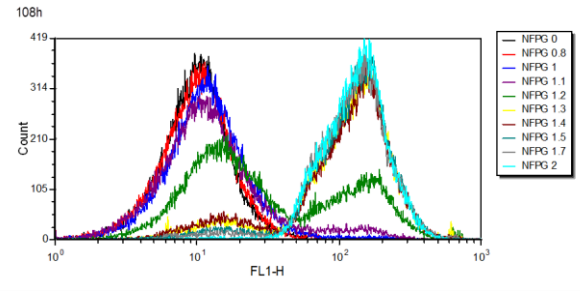
108h
Count
FL1-H
NFPG 0
NFPG 0.8
NFPG 1
NFPG 1.1
NFPG 1.2
NFPG 1.3
NFPG 1.4
NFPG 1.5
NFPG 1.7
NFPG 2

J

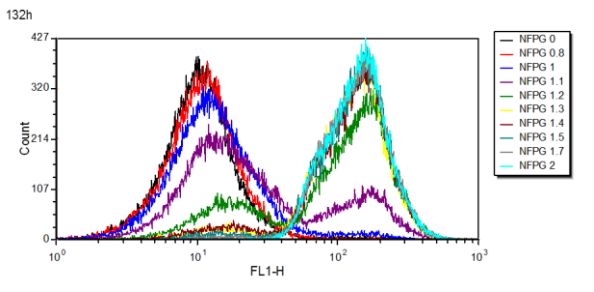
132h
Count
FL1-H
NFPG 0
NFPG 0.8
NFPG 1
NFPG 1.1
NFPG 1.2
NFPG 1.3
NFPG 1.4
NFPG 1.5
NFPG 1.7
NFPG 2

K

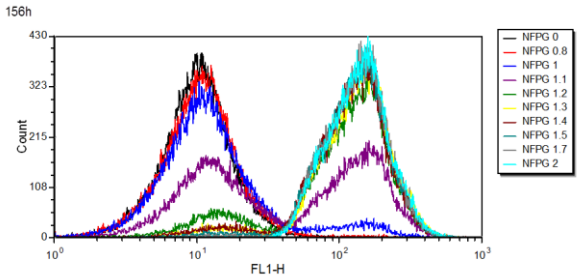
156h
Count
FL1-H
NFPG 0
NFPG 0.8
NFPG 1
NFPG 1.1
NFPG 1.2
NFPG 1.3
NFPG 1.4
NFPG 1.5
NFPG 1.7
NFPG 2

L

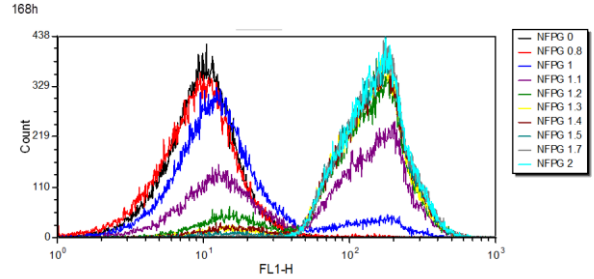
168h
Count
FL1-H
NFPG 0
NFPG 0.8
NFPG 1
NFPG 1.1
NFPG 1.2
NFPG 1.3
NFPG 1.4
NFPG 1.5
NFPG 1.7
NFPG 2

M

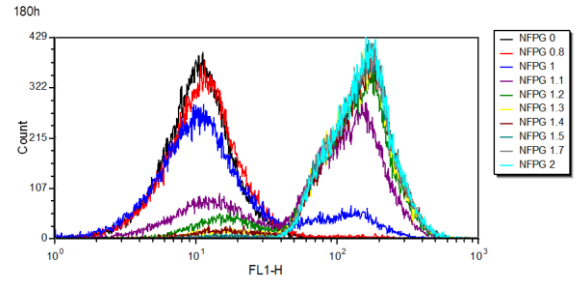
180h
Count
FL1-H
NFPG 0
NFPG 0.8
NFPG 1
NFPG 1.1
NFPG 1.2
NFPG 1.3
NFPG 1.4
NFPG 1.5
NFPG 1.7
NFPG 2

N

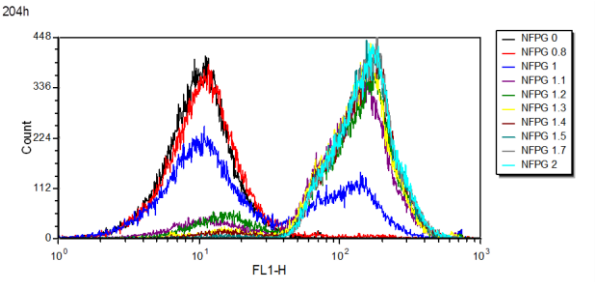
204h
Count
FL1-H
NFPG 0
NFPG 0.8
NFPG 1
NFPG 1.1
NFPG 1.2
NFPG 1.3
NFPG 1.4
NFPG 1.5
NFPG 1.7
NFPG 2

O

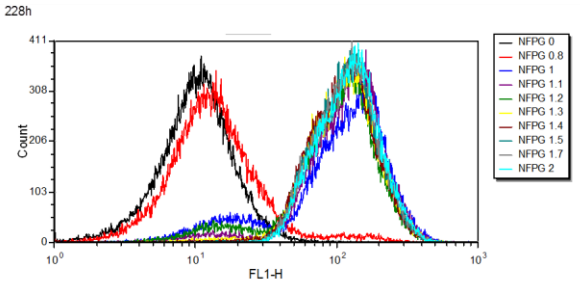
228h
Count
FL1-H
NFPG 0
NFPG 0.8
NFPG 1
NFPG 1.1
NFPG 1.2
NFPG 1.3
NFPG 1.4
NFPG 1.5
NFPG 1.7
NFPG 2

P

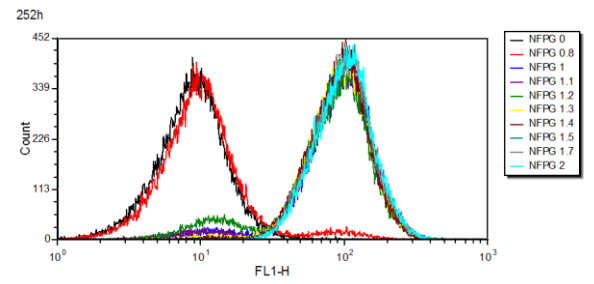
252h
Count
FL1-H
NFPG 0
NFPG 0.8
NFPG 1
NFPG 1.1
NFPG 1.2
NFPG 1.3
NFPG 1.4
NFPG 1.5
NFPG 1.7
NFPG 2

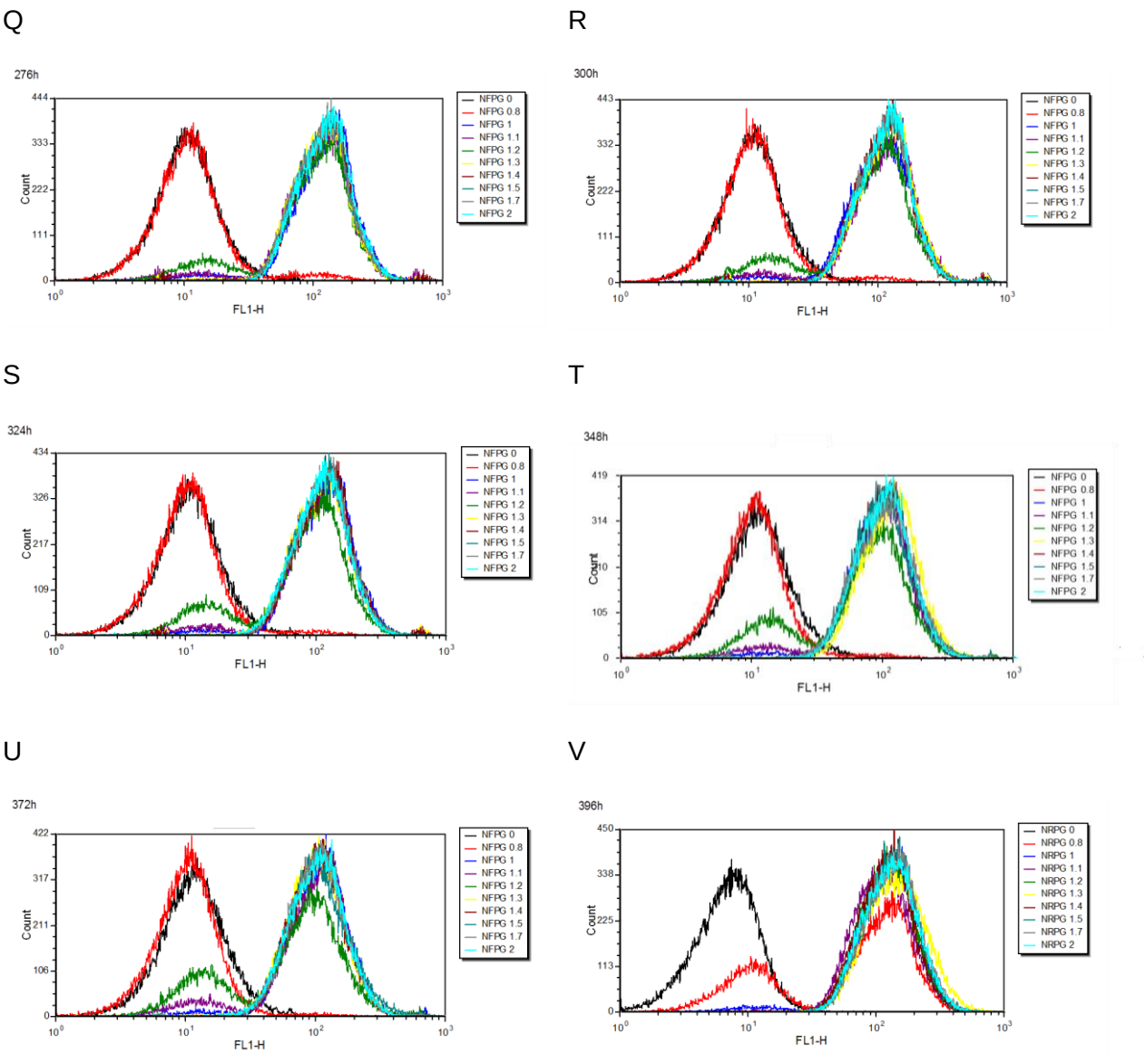

Figure 5.10 NFpump histograms in the fluconazole concentrations of 0 – 2 µg/ml.

(A) to (V) 12 hours after treatment to 396 hours after treatment. 10 Fluconazole concentrations were used: 0, 0.8, 1, 1.1, 1.2, 1.3, 1.4, 1.5, 1.7 and 2 µg/ml. In each sample, cell culture was started with 0.5 x 10^6 cells/ml, and every 12 hours, cell density was measured by Nexcelom, a small amount of cell culture based on the calculation was inoculated into fresh medium to start new culture with the same cell density, 0.5 x 10^6 cells/ml. Cell growth rate was then calculated and plotted. *PDR5::GFP* expression was measured by flow cytometry every 24 hours.

5.4 Conclusion and Discussion

In this project, I have shown that Pdr5 was able to protect *Saccharomyces cerevisiae* cells from the fluconazole treatment up to a concentration of 10 µg/ml. Non-tetracycline family molecule induced NRpump, NFpump and PFpump treated with fluconazole all showed dramatic reduction of growth rate in the first 12 hours. However, NRpump and NFpump cells fully recovered their growth rate to the normal level after 48 to 60 hours in the presence offluconazole, while the growth rate of PFpump cells remained extremely low during the entire fluconazole treatment. This discovery suggested a possibility that NRpump and NFpump gene circuits were broken in the presence of fluconazole, so that TetR was not able to repress *PDR5* transcription even in the absence of tetracycline family inducers, which led to the expression of Pdr5 from the two synthetic gene circuits. In order to test this hypothesis, flow cytometry was used to monitor *PDR5::GFP* expression after fluconazole treatment. The result confirmed the correlation between growth rate and *PDR5::GFP* expression level. The reduced growth rate in the initial fluconazole treatment was associated with basal *PDR5::GFP* expression, while the increased *PDR5::GFP* expression was associated with the recovery of growth rate in NRpump and NFpump cells. The histograms of *PDR5::GFP* expression remained the same even after the fluconazole removal, supporting the hypothesis of gene circuits' being broken in both NRpump and NFpump cases. These results suggested that the recovered growth rate was due to expression of Pdr5 from the gene circuits. Genetic mutations causing this most likely might contributed to the appearance of resistant cells. This needs further investigation by whole genome sequencing.

During the process of growth rate slow-down and recovery, NRpump and NFpump cells treated with six different fluconazole concentrations behaved similarly. The results suggested that the fluconazole concentrations between 2 µg/ml and 10 µg/ml were not able to differentiate NRpump and NFpump. Therefore, the question arose whether fluconazole was able to elicit

different distribution of Pdr5 expression. In order to answer this question, lower sets of fluconazole concentrations were used to treat NRpump and NFpump cells. The results indicated that the fluconazole concentration of 0.8 μg/ml was the threshold for generating resistance by increased expression in both NRpump and NFpump cells. It's also been noticed that the lower the fluconazole concentration was, the longer it took to elicit resistance in NRpump and NFpump cells; and the appearance of resistance was again confirmed to involve Pdr5 expression from the gene circuits. However, at intermediate fluconazole concentration, Pdr5 expression showed bimodality, which was not normal, because negative feedback loop has been proved to reduce gene expression noise, and NFpump showed unimodal distribution of Pdr5 expression when induced by doxycycline, no matter what concentration was used (Data shown in Chapter 3). This data suggested the existence of another subpopulation, which was resistance to fluconazole without Pdr5 expression from the gene circuit, or stochastic switching in a genetically homogenous population.

In order to further confirm the bimodality of Pdr5 expression in both NRpump and NFpump cells, more fluconazole concentrations in between 1 μg/ml and 1.5 μg/ml were used to elicit NRpump and NFpump cells, and the experiment lasted much longer to observe the dynamics of Pdr5 expression in the fluconazole environment. In the experiment, both NRpump and NFpump cells were induced at 10 fluconazole concentrations ranging from 0 μg/ml to 2 μg/ml for 396 hours. In the initial treatment, the growth rate of NRpump and PFpump cells slowed down with all the cells expressed low level of Pdr5 as expected. After 48 hours, both NRpump and NFpump cells started to recover their growth rate. During this process, a portion of cells became Pdr5 high expressers while others remained as low expressers. With longer treatment, an increasing percentage of cells became high expressers, until all the cells expressed a high level of Pdr5, and that was the time that NRpump and NFpump cells fully recovered their growth rate. However, at certain fluconazole concentration (1.1 μg/ml for

NRpump and 1.2 μg/ml for NFpump), a backward switch of Pdr5 expression showed up in both NRpump and NFpump cells. In other words, when all the cells became Pdr5 high expressers, a fraction of low Pdr5 expressers started to show up and increase, on the contrary, the percentage of high expressers shrank. This process lasted for around 100 hours and the low expressers eventually disappeared, then all of the cells became high expressers again. The sudden disappearance of low Pdr5 expressers at 396th hour after fluconazole treatment was suspicious, because the peak of low expressers had been increasing until the last time point before 396th hour. Unknown mechanisms must have occurred during this 12 hours time period. These results suggested several possibilities. First of all, there was no genetic mutation occurred during the entire fluconazole treatment, but two genetically identical subpopulations with different Pdr5 expression level existed, which contributed to the bimodality. The appearance of high expressers and recurrence of low expressers were due to stochastic switching. This is only possible when fluconazole induces the gene circuits' expression. Second possibility was genetic mutations on the synthetic gene circuits. The appearance of high expressers was due to the breakdown of NRpump and NFpump gene circuits, meaning that TetR was not able to repress Pdr5 expression any more, which might be due to two potential mechanisms: the TetR sequence mutated so that it could not bind to the promoter of *PDR5::GFP*, and the mutation of TetO sequence, which was the binding sites of TetR. As a result, the expression of Pdr5 conferred cells resistance to fluconazole and had the higher growth rate than cells without gene circuit breakdown, which explained the show-up of high expressers. The recurrence of low expressers was probably due to other genetic mutations occurred that conferred cells resistance to fluconazole. Overall, the results were more likely due to the combination of the last two possibilities, genetic mutation on both gene circuits and other places on the genome occurred during fluconazole treatment.

5.5 Future direction

Fluconazole was discovered to induce resistance in NRpump and NFpump cells in no tetracycline family molecule environment. Three major hypotheses were proposed to explain this result, stochastic switching, genetic mutation on the gene circuits and genetic mutation of other genes involved in cell membrane synthesis, which was the target of fluconazole resistance. The next step will be to test these hypotheses. First of all, stochastic switching theory will be tested. NRpump and NFpump cells treated with fluconazole concentrations that induced different distribution of Pdr5 expression will be used to culture in no fluconazole environment. If the histogram of Pdr5 expression remained the same after fluconazole removal, it proved that the emergence of Pdr5 high expressers was not a result of stochastic switching. However, if the percentage of high expressers decreased with the increase low expressers and eventually low expressers take over the population, then two possibilities exist. 1) stochastic switching; 2) low expressers took over the population because of their higher fitness compared to high expressers. Therefore, the next step will be to test if NRpump and NFpump gene circuits were broken. Expression of *PDR5::GFP* suggested the loss of function of TetR repression. Two possible events will contribute to this, mutation of TetR or mutation of TetO sites on the modified *GAL1* promoter. Thus, TetR and modified *GAL1* promoter on NRpump and NFpump gene circuits will be amplified by PCR and sequenced. The appearance of mutation on the sequencing results will suggest the breakdown of gene circuits, but confirmation experiments still need to be done. For example, replacing the wild type TetR or TetO sites with mutated ones to see if they are inducible by tetracycline family molecules. However, it is possible that no mutation will show up in the entire cell population or some cells in the population, for example, the NFpump low expresser subpopulation emerged after 276 hours in 1.2 μg/ml fluconazole. In that case, genes that will confer resistance to fluconazole will be tested. *ERG2*, *ERG3*, *ERG4*, *ERG6* and *ERG11*, which are involved in the alteration of sterol biosynthesis will be tested

because fluconazole blocks the natural synthesis of ergosterol which is an important component in cell membrane. Expression of other ABC family members will be tested as well. Although the endogenous Pdr5 has been knocked out in NRpump and NFpump cells, mutations of other multidrug resistance pumps, such as *PDR10*, *PDR11*, etc., might be able to compensate for its function.

Besides testing fluconazole resistance mechanisms in non-doxycycline induced NRpump and NFpump cells, the evolution dynamics of NRpump, NFpump and PFpump gene circuits in fluconazole was interesting and worth investigation as well. Study of their evaluation dynamics will help us better understand their natural selection process, and discover the evolution process of drug resistance, which might provide insight on our treatment of drug resistance. In order to better mimic natural systems and environment, fluctuating fluconazole concentrations will be used to treat these three gene circuits, because natural environment always keeps changing, a constant lasting environment rarely exists in nature. However, the evolution mechanisms discovered when the three gene circuits in constant fluconazole environment will lay the foundation for further study of evolution in fluctuating environment.

Chapter 6 Discussion and perspectives

In this dissertation research, I studied the interaction between a protein pump, Pdr5, and three synthetic gene circuits that regulate it. I compared the dose-response behavior of NRpump, NFpump and PFpump gene circuits with that of their non-pump counterparts, NR, NF and PF. The results indicated that Pdr5 changed the dose-response behavior of the original gene circuits. The change came from two resource. One was the efflux pumping function of Pdr5, and the other was reduced TetR expression in the pump strains. The additional change that Pdr5 caused in PF gene circuit was largely reduced cellular memories in the two subpopulations. Then I studied the molecular evolution of the three pump gene circuits in constant fluconazole containing environment, the resulted suggested the breakdown of NRpump and NFpump supported by the fact that *PDR5::GFP* was expressed from these two gene circuits. However, PFpump did not show any sign of change of growth rate and dose-response in 120 hours.

This study was the first one to characterize the behavior of NR, NF and PF gene circuits controlling an active target gene that affects the upstream regulatory elements experimentally in *Saccharomyces cerevasiae*, although mathematical models simulated the dose-response of another pump under the control of interlinked negative feedback and positive feedback loops in *E. coli* before [123]. The results of this study established the connection between experimental data and mathematical models, as my data was used to tune the stochastic simulations of pump gene circuits dose-response developed by my collaborator (Data not shown). The models he simulated matched well with experimental results, and it also provided insight to advance my research in the search of factors contributing to the change of dose-response in pump strains.

In this search, I discovered that the tetR expression was reduced in all the pump strains, which contributed to the dose-response change by decreasing its repression on the transcription

of *PDR5::GFP*. As a result, reduced tetR expression increase pump strains' sensitivity to the inducer, doxycycline. This increased sensitivity was not related to the efflux pumping function of Pdr5, supported by the evidence that pump strains with non-functional Pdr5 still showed the same level of sensitivity to doxycycline. In the search for potential causes of reduced TetR in pump strains, I narrowed them down to transcriptional level regulation, and the result was likely due to gene circuit's construction for the pump strains. Because *PDR5* was over 5kb nucleic acids long and was right preceding the promoter region of TetR, it is highly possible that the large *PDR5* gene sequence negatively affected the downstream transcription of TetR. Although other possibilities still exist, such as epigenetic modification of *PDR5*, researchers studying *PDR5* should pay more attention to the gene circuits' construction to avoid potential problems.

Another factor that contributed to the change of dose-response in the pump strains was the efflux pumping function of Pdr5. Besides, I also showed the exact difference it caused, such as the loss of linearity in NF. These results laid the foundation for further study on *PDR5* under other genetic circuits and even the behaviors of other active target genes (other protein pumps) in different regulatory networks. For example, genetic toggle switches might need higher inducer concentration to complete the switch when they are controlling *PDR5*, the concave dose-response curve might become less concave, or even linear. This might create a gradual switch, which can be used to fine tune desired output. Oscillator involves *PDR5* might lose oscillation since the key for oscillator requires delayed negative feedback [71], the addition of another *PDR5* induce negative feedback might destroy oscillation. However, oscillation might appear when *PDR5* is under control of a positive feedback loop and worth trying in the future since this potential genetic oscillator is simpler than other existing ones.

Besides insight to other gene circuits, this study has numerous applications as well. Since *PDR5* is involved in a number of biological processes, and has a variety of substrates, we are able to deliver precise control over them using our system. Although Pdr5 changed the linearity in NF, but the noise reduction nature of negative feedback still makes NFpump more

precise than NRpump in controlling target gene expression, and the subsequent exclusion of target gene substrates. Recent research discovered that protein pump helped to increase production of biofuel in *E. coli* by exporting biofuel molecules outside the bacteria to reduce toxicity and increase growth rate of host microorganisms [123]. We can do better by using our system to regulate the intracellular biofuel molecules precisely so that the cells growth rate and productivity will stay at the optimal level. Even more, we can combine our system with a biosensor system to detect certain molecules and respond automatically. For example, a recently engineered biosensor in yeast cells is able to detect steroids hormones [147], we can build an automatic system for production of steroids by adding biosensor to our system to deliver multilevel regulation. Different concentration of intracellular steroids will automatically results in different Pdr5 expression to maintain the production at the optimal level. Besides regulation of biomaterial production, our *PDR5* system can be used to advance basic research as well. A group of Pdr proteins in *Saccharomyces cerevasiae* have been shown to play a major role in the aging [148], our NFpump gene circuit can be used to study the dynamics and effect of ageing process more precisely. Besides, our system can facilitate research on multidrug resistance (MDR) pump mediated drug resistance. Earlier studies discovered that transcriptional noise led to phenotypic consequences [25, 34, 39, 40, 46], one cause for drug resistance is MDR gene expression noise. Since NF gene circuit reduces transcriptional noise, using NF controlling MDR pump is able to study drug resistance appearance and treatment more specifically.

This research also identified the change of growth rate and cellular memory caused by Pdr5 in PF strain. Although exceptions exist, positive feedback loop is considered to produce bimodal distribution [1, 79, 149-152], which means the existence of two stable steady states in terms of expression, ‘ON’ and ‘OFF’. In order to describe the transition between the two stable states, cellular memory was used, which was defined as the average time of an individual cell stays in one stable steady state. The results showed that Pdr5 reduced the cellular memory of high expresser significantly. Although it still needs further confirmation, the reduction was highly likely

due to the efflux pumping function of Pdr5. This data suggested a possibility to change cellular memory by introducing negative feedback loops. By doing so, another interesting question rose, if the strength of negative feedback loop affects the cellular memory as well. It's been know that positive feedback coupled with delayed negative feedback produces oscillator [1, 2, 21, 71, 131], it will be interesting to see the correlation between the strength of negative feedback and the frequency of the oscillator.

Finally, this dissertation also studied the evolution of synthetic gene circuits, and discovered that the gene circuits involving TetR repression was likely to break down in fluconazole environment. Besides the insight it provided to study of evolutionary course of regulatory networks in biological systems, it also showed the weakness of TetR based regulatory systems when facing adverse environment containing drugs. Further improvement of drug resistant TetR systems should be done, concerning the wide usage of Tet systems in the study of drug resistance in biomedical sciences.

Although the chances are low, there are a few things in the projects that might lead to alternative conclusions. First of all, the original NR and NF gene circuits used yEGFP as reporter, while all the pump stains used GFP. The fluorescence intensity of GFP is one tenth of that of yEGFP. Therefore, all the data has to be normalized for comparison of dose-responses between non-pump and pump strains. In this case, we can not compare the actual fluorescence intensity value, which indicates the actual expression level of ZeoR and Pdr5. It is possible that the expression of these two target genes is different. However, the normalization works for my study because here we only compare the difference between non-pump and pump strains.

The second experiment that might need improvement is the dose-response experiment for NR strain. NRpump and NRpump mutant strains were all induced by doxycycline concentration up to 15 μg/ml, but NR was induced up to 10 μg/ml. The reason I only used up to 10 μg/ml was that NR dose-response experiment was done first, and I found that the histograms of NR did not change after doxycycline concentration reached 7 μg/ml, indicating that the

expression of target gene reached saturation in the cell population. However, when I did the dose-response experiment for NRpump, I found that they saturated at higher doxycycline concentration compared to NR. Therefore, I used higher doxycycline concentration for NRpump. However, this might have introduced an uncertainty that affects the conclusion of my study. Because all the data was normalized to the fluorescence intensity value at the highest doxycycline concentrations for all the strains, and the fluorescence intensity values are different at doxycycline concentration 10 μg/ml and 15 μg/ml for NRpump. Therefore, if the data is normalized to the fluorescence intensity value at doxycycline concentration 10 μg/ml as it was done for NR, it might cause the increase of the fluorescence intensity mean at all the doxycycline concentrations. This might result in a closer gap between NR and NRpump mean dose-response at doxycycline concentration 7 μg/ml. Right now, the ANOVA test confirmed significant difference between NR and NRpump mean at doxycycline concentration 7 μg/ml. However, the difference is not guaranteed to be significant if the data is normalized to fluorescence intensity value at doxycycline concentration at 10 μg/ml. Therefore, in order to prove that, higher doxycycline concentration should be used to induce target gene expression until no more increase of fluorescence intensity is observed from doxycycline concentration increase.

BIBLIOGRAPHY

[1] Gardner, T. S., Cantor, C. R., and Collins, J. J. (2000) Construction of a genetic toggle switch in Escherichia coli, *Nature 403*, 339-342.

[2] Elowitz, M. B., and Leibler, S. (2000) A synthetic oscillatory network of transcriptional regulators, *Nature 403*, 335-338.

[3] Arber, W. (1974) DNA modification and restriction, *Prog Nucleic Acid Res Mol Biol 14*, 1-37.

[4] Arber, W. (1978) Restriction endonucleases, *Angew Chem Int Ed Engl 17*, 73-79.

[5] Arber, W. (2010) The 2009 Lindau Nobel Laureate Meeting: Werner Arber, physiology or medicine 1978, *J Vis Exp*.

[6] Nathans, D., and Smith, H. O. (1975) Restriction endonucleases in the analysis and restructuring of dna molecules, *Annu Rev Biochem 44*, 273-293.

[7] Smith, H. O., and Wilcox, K. W. (1970) A restriction enzyme from Hemophilus influenzae. I. Purification and general properties, *J Mol Biol 51*, 379-391.

[8] Kelly, T. J., Jr., and Smith, H. O. (1970) A restriction enzyme from Hemophilus influenzae. II, *J Mol Biol 51*, 393-409.

[9] Smith, H. O., and Birnstiel, M. L. (1976) A simple method for DNA restriction site mapping, *Nucleic Acids Res 3*, 2387-2398.

[10] Lee, T. S., Krupa, R. A., Zhang, F., Hajimorad, M., Holtz, W. J., Prasad, N., Lee, S. K., and Keasling, J. D. (2011) BglBrick vectors and datasheets: A synthetic biology platform for gene expression, *J Biol Eng 5*, 12.

[11] De Mey, M., Maertens, J., Lequeux, G. J., Soetaert, W. K., and Vandamme, E. J. (2007) Construction and model-based analysis of a promoter library for E. coli: an indispensable tool for metabolic engineering, *BMC Biotechnol 7*, 34.

[12] Hartner, F. S., Ruth, C., Langenegger, D., Johnson, S. N., Hyka, P., Lin-Cereghino, G. P., Lin-Cereghino, J., Kovar, K., Cregg, J. M., and Glieder, A. (2008) Promoter library designed for fine-tuned gene expression in Pichia pastoris, *Nucleic Acids Res 36*, e76.

[13] Blount, B. A., Weenink, T., Vasylechko, S., and Ellis, T. (2012) Rational diversification of a promoter providing fine-tuned expression and orthogonal regulation for synthetic biology, *PLoS One 7*, e33279.

[14] Blazeck, J., and Alper, H. S. (2013) Promoter engineering: recent advances in controlling transcription at the most fundamental level, *Biotechnol J 8*, 46-58.

[15] Lubliner, S., Keren, L., and Segal, E. (2013) Sequence features of yeast and human core promoters that are predictive of maximal promoter activity, *Nucleic Acids Res 41*, 5569-5581.

[16] Salis, H. M., Mirsky, E. A., and Voigt, C. A. (2009) Automated design of synthetic ribosome binding sites to control protein expression, *Nature biotechnology 27*, 946-950.

[17] Mutalik, V. K., Guimaraes, J. C., Cambray, G., Lam, C., Christoffersen, M. J., Mai, Q. A., Tran, A. B., Paull, M., Keasling, J. D., Arkin, A. P., and Endy, D. (2013) Precise and reliable gene expression via standard transcription and translation initiation elements, *Nat Methods 10*, 354-360.

[18] Alper, H., Fischer, C., Nevoigt, E., and Stephanopoulos, G. (2005) Tuning genetic control through promoter engineering, *Proc Natl Acad Sci U S A 102*, 12678-12683.

[19] Gorochowski, T. E., van den Berg, E., Kerkman, R., Roubos, J. A., and Bovenberg, R. A. (2014) Using synthetic biological parts and microbioreactors to explore the protein expression characteristics of Escherichia coli, *ACS synthetic biology 3*, 129-139.

[20] Ferrari, S., Lougaris, V., Caraffi, S., Zuntini, R., Yang, J., Soresina, A., Meini, A., Cazzola, G., Rossi, C., Reth, M., and Plebani, A. (2007) Mutations of the Igbeta gene cause agammaglobulinemia in man, *J Exp Med 204*, 2047-2051.

[21] Atkinson, M. R., Savageau, M. A., Myers, J. T., and Ninfa, A. J. (2003) Development of genetic circuitry exhibiting toggle switch or oscillatory behavior in Escherichia coli, *Cell 113*, 597-607.

[22] Antunes, M. S., Ha, S. B., Tewari-Singh, N., Morey, K. J., Trofka, A. M., Kugrens, P., Deyholos, M., and Medford, J. I. (2006) A synthetic de-greening gene circuit provides a reporting system that is remotely detectable and has a re-set capacity, *Plant Biotechnol J 4*, 605-622.

[23] Gibson, D. G., Glass, J. I., Lartigue, C., Noskov, V. N., Chuang, R. Y., Algire, M. A., Benders, G. A., Montague, M. G., Ma, L., Moodie, M. M., Merryman, C., Vashee, S., Krishnakumar, R., Assad-Garcia, N., Andrews-Pfannkoch, C., Denisova, E. A., Young, L., Qi, Z. Q., Segall-Shapiro, T. H., Calvey, C. H., Parmar, P. P., Hutchison, C. A., 3rd, Smith, H. O., and Venter, J. C. (2010) Creation of a bacterial cell controlled by a chemically synthesized genome, *Science 329*, 52-56.

[24] Church, G. M., Gao, Y., and Kosuri, S. (2012) Next-generation digital information storage in DNA, *Science 337*, 1628.

[25] Elowitz, M. B., Levine, A. J., Siggia, E. D., and Swain, P. S. (2002) Stochastic gene expression in a single cell, *Science 297*, 1183-1186.

[26] Khalil, A. S., and Collins, J. J. (2010) Synthetic biology: applications come of age, *Nature reviews. Genetics 11*, 367-379.

[27] Brown, M., Figge, J., Hansen, U., Wright, C., Jeang, K. T., Khoury, G., Livingston, D. M., and Roberts, T. M. (1987) lac repressor can regulate expression from a hybrid SV40 early promoter containing a lac operator in animal cells, *Cell 49*, 603-612.

[28] Gossen, M., and Bujard, H. (1992) Tight control of gene expression in mammalian cells by tetracycline-responsive promoters, *Proc Natl Acad Sci U S A 89*, 5547-5551.

[29] Nevozhay, D., Adams, R. M., Murphy, K. F., Josic, K., and Balazsi, G. (2009) Negative autoregulation linearizes the dose-response and suppresses the heterogeneity of gene expression, *Proc Natl Acad Sci U S A 106*, 5123-5128.

[30] Qi, L., Haurwitz, R. E., Shao, W., Doudna, J. A., and Arkin, A. P. (2012) RNA processing enables predictable programming of gene expression, *Nature biotechnology 30*, 1002-1006.

[31] Novick, A., and Weiner, M. (1957) Enzyme Induction as an All-or-None Phenomenon, *Proc Natl Acad Sci U S A 43*, 553-566.

[32] Ko, M. S., Nakauchi, H., and Takahashi, N. (1990) The dose dependence of glucocorticoid-inducible gene expression results from changes in the number of transcriptionally active templates, *EMBO J 9*, 2835-2842.

[33] Chalancon, G., Ravarani, C. N., Balaji, S., Martinez-Arias, A., Aravind, L., Jothi, R., and Babu, M. M. (2012) Interplay between gene expression noise and regulatory network architecture, *Trends Genet 28*, 221-232.

[34] Ozbudak, E. M., Thattai, M., Kurtser, I., Grossman, A. D., and van Oudenaarden, A. (2002) Regulation of noise in the expression of a single gene, *Nature genetics 31*, 69-73.

[35] Thattai, M., and van Oudenaarden, A. (2001) Intrinsic noise in gene regulatory networks, *Proc Natl Acad Sci U S A 98*, 8614-8619.

[36] Rosenfeld, N., Young, J. W., Alon, U., Swain, P. S., and Elowitz, M. B. (2005) Gene regulation at the single-cell level, *Science 307*, 1962-1965.

[37] Golding, I., Paulsson, J., Zawilski, S. M., and Cox, E. C. (2005) Real-time kinetics of gene activity in individual bacteria, *Cell 123*, 1025-1036.

[38] Becskei, A., Kaufmann, B. B., and van Oudenaarden, A. (2005) Contributions of low molecule number and chromosomal positioning to stochastic gene expression, *Nature genetics 37*, 937-944.

[39] Blake, W. J., Balazsi, G., Kohanski, M. A., Isaacs, F. J., Murphy, K. F., Kuang, Y., Cantor, C. R., Walt, D. R., and Collins, J. J. (2006) Phenotypic consequences of promoter-mediated transcriptional noise, *Mol Cell 24*, 853-865.

[40] Blake, W. J., M, K. A., Cantor, C. R., and Collins, J. J. (2003) Noise in eukaryotic gene expression, *Nature 422*, 633-637.

[41] Raser, J. M., and O'Shea, E. K. (2004) Control of stochasticity in eukaryotic gene expression, *Science 304*, 1811-1814.

[42] de Krom, M., van de Corput, M., von Lindern, M., Grosveld, F., and Strouboulis, J. (2002) Stochastic patterns in globin gene expression are established prior to transcriptional activation and are clonally inherited, *Mol Cell 9*, 1319-1326.

[43] Raj, A., Peskin, C. S., Tranchina, D., Vargas, D. Y., and Tyagi, S. (2006) Stochastic mRNA synthesis in mammalian cells, *PLoS biology 4*, e309.

[44] Murphy, K. F., Balazsi, G., and Collins, J. J. (2007) Combinatorial promoter design for engineering noisy gene expression, *Proc Natl Acad Sci U S A 104*, 12726-12731.

[45] Colman-Lerner, A., Gordon, A., Serra, E., Chin, T., Resnekov, O., Endy, D., Pesce, C. G., and Brent, R. (2005) Regulated cell-to-cell variation in a cell-fate decision system, *Nature 437*, 699-706.

[46] Fraser, H. B., Hirsh, A. E., Giaever, G., Kumm, J., and Eisen, M. B. (2004) Noise minimization in eukaryotic gene expression, *PLoS biology 2*, e137.

[47] Volfson, D., Marciniak, J., Blake, W. J., Ostroff, N., Tsimring, L. S., and Hasty, J. (2006) Origins of extrinsic variability in eukaryotic gene expression, *Nature 439*, 861-864.

[48] Newman, J. R., Ghaemmaghami, S., Ihmels, J., Breslow, D. K., Noble, M., DeRisi, J. L., and Weissman, J. S. (2006) Single-cell proteomic analysis of S. cerevisiae reveals the architecture of biological noise, *Nature 441*, 840-846.

[49] Shahrezaei, V., and Swain, P. S. (2008) The stochastic nature of biochemical networks, *Curr Opin Biotechnol 19*, 369-374.

[50] Raj, A., and van Oudenaarden, A. (2008) Nature, nurture, or chance: stochastic gene expression and its consequences, *Cell 135*, 216-226.

[51] Chubb, J. R., Trcek, T., Shenoy, S. M., and Singer, R. H. (2006) Transcriptional pulsing of a developmental gene, *Curr Biol 16*, 1018-1025.

[52] Beach, D. L., Salmon, E. D., and Bloom, K. (1999) Localization and anchoring of mRNA in budding yeast, *Curr Biol 9*, 569-578.

[53] Bloom, K., and Beach, D. L. (1999) mRNA localization: motile RNA, asymmetric anchors, *Curr Opin Microbiol 2*, 604-609.

[54] Bertrand, E., Chartrand, P., Schaefer, M., Shenoy, S. M., Singer, R. H., and Long, R. M. (1998) Localization of ASH1 mRNA particles in living yeast, *Mol Cell 2*, 437-445.

[55] Tsuboi, A., Yoshihara, S., Yamazaki, N., Kasai, H., Asai-Tsuboi, H., Komatsu, M., Serizawa, S., Ishii, T., Matsuda, Y., Nagawa, F., and Sakano, H. (1999) Olfactory neurons expressing closely linked and homologous odorant receptor genes tend to project their axons to neighboring glomeruli on the olfactory bulb, *J Neurosci 19*, 8409-8418.

[56] Touhara, K., Sengoku, S., Inaki, K., Tsuboi, A., Hirono, J., Sato, T., Sakano, H., and Haga, T. (1999) Functional identification and reconstitution of an odorant receptor in single olfactory neurons, *Proc Natl Acad Sci U S A 96*, 4040-4045.

[57] Chang, H. H., Hemberg, M., Barahona, M., Ingber, D. E., and Huang, S. (2008) Transcriptome-wide noise controls lineage choice in mammalian progenitor cells, *Nature 453*, 544-547.

[58] Mettetal, J. T., Muzzey, D., Pedraza, J. M., Ozbudak, E. M., and van Oudenaarden, A. (2006) Predicting stochastic gene expression dynamics in single cells, *Proc Natl Acad Sci U S A 103*, 7304-7309.

[59] Ozbudak, E. M., Thattai, M., Lim, H. N., Shraiman, B. I., and Van Oudenaarden, A. (2004) Multistability in the lactose utilization network of Escherichia coli, *Nature 427*, 737-740.

[60] Acar, M., Becskei, A., and van Oudenaarden, A. (2005) Enhancement of cellular memory by reducing stochastic transitions, *Nature 435*, 228-232.

[61] Kussell, E., and Leibler, S. (2005) Phenotypic diversity, population growth, and information in fluctuating environments, *Science 309*, 2075-2078.

[62] Garcia-Bernardo, J., and Dunlop, M. J. (2013) Tunable stochastic pulsing in the Escherichia coli multiple antibiotic resistance network from interlinked positive and negative feedback loops, *PLoS Comput Biol 9*, e1003229.

[63] Maamar, H., Raj, A., and Dubnau, D. (2007) Noise in gene expression determines cell fate in Bacillus subtilis, *Science 317*, 526-529.

[64] Pedraza, J. M., and van Oudenaarden, A. (2005) Noise propagation in gene networks, *Science 307*, 1965-1969.

[65] Hooshangi, S., Thiberge, S., and Weiss, R. (2005) Ultrasensitivity and noise propagation in a synthetic transcriptional cascade, *Proc Natl Acad Sci U S A 102*, 3581-3586.

[66] Rosenfeld, N., Elowitz, M. B., and Alon, U. (2002) Negative autoregulation speeds the response times of transcription networks, *J Mol Biol 323*, 785-793.

[67] Alon, U. (2007) Network motifs: theory and experimental approaches, *Nature reviews. Genetics 8*, 450-461.

[68] Takahashi, M., Degenkolb, J., and Hillen, W. (1991) Determination of the equilibrium association constant between Tet repressor and tetracycline at limiting Mg2+ concentrations: a generally applicable method for effector-dependent high-affinity complexes, *Anal Biochem 199*, 197-202.

[69] Ramsey, S., Orrell, D., and Bolouri, H. (2005) Dizzy: stochastic simulation of large-scale genetic regulatory networks, *J Bioinform Comput Biol 3*, 415-436.

[70] Samoilov, M. S., Price, G., and Arkin, A. P. (2006) From fluctuations to phenotypes: the physiology of noise, *Sci STKE 2006*, re17.

[71] Stricker, J., Cookson, S., Bennett, M. R., Mather, W. H., Tsimring, L. S., and Hasty, J. (2008) A fast, robust and tunable synthetic gene oscillator, *Nature 456*, 516-519.

[72] Stekel, D. J., and Jenkins, D. J. (2008) Strong negative self regulation of prokaryotic transcription factors increases the intrinsic noise of protein expression, *BMC Syst Biol 2*, 6.

[73] Batchelor, E., Silhavy, T. J., and Goulian, M. (2004) Continuous control in bacterial regulatory circuits, *J Bacteriol 186*, 7618-7625.

[74] Dublanche, Y., Michalodimitrakis, K., Kummerer, N., Foglierini, M., and Serrano, L. (2006) Noise in transcription negative feedback loops: simulation and experimental analysis, *Mol Syst Biol 2*, 41.

[75] Savageau, M. A. (1974) Comparison of classical and autogenous systems of regulation in inducible operons, *Nature 252*, 546-549.

[76] Austin, D. W., Allen, M. S., McCollum, J. M., Dar, R. D., Wilgus, J. R., Sayler, G. S., Samatova, N. F., Cox, C. D., and Simpson, M. L. (2006) Gene network shaping of inherent noise spectra, *Nature 439*, 608-611.

[77] Becskei, A., and Serrano, L. (2000) Engineering stability in gene networks by autoregulation, *Nature 405*, 590-593.

[78] Hasty, J., Pradines, J., Dolnik, M., and Collins, J. J. (2000) Noise-based switches and amplifiers for gene expression, *Proc Natl Acad Sci U S A 97*, 2075-2080.

[79] Isaacs, F. J., Hasty, J., Cantor, C. R., and Collins, J. J. (2003) Prediction and measurement of an autoregulatory genetic module, *Proc Natl Acad Sci U S A 100*, 7714-7719.

[80] Kramer, B. P., and Fussenegger, M. (2005) Hysteresis in a synthetic mammalian gene network, *Proc Natl Acad Sci U S A 102*, 9517-9522.

[81] Nevozhay, D., Adams, R. M., Van Itallie, E., Bennett, M. R., and Balazsi, G. (2012) Mapping the environmental fitness landscape of a synthetic gene circuit, *PLoS computational biology 8*, e1002480.

[82] Gossen, M., Freundlieb, S., Bender, G., Muller, G., Hillen, W., and Bujard, H. (1995) Transcriptional activation by tetracyclines in mammalian cells, *Science 268*, 1766-1769.

[83] Urlinger, S., Baron, U., Thellmann, M., Hasan, M. T., Bujard, H., and Hillen, W. (2000) Exploring the sequence space for tetracycline-dependent transcriptional activators: novel mutations yield expanded range and sensitivity, *Proc Natl Acad Sci U S A 97*, 7963-7968.

[84] Zhou, X., Vink, M., Berkhout, B., and Das, A. T. (2006) Modification of the Tet-On regulatory system prevents the conditional-live HIV-1 variant from losing doxycycline-control, *Retrovirology 3*, 82.

[85] Zhou, X., Vink, M., Klaver, B., Berkhout, B., and Das, A. T. (2006) Optimization of the Tet-On system for regulated gene expression through viral evolution, *Gene Ther 13*, 1382-1390.

[86] Loew, R., Heinz, N., Hampf, M., Bujard, H., and Gossen, M. (2010) Improved Tet-responsive promoters with minimized background expression, *BMC Biotechnol 10*, 81.

[87] Ames, G. F. (1986) Bacterial periplasmic transport systems: structure, mechanism, and evolution, *Annu Rev Biochem 55*, 397-425.

[88] Higgins, C. F., Hiles, I. D., Salmond, G. P., Gill, D. R., Downie, J. A., Evans, I. J., Holland, I. B., Gray, L., Buckel, S. D., Bell, A. W. (1986) A family of related ATP-binding subunits coupled to many distinct biological processes in bacteria, *Nature 323*, 448-450.

[89] Higgins, C. F. (1992) ABC transporters: from microorganisms to man, *Annual review of cell biology 8*, 67-113.

[90] Higgins, C. F., Gallagher, M. P., Hyde, S. C., Mimmack, M. L., and Pearce, S. R. (1990) Periplasmic binding protein-dependent transport systems: the membrane-associated components, *Philos Trans R Soc Lond B Biol Sci 326*, 353-364; discussion 364-355.

[91] Tomii, K., and Kanehisa, M. (1998) A comparative analysis of ABC transporters in complete microbial genomes, *Genome Res 8*, 1048-1059.

[92] Dean, M., Rzhetsky, A., and Allikmets, R. (2001) The human ATP-binding cassette (ABC) transporter superfamily, *Genome Res 11*, 1156-1166.

[93] Vasiliou, V., Vasiliou, K., and Nebert, D. W. (2009) Human ATP-binding cassette (ABC) transporter family, *Hum Genomics 3*, 281-290.

[94] Decottignies, A., and Goffeau, A. (1997) Complete inventory of the yeast ABC proteins, *Nature genetics 15*, 137-145.

[95] Lamping, E., Baret, P. V., Holmes, A. R., Monk, B. C., Goffeau, A., and Cannon, R. D. (2010) Fungal PDR transporters: Phylogeny, topology, motifs and function, *Fungal Genet Biol 47*, 127-142.

[96] Leppert, G., McDevitt, R., Falco, S. C., Van Dyk, T. K., Ficke, M. B., and Golin, J. (1990) Cloning by gene amplification of two loci conferring multiple drug resistance in Saccharomyces, *Genetics 125*, 13-20.

[97] Leonard, P. J., Rathod, P. K., and Golin, J. (1994) Loss of function mutation in the yeast multiple drug resistance gene PDR5 causes a reduction in chloramphenicol efflux, *Antimicrob Agents Chemother 38*, 2492-2494.

[98] Kolaczkowski, M., van der Rest, M., Cybularz-Kolaczkowska, A., Soumillion, J. P., Konings, W. N., and Goffeau, A. (1996) Anticancer drugs, ionophoric peptides, and steroids as substrates of the yeast multidrug transporter Pdr5p, *J Biol Chem 271*, 31543-31548.

[99] Rogers, B., Decottignies, A., Kolaczkowski, M., Carvajal, E., Balzi, E., and Goffeau, A. (2001) The pleitropic drug ABC transporters from Saccharomyces cerevisiae, *Journal of molecular microbiology and biotechnology 3*, 207-214.

[100] Subba Rao, G., Bachhawat, A. K., and Gupta, C. M. (2002) Two-hybrid-based analysis of protein-protein interactions of the yeast multidrug resistance protein, Pdr5p, *Funct Integr Genomics 1*, 357-366.

[101] Golin, J., and Ambudkar, S. V. (2015) The multidrug transporter Pdr5 on the 25th anniversary of its discovery: an important model for the study of asymmetric ABC transporters, *Biochem J 467*, 353-363.

[102] Rutledge, R. M., Ghislain, M., Mullins, J. M., de Thozee, C. P., and Golin, J. (2008) Pdr5-mediated multidrug resistance requires the CPY-vacuolar sorting protein Vps3: are xenobiotic compounds routed from the vacuole to plasma membrane transporters for efflux?, *Mol Genet Genomics 279*, 573-583.

[103] Rutledge, R. M., Esser, L., Ma, J., and Xia, D. (2011) Toward understanding the mechanism of action of the yeast multidrug resistance transporter Pdr5p: a molecular modeling study, *J Struct Biol 173*, 333-344.

[104] Kolaczkowska, A., Kolaczkowski, M., Goffeau, A., and Moye-Rowley, W. S. (2008) Compensatory activation of the multidrug transporters Pdr5p, Snq2p, and Yor1p by Pdr1p in Saccharomyces cerevisiae, *FEBS Lett 582*, 977-983.

[105] Kolaczkowski, M., Kolaczkowska, A., Motohashi, N., and Michalak, K. (2009) New high-throughput screening assay to reveal similarities and differences in inhibitory sensitivities of multidrug ATP-binding cassette transporters, *Antimicrob Agents Chemother 53*, 1516-1527.

[106] Kolaczkowski, M., Michalak, K., and Motohashi, N. (2003) Phenothiazines as potent modulators of yeast multidrug resistance, *Int J Antimicrob Agents 22*, 279-283.

[107] Golin, J., Ambudkar, S. V., Gottesman, M. M., Habib, A. D., Sczepanski, J., Ziccardi, W., and May, L. (2003) Studies with novel Pdr5p substrates demonstrate a strong size dependence for xenobiotic efflux, *J Biol Chem 278*, 5963-5969.

[108] Golin, J., Ambudkar, S. V., and May, L. (2007) The yeast Pdr5p multidrug transporter: how does it recognize so many substrates?, *Biochem Biophys Res Commun 356*, 1-5.

[109] de Thozee, C. P., Cronin, S., Goj, A., Golin, J., and Ghislain, M. (2007) Subcellular trafficking of the yeast plasma membrane ABC transporter, Pdr5, is impaired by a mutation in the N-terminal nucleotide-binding fold, *Mol Microbiol 63*, 811-825.

[110] Golin, J., Kon, Z. N., Wu, C. P., Martello, J., Hanson, L., Supernavage, S., Ambudkar, S. V., and Sauna, Z. E. (2007) Complete inhibition of the Pdr5p multidrug efflux pump ATPase activity by its transport substrate clotrimazole suggests that GTP as well as ATP may be used as an energy source, *Biochemistry 46*, 13109-13119.

[111] Ernst, R., Kueppers, P., Stindt, J., Kuchler, K., and Schmitt, L. (2010) Multidrug efflux pumps: substrate selection in ATP-binding cassette multidrug efflux pumps--first come, first served?, *FEBS J 277*, 540-549.

[112] Panagiotopoulos, I. A., Bakker, R. R., de Vrije, T., Claassen, P. A., and Koukios, E. G. (2013) Integration of first and second generation biofuels: fermentative hydrogen production from wheat grain and straw, *Bioresour Technol 128*, 345-350.

[113] Nosaka, K., Muthalib, M., Lavender, A., and Laursen, P. B. (2007) Attenuation of muscle damage by preconditioning with muscle hyperthermia 1-day prior to eccentric exercise, *Eur J Appl Physiol 99*, 183-192.

[114] Bokinsky, G., Peralta-Yahya, P. P., George, A., Holmes, B. M., Steen, E. J., Dietrich, J., Lee, T. S., Tullman-Ercek, D., Voigt, C. A., Simmons, B. A., and Keasling, J. D. (2011) Synthesis of three advanced biofuels from ionic liquid-pretreated switchgrass using engineered Escherichia coli, *Proc Natl Acad Sci U S A 108*, 19949-19954.

[115] Steen, E. J., Kang, Y., Bokinsky, G., Hu, Z., Schirmer, A., McClure, A., Del Cardayre, S. B., and Keasling, J. D. (2010) Microbial production of fatty-acid-derived fuels and chemicals from plant biomass, *Nature 463*, 559-562.

[116] Steen, E. J., Chan, R., Prasad, N., Myers, S., Petzold, C. J., Redding, A., Ouellet, M., and Keasling, J. D. (2008) Metabolic engineering of Saccharomyces cerevisiae for the production of n-butanol, *Microb Cell Fact 7*, 36.

[117] Srirangan, K., Pyne, M. E., and Perry Chou, C. (2011) Biochemical and genetic engineering strategies to enhance hydrogen production in photosynthetic algae and cyanobacteria, *Bioresour Technol 102*, 8589-8604.

[118] Lan, E. I., and Liao, J. C. (2013) Microbial synthesis of n-butanol, isobutanol, and other higher alcohols from diverse resources, *Bioresour Technol 135*, 339-349.

[119] Stephanopoulos, G. (2007) Challenges in engineering microbes for biofuels production, *Science 315*, 801-804.

[120] Delebecque, C. J., Lindner, A. B., Silver, P. A., and Aldaye, F. A. (2011) Organization of intracellular reactions with rationally designed RNA assemblies, *Science 333*, 470-474.

[121] Peskind, E. R., Raskind, M. A., Wingerson, D., Pascualy, M., Thal, L. J., Dobie, D. J., Veith, R. C., Dorsa, D. M., Murray, S., Sikkema, C. (1995) Enhanced hypothalamic-pituitary-adrenocortical axis responses to physostigmine in normal aging, *J Gerontol A Biol Sci Med Sci 50*, M114-120.

[122] Nicolaou, S. A., Gaida, S. M., and Papoutsakis, E. T. (2010) A comparative view of metabolite and substrate stress and tolerance in microbial bioprocessing: From biofuels and chemicals, to biocatalysis and bioremediation, *Metab Eng 12*, 307-331.

[123] Dunlop, M. J., Dossani, Z. Y., Szmidt, H. L., Chu, H. C., Lee, T. S., Keasling, J. D., Hadi, M. Z., and Mukhopadhyay, A. (2011) Engineering microbial biofuel tolerance and export using efflux pumps, *Mol Syst Biol 7*, 487.

[124] Dunlop, M. J. (2011) Engineering microbes for tolerance to next-generation biofuels, *Biotechnol Biofuels 4*, 32.

[125] Stephanopoulos, G. (2012) Synthetic biology and metabolic engineering, *ACS synthetic biology 1*, 514-525.

[126] Nielsen, J., Fussenegger, M., Keasling, J., Lee, S. Y., Liao, J. C., Prather, K., and Palsson, B. (2014) Engineering synergy in biotechnology, *Nat Chem Biol 10*, 319-322.

[127] Way, J. C., Collins, J. J., Keasling, J. D., and Silver, P. A. (2014) Integrating biological redesign: where synthetic biology came from and where it needs to go, *Cell 157*, 151-161.

[128] Purnick, P. E., and Weiss, R. (2009) The second wave of synthetic biology: from modules to systems, *Nature reviews. Molecular cell biology 10*, 410-422.

[129] Brophy, J. A., and Voigt, C. A. (2014) Principles of genetic circuit design, *Nature methods 11*, 508-520.

[130] Slusarczyk, A. L., Lin, A., and Weiss, R. (2012) Foundations for the design and implementation of synthetic genetic circuits, *Nature reviews. Genetics 13*, 406-420.

[131] Tigges, M., Marquez-Lago, T. T., Stelling, J., and Fussenegger, M. (2009) A tunable synthetic mammalian oscillator, *Nature 457*, 309-312.

[132] Siuti, P., Yazbek, J., and Lu, T. K. (2013) Synthetic circuits integrating logic and memory in living cells, *Nature biotechnology 31*, 448-452.

[133] Xie, Z., Wroblewska, L., Prochazka, L., Weiss, R., and Benenson, Y. (2011) Multi-input RNAi-based logic circuit for identification of specific cancer cells, *Science 333*, 1307-1311.

[134] Moon, T. S., Lou, C., Tamsir, A., Stanton, B. C., and Voigt, C. A. (2012) Genetic programs constructed from layered logic gates in single cells, *Nature 491*, 249-253.

[135] Nandagopal, N., and Elowitz, M. B. (2011) Synthetic biology: integrated gene circuits, *Science 333*, 1244-1248.

[136] Harrison, M. E., and Dunlop, M. J. (2012) Synthetic feedback loop model for increasing microbial biofuel production using a biosensor, *Front Microbiol 3*, 360.

[137] Lage, H. (2003) ABC-transporters: implications on drug resistance from microorganisms to human cancers, *International journal of antimicrobial agents 22*, 188-199.

[138] Charlebois, D. A., Balazsi, G., and Kaern, M. (2014) Coherent feedforward transcriptional regulatory motifs enhance drug resistance, *Phys Rev E 89*.

[139] Huh, W. K., Falvo, J. V., Gerke, L. C., Carroll, A. S., Howson, R. W., Weissman, J. S., and O'Shea, E. K. (2003) Global analysis of protein localization in budding yeast, *Nature 425*, 686-691.

[140] Nevozhay, D., Adams, R. M., and Balazsi, G. (2011) Linearizer Gene Circuits with Negative Feedback Regulation, *Methods Mol Biol 734*, 81-100.

[141] Gietz, R. D., Schiestl, R. H., Willems, A. R., and Woods, R. A. (1995) Studies on the transformation of intact yeast cells by the LiAc/SS-DNA/PEG procedure, *Yeast 11*, 355-360.

[142] Gietz, R. D., and Schiestl, R. H. (2007) High-efficiency yeast transformation using the LiAc/SS carrier DNA/PEG method, *Nat Protoc 2*, 31-34.

[143] Sauna, Z. E., Bohn, S. S., Rutledge, R., Dougherty, M. P., Cronin, S., May, L., Xia, D., Ambudkar, S. V., and Golin, J. (2008) Mutations define cross-talk between the N-terminal nucleotide-binding domain and transmembrane helix-2 of the yeast multidrug transporter Pdr5: possible conservation of a signaling interface for coupling ATP hydrolysis to drug transport, *J Biol Chem 283*, 35010-35022.

[144] Furman, C., Mehla, J., Ananthaswamy, N., Arya, N., Kulesh, B., Kovach, I., Ambudkar, S. V., and Golin, J. (2013) The deviant ATP-binding site of the multidrug efflux pump Pdr5 plays an active role in the transport cycle, *J Biol Chem 288*, 30420-30431.

[145] Nevozhay, D., Adams, R. M., and Balazsi, G. (2011) Linearizer gene circuits with negative feedback regulation, *Methods Mol Biol 734*, 81-100.

[146] Ananthaswamy, N., Rutledge, R., Sauna, Z. E., Ambudkar, S. V., Dine, E., Nelson, E., Xia, D., and Golin, J. (2010) The signaling interface of the yeast multidrug transporter Pdr5 adopts a cis conformation, and there are functional overlap and equivalence of the deviant and canonical Q-loop residues, *Biochemistry 49*, 4440-4449.

[147] Ino, K., Kitagawa, Y., Watanabe, T., Shiku, H., Koide, M., Itayama, T., Yasukawa, T., and Matsue, T. (2009) Detection of hormone active chemicals using genetically engineered

yeast cells and microfluidic devices with interdigitated array electrodes, *Electrophoresis 30*, 3406-3412.

[148] Eldakak, A., Rancati, G., Rubinstein, B., Paul, P., Conaway, V., and Li, R. (2010) Asymmetrically inherited multidrug resistance transporters are recessive determinants in cellular replicative ageing, *Nat Cell Biol 12*, 799-805.

[149] Ajo-Franklin, C. M., Drubin, D. A., Eskin, J. A., Gee, E. P., Landgraf, D., Phillips, I., and Silver, P. A. (2007) Rational design of memory in eukaryotic cells, *Genes Dev 21*, 2271-2276.

[150] Becskei, A., Seraphin, B., and Serrano, L. (2001) Positive feedback in eukaryotic gene networks: cell differentiation by graded to binary response conversion, *EMBO J 20*, 2528-2535.

[151] Ellis, T., Wang, X., and Collins, J. J. (2009) Diversity-based, model-guided construction of synthetic gene networks with predicted functions, *Nature biotechnology 27*, 465-471.

[152] May, T., Eccleston, L., Herrmann, S., Hauser, H., Goncalves, J., and Wirth, D. (2008) Bimodal and hysteretic expression in mammalian cells from a synthetic gene circuit, *PLoS One 3*, e2372.

VITA

Junchen Diao received his Bachelor of Science degree in Biological Sciences from Wuhan University, P.R. China, in June 2008. Then he worked as research assistant in Dr. Ying-Hua Chen's lab at Tsinghua University, P.R. China, where he did his research thesis for B.S degree. In this lab, Junchen studied HIV vaccine, which led to a coauthor paper published in the journal of Vaccine. In August 2010, he enrolled in the University of Texas Graduate School of Biomedical Sciences. The following year, He joined Dr. Gabor Balazsi's lab at the University of Texas M.D. Anderson Cancer Center to do dissertation research on the interaction between regulatory synthetic gene circuits and PDR5 in *Saccharomyces cerevisiae*.